

THE UNIVERSITY OF MANITOBA

EXPERIMENTAL ANALYSIS OF CELLULAR IMMUNITY

IN THE INSECT GALLERIA MELLONELLA L.



WILLIAM LIONEL DIEHL-JONES

A THESIS

SUBMITTED TO THE FACULTY OF GRADUATE STUDIES

IN PARTIAL FULFILMENT OF THE REQUIREMENTS FOR THE

DEGREE OF MASTER OF SCIENCE

DEPARTMENT OF ZOOLOGY

WINNIPEG, MANITOBA

FALL, 1986

Permission has been granted to the National Library of Canada to microfilm this thesis and to lend or sell copies of the film.

The author (copyright owner) has reserved other publication rights, and neither the thesis nor extensive extracts from it may be printed or otherwise reproduced without his/her written permission.

L'autorisation a été accordée à la Bibliothèque nationale du Canada de microfilmer cette thèse et de prêter ou de vendre des exemplaires du film.

L'auteur (titulaire du droit d'auteur) se réserve les autres droits de publication; ni la thèse ni de longs extraits de celle-ci ne doivent être imprimés ou autrement reproduits sans son autorisation écrite.

ISBN 0-315-48016-5

EXPERIMENTAL ANALYSIS OF CELLULAR IMMUNITY
IN THE INSECT GALLERIA MELLONELLA L.

BY

WILLIAM LIONEL DIEHL-JONES

A thesis submitted to the Faculty of Graduate Studies of
the University of Manitoba in partial fulfillment of the requirements
of the degree of

MASTER OF SCIENCE

© 1987

Permission has been granted to the LIBRARY OF THE UNIVERSITY OF MANITOBA to lend or sell copies of this thesis, to the NATIONAL LIBRARY OF CANADA to microfilm this thesis and to lend or sell copies of the film, and UNIVERSITY MICROFILMS to publish an abstract of this thesis.

The author reserves other publication rights, and neither the thesis nor extensive extracts from it may be printed or otherwise reproduced without the author's written permission.

ABSTRACT

The cellular immune response of Galleria mellonella L. is altered when challenged with the entomophagous nematode Steinernema feltiae Filepjev. Changes occur in phagocytosis and encapsulation, lectin binding, and hemocyte morphology and motility.

Phagocytosis of latex beads was significantly lower in granulocytes from insects infected with either xenic or axenic S. feltiae 8hrs post-infection. Serum from either xenic- or axenically-infected insects also caused a significant decrease in phagocytosis. Xenic and axenic nematodes inhibited encapsulation of ultra-violet killed nematodes by 12hrs post-infection. Granulocytes from axenically-infected insects showed significant increases in patching of concanavalin A and wheat germ agglutinin receptors by 4hrs post-infection.

There were no obvious differences between internal ultra-structure, as revealed by transmission electron microscopy, of plasmatocytes and granulocytes from control or xenically-infected insects. However, scanning electron microscopy revealed differences in their spreading morphology. Video time-lapse analysis of plasmatocyte motility in vitro showed striking differences in the rate of locomotion of plasmatocytes from infected insects. The maximum locomotory speed of plasmatocytes from control, axenic- and xenically-infected insects were $10.6 \pm 0.9\mu\text{m}/15\text{min}$, $7.5 \pm 1.3\mu\text{m}/15\text{min}$, and

3.3 \pm 0.7 μ m/15min, respectively. These speeds were attained by 135, 120, and 15min elapsed time, respectively, after video recording commenced. Plasmatocytes cultured with xenic nematodes also showed significant decreases in speed. Analysis of the microtubule and microfilament (F-actin) cytoskeleton revealed changes in the distribution of microtubules and F-actin in plasmatocytes from axenically-infected insects, and these correlated closely with observations on cell motility.

Data indicated that inhibition of plasmatocyte motility likely plays a major role in suppression of cellular immunity. Results of phagocytosis and encapsulation assays suggested that S. feltiae may also inhibit recognition of foreignness, but this is only manifested during later stages of infection.

ACKNOWLEDGEMENTS

I wish to thank Dr. Erwin Huebner for allowing me to work in his lab, and for providing me with the means and guidance to complete this research. I am honored to know him professionally and personally.

I wish to thank my examining committee, Drs. L. Graham and R. Lyric.

I would also thank Drs. D.B. Stewart and T.V.N. Persaud.

To graduate students G. Kelly and G. Valdimarsson, thank you for the help and for tolerating entropy. Thank you also to O. Bres and A. Shostak.

Thanks are also due to technicians B. Luit and G. Burgess.

I wish to thank my wife, Charlene for more than I can say.

I would like to dedicate this thesis to Dr. H.E. Welch. His expertise in science, and his personal courage and integrity have made lasting impressions on me. Thank you, Dr. Welch.

TABLE OF CONTENTS

	Page
Abstract	i
Acknowledgements	iii
Table of Contents	iv
List of Figures	vi
List of Tables	x
List of Abbreviations	xi
General Introduction	1
General Materials and Methods	10
Chapter 1: Phagocytosis and Encapsulation	16
Introduction	16
Materials and Methods	17
Results	21
Discussion	32
Chapter 2: Lectin Binding	38
Introduction	38
Materials and Methods	39
Results	43
Discussion	46
Chapter 3: Hemocyte Morphology and Motility	49
Introduction	49
Materials and Methods	50
Results	55
Discussion	91

	Page
Chapter 4: Microtubule and Microfilament Cytoskeleton	97
Introduction	97
Materials and Methods	98
Results	101
Discussion	119
General Summary	127
References	129

LIST OF FIGURES

	Page
Chapter 1	
Figure 1.	22
Figure 2.	22
Figures 3,4.	22
Figure 5.	22
Figure 6a,b.	26
Figure 7a,b.	26
Figure 8a,b.	26
Figure 9a,b.	27
Figure 10a,b.	27
Figure 11a,b.	27
Figures 13,14.	30, 31
Figure 15.	33
Chapter 2	
Figure 1a,b.	42
Figure 2a,b.	42
Figure 3.	42
Figure 4.	42
Figure 5.	45

Chapter 3

Figure 1.	Normal morphology of <u>G.</u> mellonella hemocytes	56
Figures 2,3.	Morphology of hemocyte from infected animal	58
Figure 4.	Multivesicular body	58
Figures 5,6.	GR after 2min incubation on glass	60
Figure 7.	GR after 5min incubation on glass	61
Figure 8.	GR showing type I and II filopodia	61
Figure 9.	Higher magnification of filopodia	61
Figure 10.	GR after 20min incubation on glass	62
Figure 11.	GR after 2min incubation on BMM	63
Figure 12.	GR after 20min incubation on BMM	63
Figures 13-15.	PL after 2min incubation on glass	65, 66
Figures 16-19.	Intermediate spreading stage PL on glass	66, 67
Figures 20-22.	Unipolarized PL on glass	69, 70
Figure 23.	Bipolarized PL on glass	70
Figures 24-27.	PL on glass	71
Figures 28-29.	Non-polarized PL on glass	73
Figure 30.	Early spreading PL on BMM	74
Figure 31.	Intermediate spreading PL on BMM	75
Figure 32.	PL after 2min incubation on BMM	76
Figure 33.	PL after 5min incubation on BMM	76
Figure 34.	PL after 20min incubation on BMM	78
Figure 35.	GR from infected insect	79
Figure 36.	Intermediate PL from infected insect	79

	Page
Figure 37. Unipolarized PL from infected insect	79
Figure 38. PL from infected insect	79
Figures 39-41a-f. Video time-lapse sequence of control PL's	81, 82, 84
Figure 42a-f. Video time-lapse sequence of PL's in XPI4 culture	86
Figure 43a-f. Video time-lapse sequence of PL's in XPI12 culture	88
Figure 44a-e. Rate of <u>in vitro</u> locomotion of PL's in control, AxNIC, AxPI4, XNIC and XPI4 cultures	90

Chapter 4

Figures 1-4. MT distribution in early spreading stage PL's	102
Figure 5a,b,c. MT distribution at different focal planes	104
Figures 6,7. Variation of MT's in lamellae	104
Figure 8. MT distribution in unipolarized PL	106
Figure 9a,b,c. MT distribution in unipolarized PL's at stages of posterior retraction	106
Figures 10,11. MT distribution in bipolar PL's	107
Figures 12,13. MT variation in bipolar PL's	109
Figures 14-16. MT distribution in multipolar cells	109
Figures 17-20. MT distribution in non-polarized PL's	110
Figure 21. F-actin distribution in early spreading stage PL	112

	Page
Figures 22-25. F-actin distribution in intermediate PL	112, 114
Figures 26-28. F-actin distribution in unipolarized PL	114
Figure 29. F-actin distribution in bipolar PL	115
Figure 30. F-actin distribution in multipolar PL	115
Figures 31-32. F-actin in overlapping PL's	115
Figures 33-35. F-actin distribution in non-polarized PL's	116
Figures 36-41. MT distribution in PL's from infected insects	118
Figures 42-45. F-actin distribution in PL's from infected insects	120

LIST OF TABLES

	Page
Chapter 1	
Table I. Summary of encapsulation experiments with axenic, xenic and U.V.-killed nematodes	24
Chapter 2	
Table I. Lectins, haptens, and results of lectin staining	41

LIST OF ABBREVIATIONS

Abbreviation	Meaning
Ab	antibody
AxNIC	axenic nematodes in chamber
AxPI4	4hrs post-axenic infection
AxPI12	12hrs post-axenic infection
BMM	basement membrane matrigel TM
BSS	balanced salt solution
ConA	concanavalin A
DBA	<u>Dolichos biflorus</u> agglutinin
D-Glc	D-glucose
DIC	differential interference contrast
D-Man	D-mannose
EDTA	ethylene-diaminetetra-acetic acid
ET	elapsed time
F-ConA	fluoresceinated-concanavalin A
F-DBA	fluoresceinated-Dolichos biflorus agglutinin
FITC	fluorescein iso-thiocyanate
F-WGA	fluoresceinated-wheat germ agglutinin
GIM	Grace's insect medium
GlcNAc	N-acetyl-D-glucosamine
GR	granulocyte

Abbreviation	Meaning
IgG	immunoglobulin G
J1	1 st stage juvenile
KV	kilovolt
MF	microfilament
MT	microtubule
MVB	multi-vesicular body
Oe	oenocytoide
PBS	phosphate buffered saline
PI	post-infection
PI _{inj}	post-injection
PL	plasmatocyte
PTU	phenylthiourea
RER	rough endoplasmic reticulum
SE	standard error
SEM	scanning electron micrograph
SP	sphaerulocyte
TEM	transmission electron micrograph
U.V.	ultra-violet
XNIC	xenic nematodes in chamber
XPI4	4hrs post-xenic infection

GENERAL INTRODUCTION

The immunological responses of multicellular organisms to foreign pathogens represent adaptations of great complexity (Nappi, 1975). The basic vertebrate immune mechanisms probably have their evolutionary roots among the invertebrates (Burnett, 1968), and an understanding of invertebrate immunity is essential. There are also a number of reasons why invertebrate immunity should be studied in its own right (Boman et al., 1974); and insects provide ideal experimental systems for studying immunity since they demonstrate obvious cellular immune responses. The early events of insect immunity are poorly understood, especially the mechanisms of "non-self" recognition and cell movement (Ratner and Vinson, 1983a). An examination of host-parasite interactions in insects is one interesting way of approaching these problems, especially since insect parasites frequently evade or inhibit immune responses (Lackie, 1980). Since my study utilizes this approach, a brief overview of insect immunity and insect responses to parasites is pertinent.

Mechanisms of insect immunity

Invasion by would-be parasites and pathogens is initially impeded by external barriers. Insects have a tough outer cuticle that extends into foregut, hindgut, and tracheae; the midgut in some

insects is protected by the peritrophic membrane (Ratcliffe and Rowley, 1979). In addition, living cells of the alimentary canal may limit foreign invasion by endocytosis of bacteria (Kawanishi et al., 1978) or encapsulation of nematode parasites (Cawthorn and Anderson, 1977).

Once the external barriers have been penetrated, cellular and humoral elements in the hemocoel effect immunological reactions. Cellular immunity is mediated by at least two morphologically different blood cell (hemocyte) types -- granulocytes and plasmatocytes, and is manifested by three main reactions: phagocytosis, nodule formation, and encapsulation (Gupta, 1979).

Phagocytosis is the sum of several cellular events: contact with a foreign object less than 10 μ m in diameter, recognition and attachment to the "non-self" object, and ingestion (Gotz and Boman, 1985). As opposed to the vertebrate system, immunoglobins and complement do not mediate recognition of foreignness and invertebrate hemocytes lack Fc and C3 receptors (Scott, 1971; Anderson, 1976). Phagocytosis by invertebrate blood cells relies on other, less specific but effective mechanisms as shown by the variety of test particles which are phagocytosed, such as bacteria, fungi, mycetozoa, protozoa, latex, glass, and dye (Ratcliffe and Rowley, 1979).

Nodule formation usually occurs in response to large quantities of particulate matter which cannot be eliminated by phagocytosis alone. This response occurs in two phases: the first is contact

recognition by granulocytes, followed by degeneration of these cells and release of a sticky coagulum (Ratcliffe and Gagen, 1977). Next, plasmatocytes form an outer sheath, eventually giving rise to a nodule comprised of an inner melanized core, a middle region of flattened plasmatocytes, and an outer region of newly attached cells (Ratcliffe and Gagen, 1977).

Similar to nodule formation, encapsulation is also biphasic, and occurs in response to objects too large to phagocytose (Salt, 1963). During the first phase granulocytes contact a foreign surface and lyse. The second phase involves aggregation and fusion of plasmatocytes into a capsule with a variable number of layers (Ratcliffe and Rowley, 1979). Insects form capsules against a wide range of biotic and abiotic objections; most notably, encapsulation represents the main defense mechanisms of insects against nematodes (Poinar, 1979; Nappi, 1975).

Common to all three reactions is the initial recognition of foreignness and attachment. Several theories have been postulated to account for non-self recognition by insect hemocytes. Briefly, Lackie (1981a) has proposed a two-tiered system of non-self recognition, in which 'coarse adjustment' is based on non-specific factors such as surface charge or hydrophobicity, and 'fine adjustment' is based on recognition of chemical differences in cell membrane-borne molecules like glycoproteins. With respect to the former, Vinson (1974) stated that recognition may depend on the ionic nature of the

foreign surface, as the immune response of Heliothis sp. to anion and cation exchangers were different. More recently, Lackie (1986) has also found differences in encapsulation based on surface charge. During coarse adjustment, non-specific recognition could occur when hemocyte surface and cell surface differ enough by physico-chemical parameters, and this could vary between insects.

In addition, finer, more discriminatory mechanisms of recognition may include recognition based on carbohydrate moieties on the surface of hemocytes or foreign objects. Naturally-occurring hemagglutinins or lectins (Yeaton, 1981) were found both in insect hemolymph (Scott, 1972) and reversibly bound to invertebrate blood cells (Amirante and Mazzalai, 1978; van der Knaap et al., 1983). Although these molecules differ in electrophoretic mobilities from vertebrate immunoglobulin (Brahni and Cooper, 1974), they probably play a similar role to that of the immunoglobins (Ratcliffe and Rowley, 1979).

A model using carbohydrates for non-self recognition in invertebrates was proposed by Parish (1977). This involved the polymerization of 5-glycosyl-transferases into hexamers which could react more specifically to foreign surfaces. Evidence for this model is that invertebrate agglutinins bind specifically to sugars (Renwrantz and Cheng, 1977).

Melanin may be important in immune recognition, besides acting as a barrier around foreign pathogens (Leonard et al., 1985). The

prophenoloxidase system, which is part of the biosynthetic pathway of melanin, requires the activation of phenoloxidase enzyme (Evans, 1968). Once activated, this enzyme, shown to be present in Blaberus sp. hemocytes, binds to foreign surfaces and may assist in opsonization (Leonard et al., 1985).

Finally, another process believed to be common to all three invertebrate immunological responses is that of cell movement. Chemotactic cell locomotion has been implied in phagocytosis, and was demonstrated in migration of plasmatocytes towards developing nodules (Ratcliffe and Gagen, 1977) and developing hemocyte capsules (Nappi and Stoffolano, 1972). Additional mechanisms of cell movement and shape change are involved in the latter stages of nodule and capsule formation (Gotz and Boman, 1984).

Resistance to cellular defense reactions

There are several possible outcomes of parasitic invasion of insects (Lackie, 1980). In non-susceptible hosts, the parasite is recognized, effectively encapsulated, and dies. In susceptible hosts, the parasite may not be recognized, in which case either death of the host occurs, or there is coexistence of host and parasite. In cases of immune recognition, the response may be ineffective and again, either death of the host or coexistence occurs.

There are several means by which parasites can influence or evade host immune reactions (Salt, 1968; Kitano, 1969; Lackie, 1980). Basically, these mechanisms can operate at either the coarse or fine adjustment phases of recognition or during subsequent events of the immune response. In the former, evasion of recognition may occur due to antigenic similarity between the parasite surface and host tissues, such as the case of the acanthocephalan Moniliformis sp. and its host Periplaneta sp. (Lackie and Lackie, 1979). Alternately, evasion of recognition may occur as the result of the parasite acquiring host molecules, or by secretion of non-immunoreactive substances on the surface of its eggs (Vinson and Scott, 1974; Salt, 1968).

Beyond a passive level of masking immune recognition, a more active role may be taken by the parasite in evading recognition. Since prophenoloxidase activation enhances the recognition of non-self (Ratcliffe et al., 1985), secretion of substances by the parasite that are capable of chelating cations may prevent opsonization or melanization (Brennan and Cheng, 1975). Cell surface alteration may also be a factor in interruption of immune recognition. Drosophila sp. hemocytes show a high affinity for the lectin wheat germ agglutinin under conditions which enhance encapsulation (Nappi and Silvers, 1984). Since low percentages of lectin-binding cells are found in Drosophila sp. susceptible to the parasitoid Leptopilina sp., these authors suggested that developing parasites alter the surface of blood cells of reactive hosts. This finding implies that parasites may be able to hinder recognition by cell-surface alteration.

The subsequent events of encapsulation, including chemotaxis, attachment, and flattening of cells to form a multilayered capsule (Ratcliffe and Rowley, 1979) may be inhibited by a number of means. Rizki (1962) proposed that hormonal imbalances can alter hemocyte transformations in Drosophila sp., and Nappi (1975) reported that juvenile hormone and ecdysteroid in Drosophila sp. may control encapsulation of the parasitoid Pseudocoila sp.. Since parasitoids have also been shown to affect hormone levels in host insects (Lawrence, 1986), parasite secretions could inhibit encapsulation by altering hormone levels in host insects. However, there is also evidence against this method of immune regulation. Encapsulation of Cardiochiles sp. by Heliothis sp. is not affected by juvenile hormone analogues or molting hormone (Lynn and Vinson, 1977), and no significant differences in endocrine activity occur between normal and nematode-infected Prosimulium sp. (Condon and Gordon, 1977).

Besides hormonal alterations, parasites may influence a variety of other physiological parameters which control encapsulation. Exhaustion of hemolymph nutrients (Cheung et al., 1978), inhibition of lymphokine-like factors (Chain and Anderson, 1983), and metabolic inhibition (Ratner and Vinson, 1983a) could affect plasmatocyte adhesiveness and movement. According to Ratcliffe et al. (1985), interference with chemotactic movements of hemocytes could represent a significant avoidance mechanism of parasites. The rate of movement of hemocytes is a good indicator of parasite interference with encapsulation (Lackie, 1980).

Experimental system

The insect pathogenic nematode, Steinernema feltiae (= Neoalectana carpocapsae Weiser) (G. Bedding, Pers. Comm.), is a well characterized parasite which has widely been used for biological control of insects (Poinar and Himsforth, 1967). Third stage infective juveniles are ingested by insects, and after exsheathment, they penetrate the gut wall and enter the hemocoel. The nematode transforms into an active feeding stage, molts twice to become an adult, and reproduces. The host, with a few exceptions, dies of a septicemia induced by gram negative, commensal bacteria Xenorhabdus nematophilus (Poinar and Thomas) comb. nov. (syn: Achromobacter nematophilus Poinar and Thomas) carried in the alimentary canal of the nematode. The nematode seems to play the role of vector for X. nematophilus, and the bacterium is believed to furnish nutrients for the nematode (Poinar, 1979).

More recently, Gotz et al. (1981) showed that the interaction between S. feltiae and X. nematophilus is a more sophisticated arrangement than previously thought. These authors indicated that nematodes assist the bacteria by excreting an immune inhibitor which selectively destroys insect antibacterial proteins. Although Seryczynska et al. (1974) reported that axenic S. feltiae cause changes in hemocyte numbers far more slowly than xenic S. feltiae, it has nevertheless been shown that axenic S. feltiae causes toxico-

genesis and mortality in Galleria mellonella larvae (Boemare et al., 1982).

The occurrence of toxicity and mortality in insects infected with axenic S. feltiae raises the question: how does S. feltiae overcome insect immune mechanisms? Encapsulation of nematodes, when it occurs, usually happens within 24 hours, and the first signs of hemocytic responses are present within minutes after invasion of the hemocoel (Ratcliffe and Rowley, 1979). Mortality of G. mellonella infected with S. feltiae usually does not occur before 5 days post infection, so toxicogenesis caused by S. feltiae cannot be immediate or extreme (Boemare et al., 1982). It is probable, therefore, that S. feltiae inhibits immune reactions of G. mellonella.

Inhibition of immunity by S. feltiae may occur at either, or both, the recognition/attachment phase, or during the subsequent phase of capsule formation. Recognition at the coarse adjustments stage could be avoided if the cuticle of S. feltiae is non-immunoreactive. Alternately, if initial, coarse recognition occurs, S. feltiae may disrupt elements of the fine adjustment phase. Finally, the subsequent events of capsule formation may be inhibited, preventing encapsulation even when initiated.

The object of my study is to analyze the effects of S. feltiae on the immune response of G. mellonella at both recognition and later stages of encapsulation. In Chapter 1, I present data from encapsulation and phagocytosis assays which are designed to determine the

effect of nematode secretions on recognition. In Chapter 2, results are presented on S. feltiae induced alterations in distribution of hemocyte surface-borne carbohydrates. In Chapter 3, the effects of S. feltiae on hemocyte spreading behaviour and locomotion are examined, and Chapter 4 deals with changes in hemocyte cytoskeleton which correlate with alterations in spreading and locomotion.

GENERAL MATERIALS AND METHODS

Insects and nematodes

Seventh instar larvae of the greater wax moth, Galleria mellonella L. (Insecta:Lepidoptera) were reared at 30°C on a standard synthetic diet.

All experiments were performed with the Breton strain of Steinernema feltiae (= Neoaplectana carpocapsae Weiser) (Nematoda: Rhabditida) obtained from Dr. H. Kaya (University of Southern Calif., Davis). In all experiments except those indicated, infective third stage (Dauer) juveniles were used. Xenic larvae with the commensal bacteria X. nematophilus were reared according to standard methods (Poinar, 1979). Briefly, wax moth larvae were infected either per os or per anus on moistened filter paper inoculated with dauer juveniles; mortality usually occurred within 36-48 hours, after which wax

moth cadavers were placed on White traps for collection of infective juveniles. Axenic S. feltiae were obtained by either of two methods. In the first method, a procedure described by Poinar (1979) was modified slightly. Wax moth larvae were infected with S. feltiae according to standard methods (Beck, 1960). At 4 days post-infection, mature gravid female nematodes were removed before oviposition, washed repeatedly in sterile balanced salt solution (BSS) (Lackie, 1980), and placed for 4hrs in an antibiotic solution (streptomycin 100mg/ml and kanamycin 20mg/ml) and then transferred to sterile microtitre wells (0.5mls, Falcon) filled with BSS and antibiotic. Oviposited eggs were collected, washed in fresh BSS/antibiotic for 30min, and centrifuged at 100g. The egg washing procedure was repeated twice more. Eggs were then transferred to agar plates with streptomycin and pieces of homogenized, autoclaved beef liver, and nematodes reared through one generation.

A second method (Boemare et al., 1982) involved isolating gravid female nematodes, collecting the eggs in sterile BSS, and washing eggs in sodium hypochlorite (10% w/v) for 30min, followed by repeated rinses in BSS/antibiotic. Newly hatched J1 nematodes were reared in the same manner as those nematodes collected by the previous method.

The method of Boemare et al. (1982) resulted in a relatively poor recovery rate of viable nematodes, probably because of the harsh conditions used. Axenicity of both methods was verified according to

two criteria: the absence of visible bacterial growth on agar/liver plates inoculated with nematode incubate; and by test injection of G. mellonella larvae. For the latter criteria, control larvae were injected with 15-20 axenic S. feltiae in sterile BSS. If mortality of larvae occurred before 86hrs post-infection (PI), cultures were considered contaminated (Boemare et al., 1982). Only the first generation of axenic nematodes were used to avoid accidental contamination, and development took about 18-20 days on agar/streptomycin/liver plates at 20°C. Consequently, axenic nematodes were re-cultured several times during the course of experiments.

Exsheathed J3 S. feltiae larvae were used in the video time-lapse experiments. Normally, dauer J3 S. feltiae exsheath within 1hr PI in G. mellonella (Poinar, 1979); however, dauer larvae did not exsheath in Grace's Insect Medium (GIM), and are effectively isolated within the 2nd stage cuticle. To obtain exsheathed, active larvae for incubation in vitro with hemocyte cultures, axenic S. feltiae were placed in a mixture of 1:1 BSS/hemolymph supernatant (obtained from control larvae) and incubated in sterile hanging drop preparations at 30°C. Exsheathed nematodes were then washed in sterile BSS and used in time-lapse experiments.

Injection and bleeding procedures

Before injection, all dauer nematode juveniles were washed for 30min in Hyamine 10-X (0.4% w/v) (Poinar, 1979) to insure surface

sterility, then washed repeatedly in sterile BSS. Injections were made with a 100ul Hamilton micro-syringe equipped with a 26gauge needle. Insect larvae were usually CO₂ narcotized, their ventral surface sterilized with 70% ethanol, and injections made by inserting the needle, beveled-edge up, through the second-right abdominal proleg, and gently pushing it into the third body segment anteriorly. Care was taken to not unduly damage internal body structures. The circular muscle band around each proleg usually sealed off the wound after withdrawal of the needle. If any hemolymph escaped from the wound, the larva was discarded. When two injections were performed on the same animal, the next lateral proleg was used.

Insects were bled in the following manner. Chilled (except where otherwise indicated), CO₂-narcotized larvae were surface sterilized with 70% ethanol. A drop of cold (4°C) GIM, saturated with phenylthiourea (PTU) to prevent melanization and clumping (Brewer and Vinson, 1971), was placed between the posterior pair of thoracic prolegs, and one of the prolegs was amputated. Hemolymph usually oozed into the drop of GIM and approximately 80ul of hemolymph was collected into sterile micro-capillary tubes. Hemolymph was then diluted into 0.5ml of GIM with PTU (4°C), and the mixture was gently agitated to insure mixing and to prevent coagulation of hemolymph protein.

Approximately 200ul of dilute hemolymph was placed on clean glass coverslips ringed with grease pencil, and incubated at room temperature in moist containers. Depending on the procedure, hemo-

lymph protein was then washed off with either BSS or GIM. Fixation was done with ice cold (-20°C) citrate/acetone at pH 6.2 (Sigma Chemical Co., St. Louis, Mi.) for 45sec. Fixative was washed away with 3 rinses of BSS, and the adherent cells were then processed according to experimental protocol.

Glassware

All glassware used for scanning electron microscopy and video time-lapse micrography was cleaned in the following manner. Coverslips were washed with FL-70 biodegradable cleaner, and rinsed thoroughly in distilled water. Coverlips were then cleaned in nitro-sulphuric acid for 30min, and washed several times, first in distilled water, then in double-distilled, deionized water. Rubber gaskets and other components of Sykes-Moore chambers were also washed in FL-70 cleaner, and thoroughly rinsed in distilled then deionized water.

Control, xenically- and axenically-derived serum

Cell-free hemolymph (serum) was collected in the following manner. Thirty G. mellonella larvae were injected with 10ul BSS, 10ul BSS with 15-20 xenic nematodes, or 10ul BSS with axenic nematodes. Larvae were incubated for 12hrs at 30°C , then CO_2 narcotized and chilled on ice. Using sterile technique, larvae were

quickly bled as before into GIM without PTU and collected with chilled micro-capillary tubes. Whole hemolymph was quickly diluted into cold (4°C) BSS and centrifuged at approximately 100g for 3min in chilled centrifuge tubes. The cell-free supernatant was then removed and passed through a millipore filter (0.22um pore size). Cell-free serum samples were then stored in Nunc tubes at -70°C. Protein concentration was determined by the Lowry method (Lowry et al., 1951).

Chapter 1: Phagocytosis and Encapsulation

INTRODUCTION

Humoral and/or cellular encapsulation is the primary response of insect hemocytes to most metazoan parasites such as nematodes (Poinar, 1974). Since it is unknown if the failure of G. mellonella hemocytes to encapsulate S. feltiae is due to non-recognition of the nematode cuticle, a simple assay was developed to determine if recognition occurs. Ultraviolet radiation (U.V.) has been shown to kill S. feltiae (Gaugler and Boush, 1979), yet not affect molecular determinants on the nematode cuticle. Comparison of the encapsulation response to live and U.V.-killed nematodes thus provides an experimental approach to determine the existence of nematode-derived factors which prevent encapsulation. Phagocytosis and encapsulation are fundamentally similar processes; both involve recognition of non-self and attachment of hemocytes and foreign surfaces (Lackie, 1980; Ratner and Vinson, 1983a; Cheng, 1983). In fact, the flattening of plasmatocytes (PL's) during encapsulation may represent unsuccessful attempts of these cells to engulf large objects (Nappi, 1975). Thus, presumably the ability of hemocytes to recognize and attach to particles is indicative of the ability of hemocytes to recognize and attach to larger objects such as nematodes, and a phagocytosis assay provides a measure of the effect of S. feltiae on immune recognition.

MATERIALS AND METHODS

Insects

Early 7th instar G. mellonella larvae, reared as previously described, were used in all experiments. Initial phagocytosis and encapsulation tests were conducted with larvae between 0.190-0.210g. For specific phagocytosis experiments, larvae (0.198-0.200g) in the same treatment group were selected from the same rearing container, and weighed. Only healthy, actively feeding larvae were used in these experiments, and were subjected to a minimum of handling.

Encapsulation experiments

To determine if G. mellonella hemocytes recognized and attached to S. feltiae, 15-20 U.V.-killed, axenic nematodes in 10ul sterile BSS were injected into 7th instar insect larvae. After incubation at 30°C for either 30min or 4hrs post-injection (PI_{nj}), chilled, CO₂ narcotized larvae were dissected in BSS saturated with PTU. Insects were examined with a dissecting microscope for evidence of encapsulated nematodes. When present, encapsulation was verified using a Zeiss Photo II microscope with Nomarski differential interference contrast optics.

The effects of active xenic or axenic nematode infections on encapsulation were examined by injecting 15-20 live nematodes then 15-20 U.V.-killed nematodes in 10ul sterile BSS, either simultaneously or at intervals 4, 8, or 12hrs post-infection (PI). The range of treatments are listed in Table I. Larvae were incubated at 30°C and, 4hrs PInj, were chilled, CO₂ narcotized, and dissected in BSS with PTU. The presence of encapsulated nematodes was verified as before, and in some instances encapsulated nematodes were routinely processed for future ultrastructural examination.

Phagocytosis experiments

In initial experiments, in vitro and in vivo assays of phagocytosis were attempted using 1.0um dia. fluorescently-labelled latex beads (Polysciences, Warrington, Pa.) and hemocytes of G. mellonella. Since phagocytosis did not occur in vitro, all assays were conducted using in vivo methods. As consistent results were difficult to obtain unless larvae were closely synchronized, data from initial phagocytosis assays were pooled, and total percentages of cells with beads were calculated; more specific assays were conducted with closely synchronized larvae after general trends had been established.

Six groups of 40 larvae each were used in the initial phagocytosis experiments. Group a) larvae were injected with 10ul

sterile BSS; larvae in groups b) and c) were injected with 15-20 xenic or axenic nematodes, respectively. Larvae in all groups were incubated for 1-8hrs PI, and at 1hr intervals, 5 larvae/group were CO₂ narcotized and injected with 5ul Fluoresbrite™ latex beads in BSS (0.25% latex w/v), and incubated for an additional 20min at 30°C. Larvae were then bled into GIM with PTU and hemocytes attached to glass coverslips were fixed as previously described. Larvae in group d) were injected with 10ul of control serum, and groups e) and f) larvae injected with 10ul of xenically- or axenically-derived serum, respectively, which was prepared as previously described. Larvae in groups d), e) and f) were treated similar to the previous larvae, as summarized in Fig. 12a-f.

On the basis of results from these experiments, a more specific analysis of the effects of nematode infection and serum injections was conducted as follows. Twenty larvae in 4 groups of 5 larvae each were each injected with either 15-20 (low dose) or 40-50 (medium dose) xenic or axenic nematodes in 20ul sterile BSS. Following incubation at 30°C for 8hrs PI, larvae were CO₂ narcotized, each injected with 5ul latex beads, and incubated at 30°C for 20min. Hemocytes were then collected as previously described.

To statistically assess the effects of nematode secretions in serum on phagocytosis, 30 larvae in 6 groups of 5 larvae each were each injected with 20ul of either control, xenically- or axenically-derived serum at low (0.1mg/ml), medium (1.0mg/ml), and high (10mg/ml)

concentrations of protein. Larvae were incubated for 1hr PI_{inj}, and injected with 5ul beads in BSS, and treated as before. Finally, the effect of boiled serum was examined with control and axenically-derived serum boiled for 15min; 5 larvae in both treatment groups were used, and the same procedures previously used were applied.

Analysis

Fixed hemocyte preparations on glass slides were stored in light-proof containers at 4°C with no apparent loss of fluorescence activity. A Zeiss Photo II microscope with phase contrast and epifluorescence optics was used to make random counts of hemocytes with and without latex beads. This was done by systematically scanning slide-mounted coverslips under phase contrast, selecting a field with hemocytes in it, then switching to fluorescence optics. Approximately 400-500 cells were counted from all 5 larvae in each group in the initial assay, while exactly 50 cells/larvae were counted in the specific assays, and the number of hemocytes containing low (1-3), medium (5-10), and high (10) numbers of beads/hemocyte was scored. Although no attempt to differentiate between PL's and GR's was made, possible differences between affinity for beads and relative number of PL's and GR's in each population were not important, as all hemocyte preparations made in these assays contained far more GR's than PL's. Differences between control and treatment groups in the

specific assay were analyzed statistically with Students t-test (Zar, 1974), and were considered significant when $p=0.05$. Preparations which showed non-specific binding of beads to the substrate, presumably because of adherent hemolymph protein, were discarded. To rule-out the possibility of electro-static binding of beads to the substrate, fixed coverslip preparations were incubated with latex beads in BSS; these controls were negative. Photographic records were made with Kodak Pan-X film (ISO 32) for Nomarski DIC micrographs, or with Kodak Tri-X film (ISO 400) for phase contrast and fluorescence micrographs.

RESULTS

Encapsulation

U.V.-killed, axenic nematodes were encapsulated in all instances. Hemocyte capsules were detected by 30min PI_{inj}, and did not initially cover the entire nematode (Fig. 1). Capsules appeared to have been initiated in a localized area on the nematode, and were comprised of several layers of cells interspersed with a dark, granular substance, presumably melanin, which was also present in areas on the cuticle of the nematode. The innermost cell layer of early capsules consisted of PL's and GR's as well as some cellular

Figures 1-5. Encapsulated nematodes at 30min and 4hrs PInj. Coverslip preparations of live cells in BSS. Nomarski DIC optics.

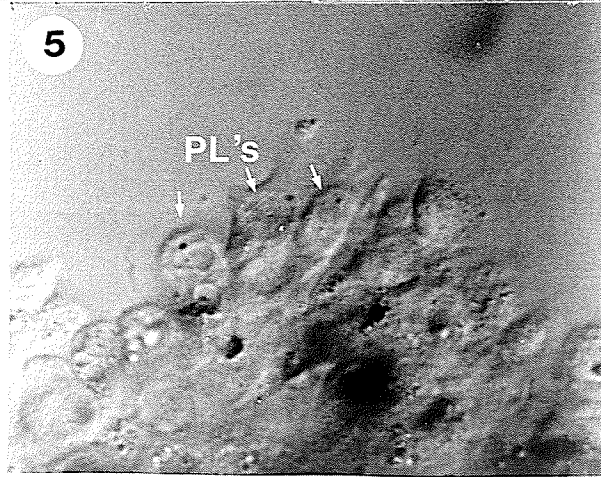
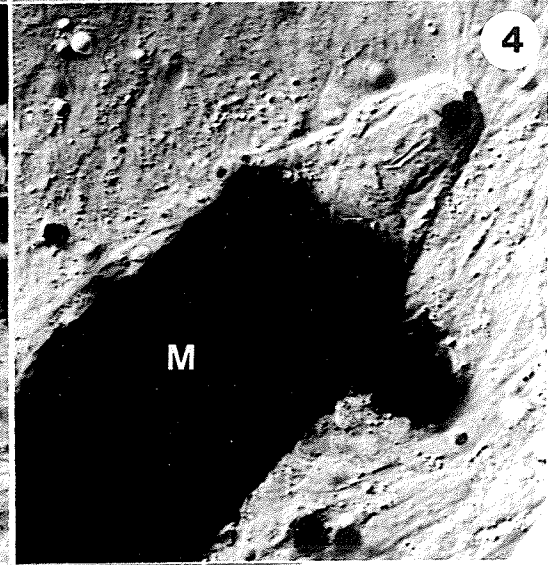
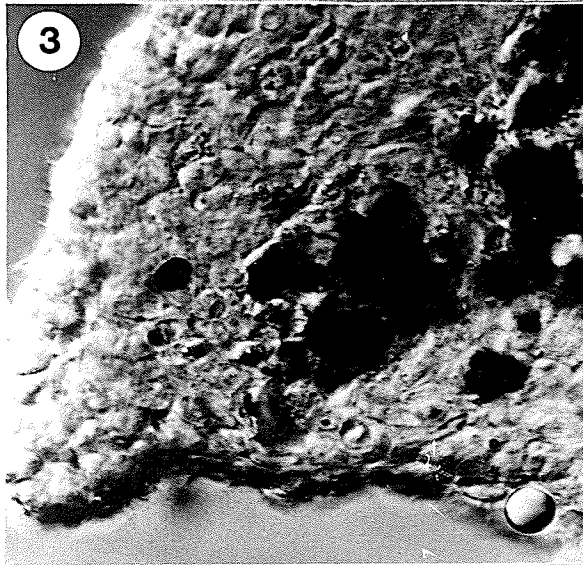
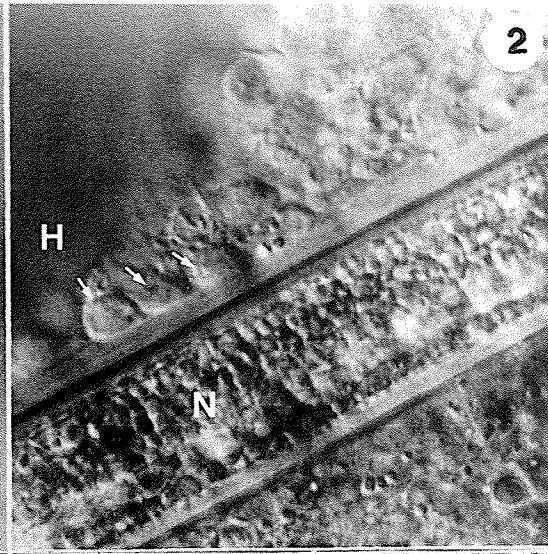
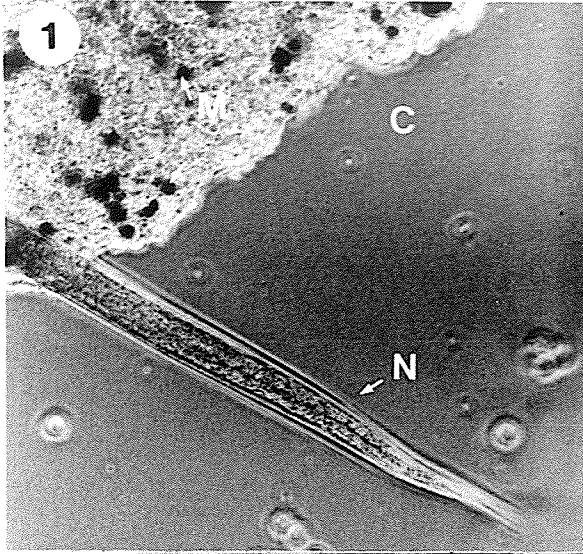
Figure 1. Hemocyte capsule (C) at 30min PInj. Nematode (N) is not completely encapsulated. Dark patches are melanin (M). x240.

Figure 2. Adherent hemocytes (H) on cuticle of nematode, 30min PInj. x700.

Figure 3. Portion of encapsulated nematode 4hrs PInj. x340.

Figure 4. Cephalic end of encapsulated nematode 4hrs PInj. Melanin covers most of nematode. x700.

Figure 5. Outer layer of cells of capsule 4hrs PInj. PL's adhering to coverslip were observed migrating towards capsule. x1,700.



debris, and isolated PL's could also be observed in the process of flattening on the cuticle (Fig. 2). After 4hrs PInj, multilayered capsules completely enveloping nematodes were found (Fig. 3). Extensive deposits of melanin on the nematode cuticle were evident and the innermost layer of cells consisted of flattened PL's (Fig. 4), while the outer layer PL's were more rounded (Fig. 5). The general morphology of hemocyte capsules around S. feltiae was consistent with other reports of nematode encapsulation (Ratcliffe and Rowley, 1979; Poinar et al., 1968).

Xenic nematodes were not encapsulated; however, xenic and U.V.-killed nematodes injected simultaneously usually elicited encapsulation reactions (Table I). Similarly, U.V.-killed nematodes injected 4 and 8hrs PI with xenic nematodes elicited encapsulation reactions. When U.V.-killed nematodes were injected 12hrs PI, however, encapsulation did not occur. Axenic nematodes also did not elicit encapsulation (Table I), only in rare instances was an encapsulated nematode was found. There was never more than one encapsulated nematode in such larvae, and the nematode was apparently dead. Presumably, these represented nematodes which were dead prior to injection, despite screening for viability. When U.V.-killed nematodes were injected either simultaneously with or at intervals up to 8hrs PInj of axenic nematodes, encapsulation usually occurred. By 12hrs PI with axenic nematodes, however, U.V.-killed nematodes apparently did not elicit encapsulation.

TABLE I. Hemocytic response to U.V.-killed nematodes injected into G. mellonella larvae simultaneously or at 4, 8, or 12hrs PI with xenic or axenic nematodes. Larvae were dissected 4hrs PIinj. (+) or (-) indicates whether or not encapsulation occurred.

Treatment	Encapsulation	Comments
Xenic	-	No capsules found; no evidence of melanization
Xenic + U.V.-killed	+	
Xenic + U.V.-killed (4hrs PI)	+	
Xenic + U.V.-killed (8hrs PI)	+/-	Capsules not found in all larvae
Xenic + U.V.-killed (12hrs PI)	-	
Axenic	-	No capsules found; no evidence of melanization
Axenic + U.V.-killed	+	
Axenic + U.V.-killed (4hrs PI)	+	
Axenic + U.V.-killed (8hrs PI)	+	Capsules usually present
Axenic + U.V.-killed (12hrs PI)	-	

Phagocytosis

Fluoresbrite TM latex beads were readily phagocytosed by GR's (Fig. 6a,b), and usually not by PL's (Fig. 7a,b). GR's often had beads at different focal planes within the same cell, indicating that the beads were internalized (Fig. 8a,b). Most GR's ingested less than 10 beads, although a few had markedly more (Fig. 9a,b), and level of phagocytosis varied according to treatment (Figs. 10a,b and 11a,b).

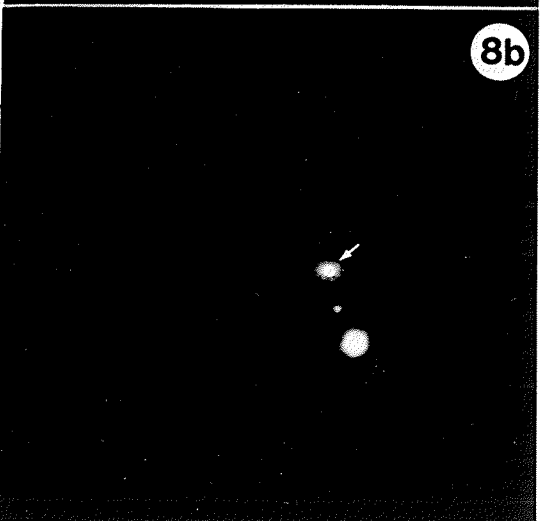
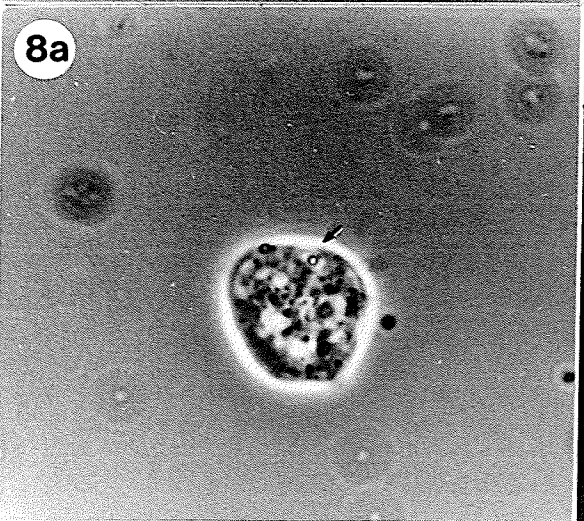
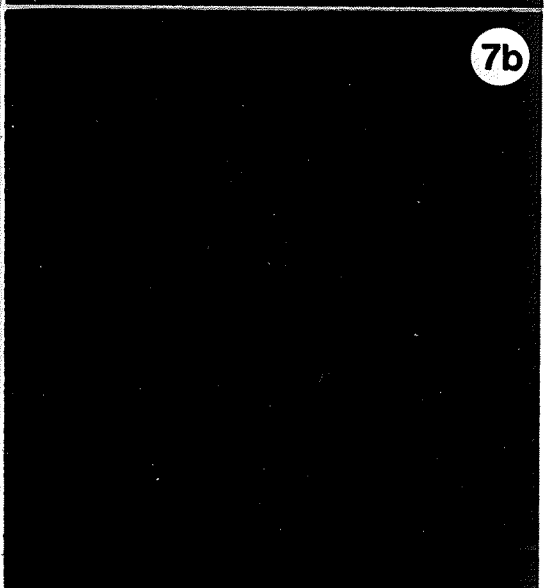
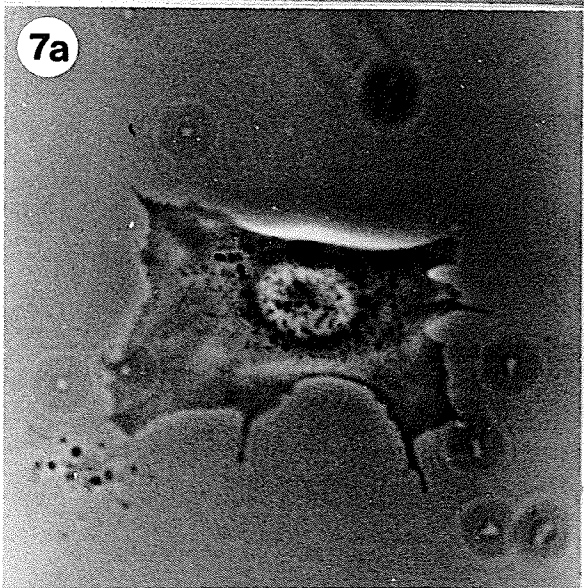
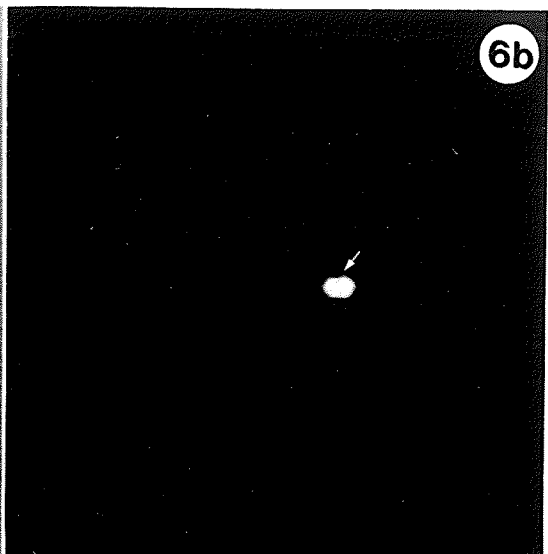
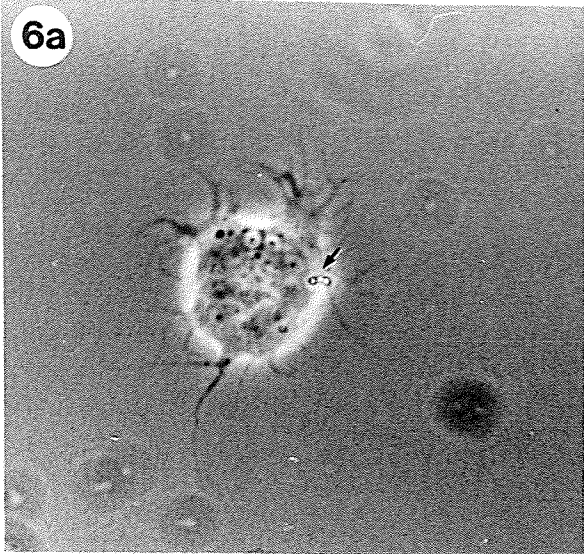
Initial phagocytosis experiments did not reveal any major differences between controls and nematode infected larvae during the first 7hrs PI (Fig. 12a,b,c). Xenic and axenic infections resulted in slightly higher levels of phagocytosis 1hr PI, but this could have been due to random variation. Variable, but relatively similar levels of phagocytosis were evident during the remaining interval until 8hrs PI, when definite decreases in phagocytosis occurred in xenic and axenic infections. This trend was reversed in serum-injected larvae (Fig. 12d,e,f). At 1hr PI, larvae injected with xenically- or axenically-derived serum exhibited definite decreases in phagocytosis compared to controls. Phagocytosis in xenically-derived and axenically-derived groups increased during the remaining interval PIinj; by 4hrs PIinj, rate of phagocytosis of the axenic group matched that of controls, and rate of phagocytosis of xenic groups matched controls by 5hrs PIinj. There were slight decreases in phagocytosis by 8hrs PIinj in both xenic and axenic groups, but not in controls. Most

Figures 6-8. Coverslip preparations of live hemocytes in BSS. Cells are from control insects injected with fluorescently-labelled latex beads. Phase contrast and corresponding epifluorescence micrographs show position of beads (arrows) x900.

Figure 6a,b. GR with 3 beads, all in same focal plane.

Figure 7a,b. PL typically showing no beads.

Figure 8a,b. GR with 3 beads. Some beads lie within the cell, as indicated in Fig. 8b by the diffraction pattern of beads in different focal planes.

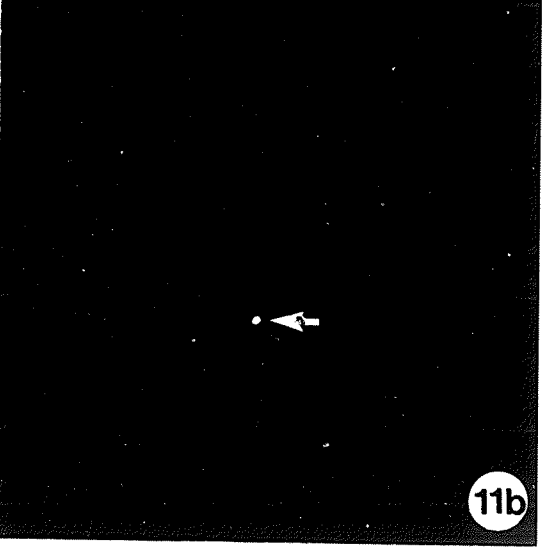
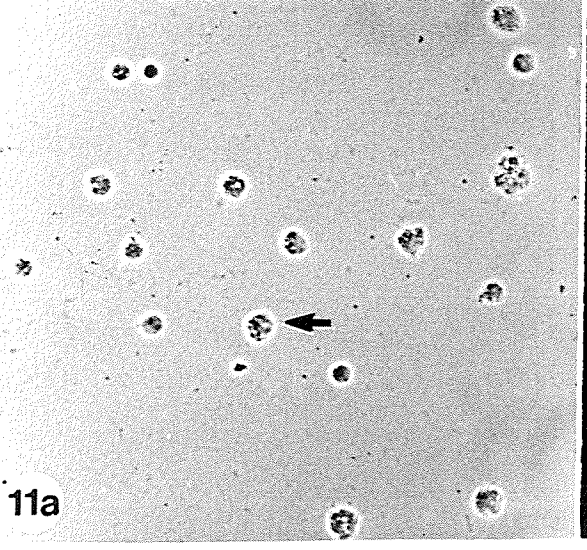
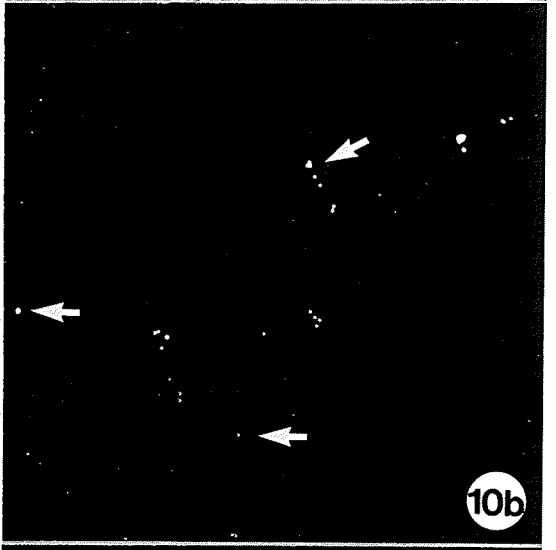
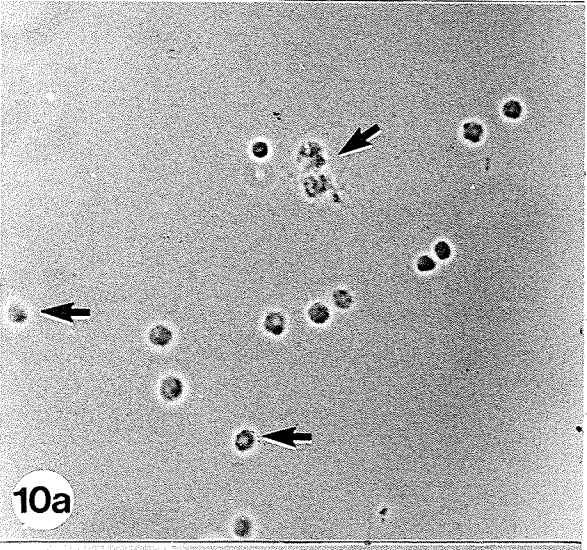
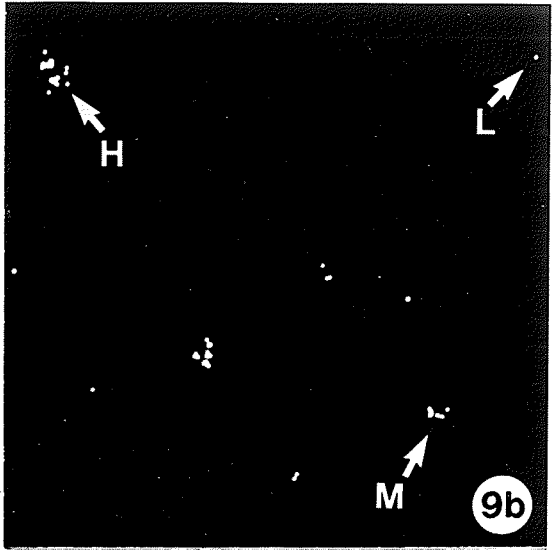
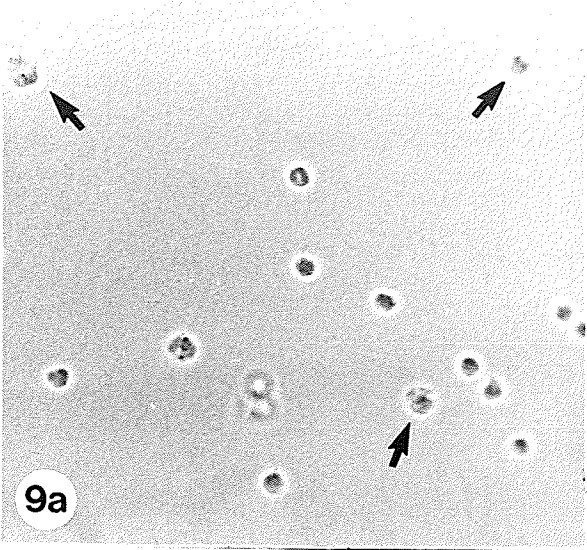


Figures 9-11. Coverslip preparations of fixed hemocytes from control and infected insects injected with fluorescently-labelled latex beads. Phase contrast and corresponding epifluorescence micrographs show number of cells with beads and number of beads/cell. x260.

Figure 9a,b. High (H), medium (M) and low (L) numbers of beads/cell in specific cells are indicated by arrows. Hemocytes are from a control larva.

Figure 10a,b. Hemocytes from axenically-infected larva 4hrs PI. There is no difference in number of cells with beads.

Figure 11a,b. Hemocytes from axenically-infected larva 8hrs PI. Note conspicuous absence of beads.



obvious differences between controls and nematode-infected larvae occurred at 8hrs PI, and those between controls and xenic or axenically-derived treatments occurred at 1hr PInj, therefore, specific phagocytosis assays were undertaken at those times to determine if differences were statistically significant.

Rate of phagocytosis by hemocytes of xenically- and axenically-infected larvae were significantly lower at 8hrs PI (Fig. 13). Phagocytosis in larvae infected with low numbers of xenic nematodes was significantly lower than that of low axenic infections. Infection with high numbers of either xenic or axenic nematodes resulted in significantly lower rate of phagocytosis than either of the low-nematode treatments. High axenic and xenic nematode treatments were not significantly different from each other. The relative proportion of hemocytes with high, medium, and low numbers of beads/cell was relatively constant.

The effects of control, xenically- and axenically-derived serum injections on phagocytosis are presented in Fig. 14. There were no significant differences between larvae injected with high, medium, and low concentrations of control hemolymph protein. Both xenic and axenic groups had significantly lower rates of phagocytosis than controls. The decrease in phagocytosis in both xenic and axenic groups was dose dependant, as high protein concentrations resulted in the lowest rates. Medium xenically-derived concentrations resulted in lower levels of phagocytosis than low concentrations, but this was not

Figure 12a-f. Percentage phagocytosis of beads in control and treatment groups 1-8hrs post-treatment. BSS-injected insects (Fig. 12a) were controls for insects injected with xenic and axenic nematodes (Figs. 12b and 12c, respectively). Insects injected with normal serum (Fig. 12d) were controls for insects injected with xenically- and axenically-derived serum (Figs. 12e and 12f, respectively).

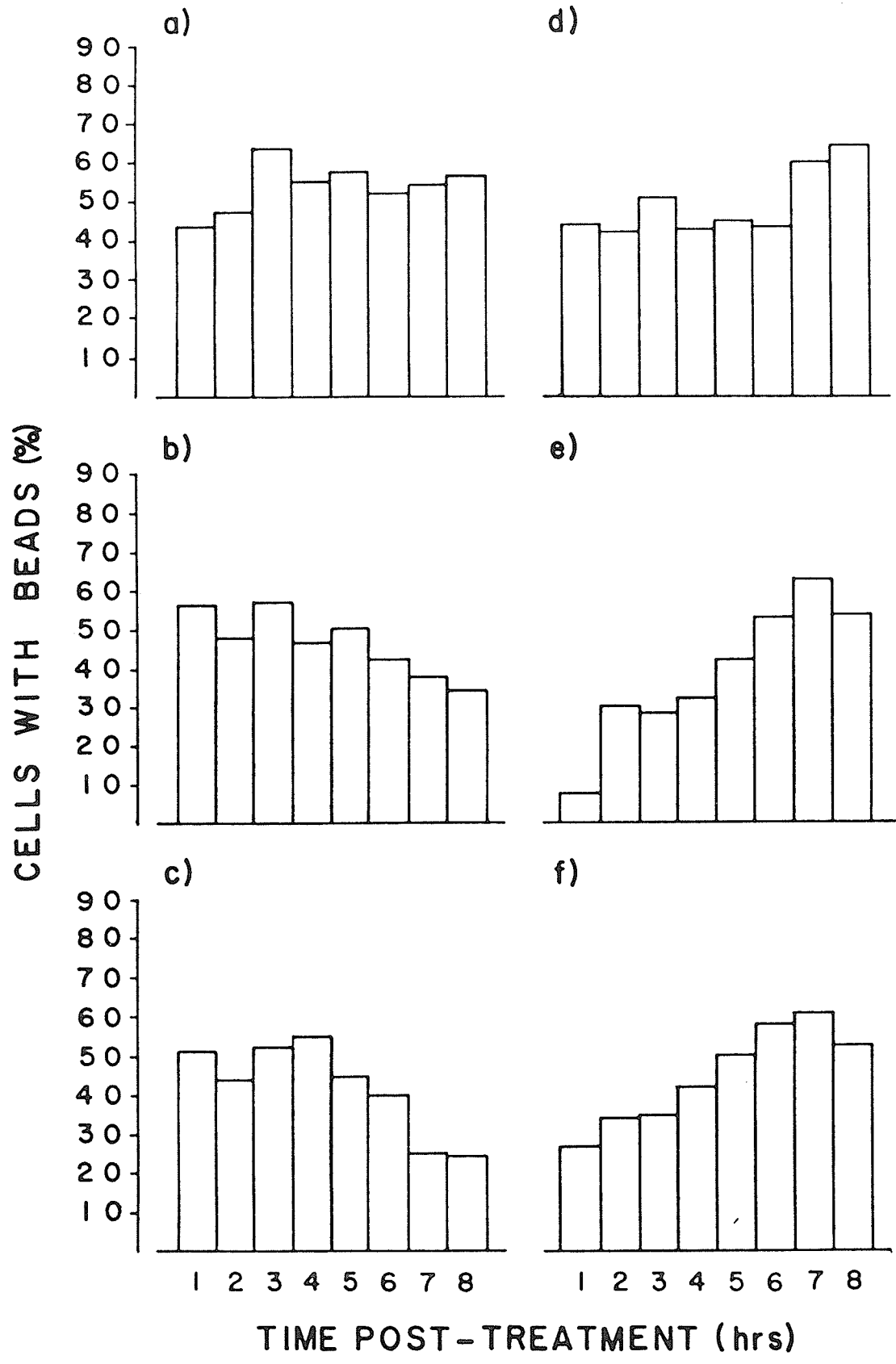


Figure 13. Average level of phagocytosis of beads by GR's from control (C), xenic- (X) and axenically- (A) infected larvae. Subscripts (L) and (H) indicate low (15-20) and medium (40-50) doses of nematodes, respectively. C indicates controls. There were 5 replicates/treatment, and 50 cells/replicate. Bars indicate standard error.

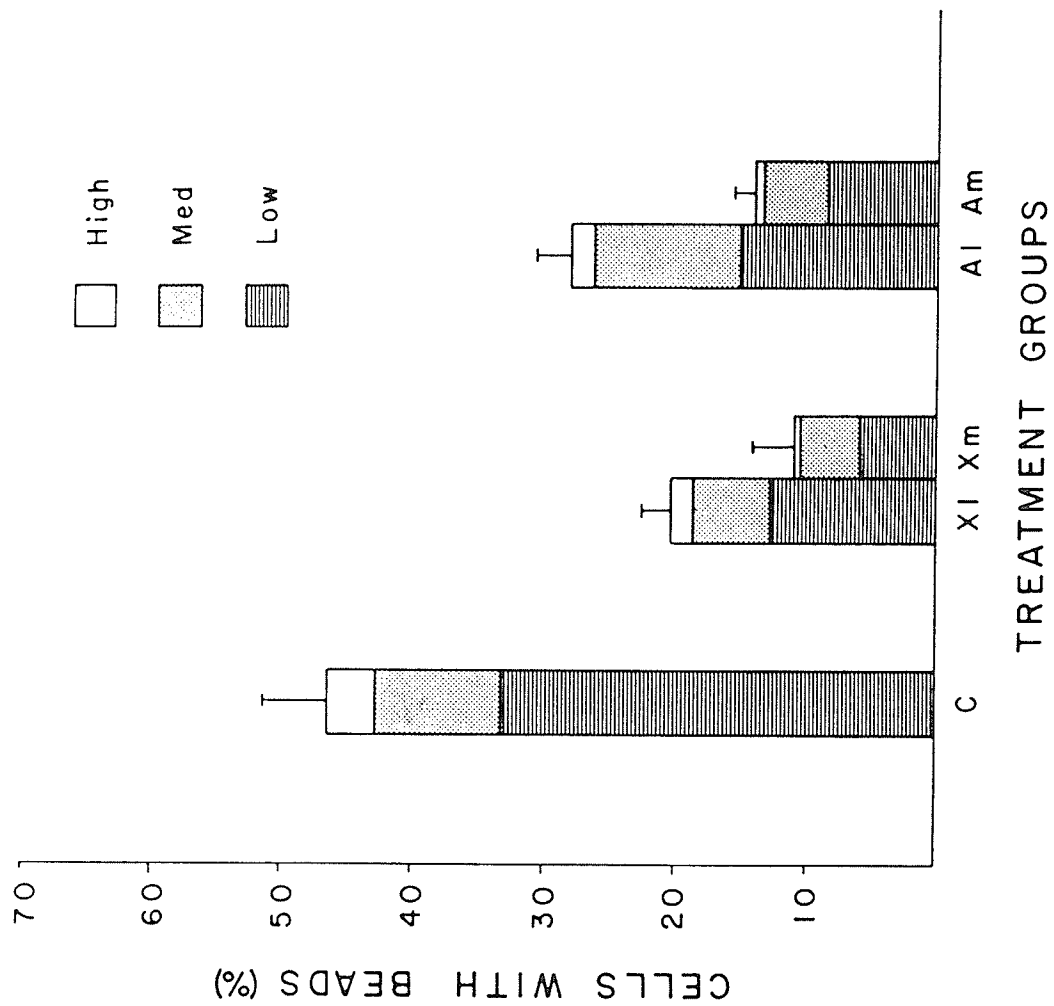
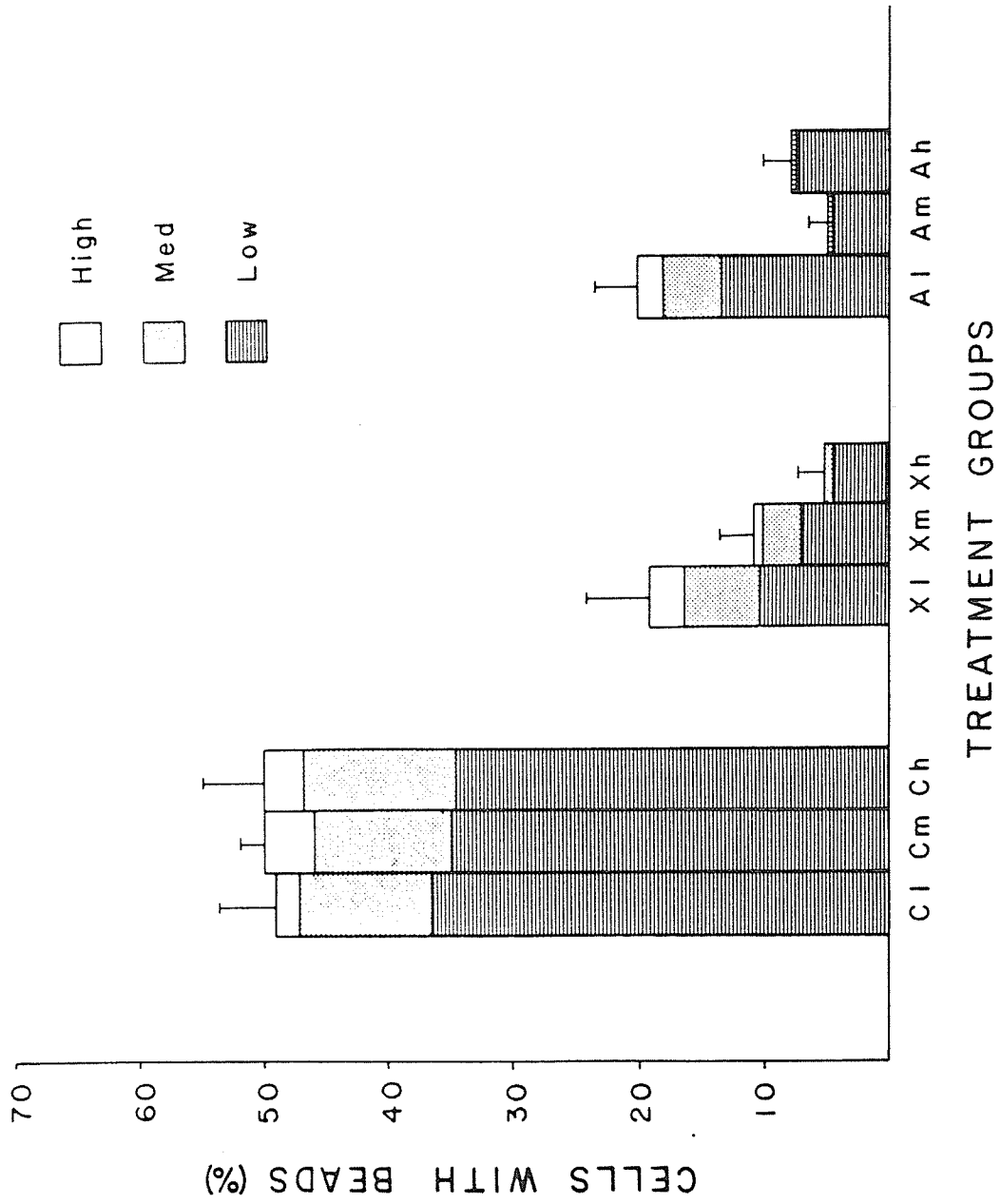


Figure 14. Average level of phagocytosis of beads by GR's from larvae injected with control (C), xenic- (X), and axenically- (A) derived serum. Subscripts (L), (M), and (H) indicate low (0.1mg/ml), medium (1.0mg/ml) and high (10.0mg/ml) concentrations of hemolymph protein, respectively. Subscripts preceded by C indicate corresponding controls. Bars indicate standard error.



significant; nor were differences between medium axenically-derived concentrations and low concentrations. Finally, the level of phagocytosis by hemocytes from larvae injected with boiled axenically-derived serum was not significantly less than controls (Fig. 15). Hemocytes from the former group did not take up high numbers of beads, but relative to the low percentage of hemocytes in controls which phagocytosed high numbers of beads, this was not significant.

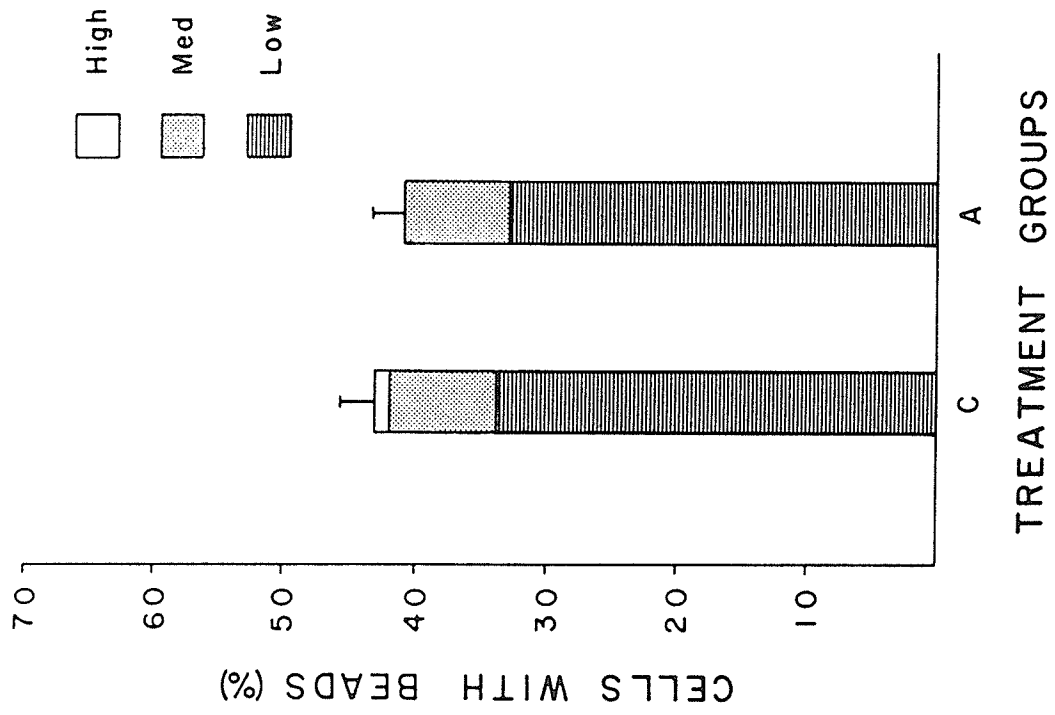
DISCUSSION

Encapsulation

Vinson (1977) proposed several methods by which parasites could avoid insect immune reactions, including acquisition of host hemolymph molecules and masking of recognition, or by possession of non-immunoreactive surfaces. I concluded from my research that S. feltiae cuticle is recognized as non-self by G. mellonella hemocytes, and that the nematode, at least passively, does not acquire masking molecules from the host hemolymph.

Live axenic and xenic nematodes did not prevent encapsulation of U.V.-killed nematodes up to and including 8hrs PI. This implied that live nematodes were themselves capable of evading encapsulation, but were not capable of preventing encapsulation of dead ones. This

Figure 15. Average level of phagocytosis of beads by GR's from larvae injected with boiled control (C) and axenically-derived serum. Bars indicate standard error.



was probably due to two conditions. Welch and Bronskill (1962) reported that S. feltiae were sometimes capable, through active movement, of escaping from capsules formed by Aedes aegypti. Live nematodes may also have been able to secrete factors which could have produced a local inhibition of encapsulation, but which were not in high enough concentration to extend to dead nematodes.

The latency of inhibition of encapsulation may have been due to insufficient concentration of nematode excretions within the hemolymph. By 12hrs PI, when encapsulation of dead nematodes did not occur, excretions had either accumulated within the insect at a level high enough to prevent encapsulation, or continued growth of nematodes was concomitant with an increase in excretory activity. The result was that live nematodes produced a sufficient quantity of factor(s) to prevent the encapsulation of U.V.-killed nematodes. This may have been due to inhibition of recognition, probably at Lackie's second tier of recognition (Lackie, 1980), or from inhibition of subsequent events during encapsulation.

Phagocytosis

Clearly, both xenic and axenic S. feltiae caused lower levels of phagocytosis. The significantly lower degree of phagocytosis in larvae infected with low numbers of S. feltiae than in axenic-infected larvae indicates that the commensal bacterium X. nematophilus,

directly or indirectly contributed to inhibition of phagocytosis. This may have been due to the pathogenicity of this bacterium (Lysenko and Weiser, 1974), or may be due to the dependence of S. feltiae on X. nematophilus for most of its nutritional requirements (Poinar, 1979). The effect of axenic nematodes, however, demonstrated that the nematodes alone can inhibit phagocytosis of latex beads by hemocytes.

It is unknown at what level the inhibition of phagocytosis occurred, and there are different phases during which it might have been interrupted. The first phase involves contact between a hemocyte and a foreign body, and this may be facilitated by unidirectional chemotaxis (Ratcliffe and Gagen, 1976). Inhibition of this phase might have reduced contact between cells and beads; however, it is commonly believed that most contact between hemocytes and foreign particles occurs randomly within the hemocoel (Salt, 1970; Gotz and Boman, 1985) and therefore, this was probably not a major cause of the decreased phagocytosis.

Second, and more likely, inhibition of recognition and/or attachment might have reduced phagocytosis. There is considerable information on the recognition of foreignness and attachment (Ratcliffe and Rowley, 1979; Lackie, 1980; Ratner and Vinson, 1983a), but precisely how these occur is unknown. If insect hemagglutinins are involved (Scott, 1972), destruction of these could have prevented opsonization and attachment of beads. Alternately, serum-independent recognition may be mediated by cell surface receptors (Anderson,

1976). Scott (1971) showed that phagocytosis by Periplaneta sp. hemocytes mainly depended on trypsin-labile surface receptors. More recently, cell-bound carbohydrates have been implicated (Parish, 1977; van der Knaap et al., 1983). Either destruction or rearrangement of these receptors might have resulted in non-recognition or attachment.

Since distribution of concanavalin-A receptors is altered by metabolic inhibitors (Yoshino et al., 1979), metabolic inhibition may also have interfered with recognition. Finally, cytochalasin-B-sensitive microfilaments are involved in cell movement and filopod formation (Anderson, 1976), and disruption of filopodia could also have interfered with phagocytosis, particularly during attachment.

Whatever the actual mechanism, the failure of axenic and xenic nematodes to produce detectable inhibitory effects prior to 8hrs PI could have been due to a relatively low concentration of excreted factor(s); reduced phagocytosis was likely manifested only when nematodes were producing a sufficient quantity of secretions, or when a sufficient concentration had accumulated. The dramatic decrease in phagocytosis which also occurred after injection of serum suggests that the inhibitory factor(s) were free in hemolymph. The effect of boiled serum indicated that the causative factors are heat labile, and may be a protein or peptide. Also, the factor was either unstable or are degraded by the insect, as the inhibitory effect of serum from parasitized insects was not obvious after 4hrs PInj.

The results of the phagocytosis experiments have implications in two areas. First, axenic S. feltiae secrete "immune inhibitors" which destroy antibacterial proteins in G. mellonella and Hyalophora cecropia (Gotz et al., 1981). The inhibitory effects of S. feltiae on phagocytosis suggests that the interaction between the nematode and the insect immune response is complex, and that the nematode secretions have wider-ranging effects. Second, while inhibition of phagocytosis does not definitively indicate an inhibition of encapsulation, it is implied that S. feltiae secretions can influence encapsulation, particularly during the recognition/attachment phase. This probably is not effective until later stages of infection.

In summary, recognition of S. feltiae does occur, and as the phagocytosis experiments indicate, S. feltiae secretions may inhibit recognition. S. feltiae possibly also affects later stages of encapsulation. Research in the subsequent chapters aims to: (1) determine if inhibition of recognition is reflected by alterations in cell surface binding sites; and (2) examine the effect of S. feltiae on hemocyte locomotion, spreading behaviour, and intracellular components involved in movement.

Chapter 2: Lectin Binding

INTRODUCTION

Carbohydrate moieties on the plasma membrane of insect hemocytes may play an important role in mediating recognition of 'non-self' and/or cell activation (Lackie, 1980; Parish, 1977). Alterations in the distribution of carbohydrates on the cell membrane may affect adhesion of hemocytes to parasites and to one another (Nappi and Silvers, 1984). Since the immune response of G. mellonella larvae to S. feltiae may be inhibited during either the recognition or later phases of cellular encapsulation, this may be reflected by alterations in the hemocyte surface membrane.

Lectins are known to interact with oligosaccharides on cell surface glycoproteins by binding to specific sugar molecules (Nicolson, 1974). Several different lectins bind to hemocytes of the Indian meal moth, Plodia sp. (Beeman et al., 1983), and wheat germ agglutinin (WGA) binds to hemocytes of Drosophila sp. (Nappi and Silvers, 1984). In the latter, changes in affinity to WGA correlate with immunosuppressive conditions. The results of a binding assay between G. mellonella hemocytes and three different fluorescein-conjugated lectins are presented in this chapter, and the effects of S. feltiae on hemocyte surface carbohydrate distribution are described.

MATERIALS AND METHODS

Treatment groups

Hemocytes from early 7th instar G. mellonella were used for the lectin-binding experiments. Three groups of fifteen larvae each were treated as follows: larvae in the first group received no treatment; larvae in the other two groups were routinely injected with either 10ul sterile BSS, or with 15-20 axenic S. feltiae in 10ul sterile BSS. The latter two groups were incubated for 4hrs PInj and PI, respectively, after which hemocytes were collected using standard techniques. Three 200ul samples of dilute, whole hemolymph from each larva were placed on separate glass coverslips and incubated for 20min at 25°C in moist, humid chambers. Each coverslip with adherent cells was then further processed for staining with one of the three lectins.

Lectin staining

Fluorescein-conjugated lectins were obtained from Vector labs (Mississauga, Ont.). These included concanavalin A (F-ConA), wheat germ agglutinin (F-WGA), and Dolichos biflorus agglutinin (F-DBA). The appropriate specific haptens were obtained from the Sigma Chemical Co. (St. Louis, Miss.). Concentrations of lectins and haptens are

given in Table I. The concentrations of haptens were derived by determining the minimum amount of hapten required to prevent binding.

Staining protocol was modified from Beeman et al. (1983). Briefly, coverslips were washed 3 times with BSS, and routinely fixed in cold (-20°C) citrate/acetone fixative. Following fixation, cells were rinsed with phosphate buffered saline (PBS) (pH 7.2) and incubated in PBS for 30min at 25°C. Cells were then incubated for 30min at 25°C in 25ul of each lectin in PBS. Controls were performed by incubating cell preparations in 25ul specific lectin/hapten complexes. After incubations, coverslips were washed 3 times for 5min each in PBS, and were mounted on slides in PBS/glycerol (4:1). Cells were located on a Zeiss Photo II microscope with phase contrast optics, then examined by epi-fluorescence microscopy. One hundred GR's on each coverslip were scored as either patched (2 or more discrete areas of fluorescence per cell) or non-patched (continuous staining pattern). Photomicrographs were made with Kodak Tri-X Pan film (ISO 400). Data was analyzed statistically with Students t-test (Zar, 1974) and considered significant at $p=0.05$.

TABLE I: Composition and concentrations of lectins and haptens; staining pattern of GR's and PL's.

<u>Lectin</u> (concentration)	<u>Hapten</u> (concentration)	<u>Hemocyte staining pattern</u> GR's	<u>PL's</u>
ConA (20ug/ml)	α -methyl-D-mannoside (6mM)	strong, continuous staining; a few cells with patches	Weak, non-specific staining; peri-nuclear granuales present
WGA (10ug/ml)	N-acetyl-D-glucosamine (20mM)	strong, continuous staining; a few cells with patches	Weak, non-specific staining; peri-nuclear granuales present
DBA (10ug/ml)	N-acetyl-D-galactosamine (20mM)	strong, continuous staining; a few cells with patches	Weak, non-specific staining; peri-nuclear granuales present

ConA = concanavalin A
WGA = wheat germ agglutinin
DBA = Dolichos biflorus agglutinin

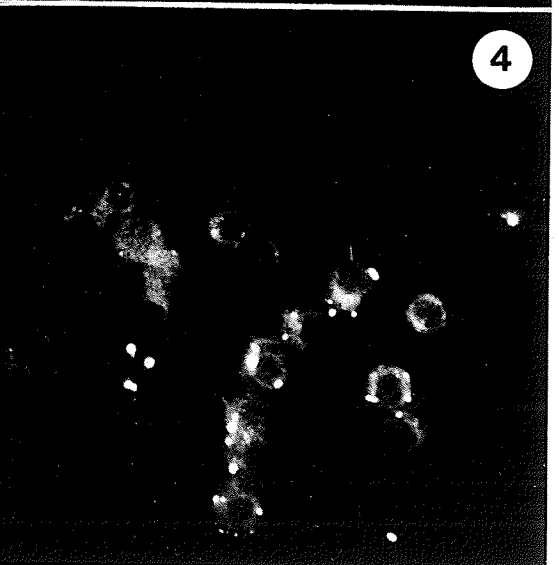
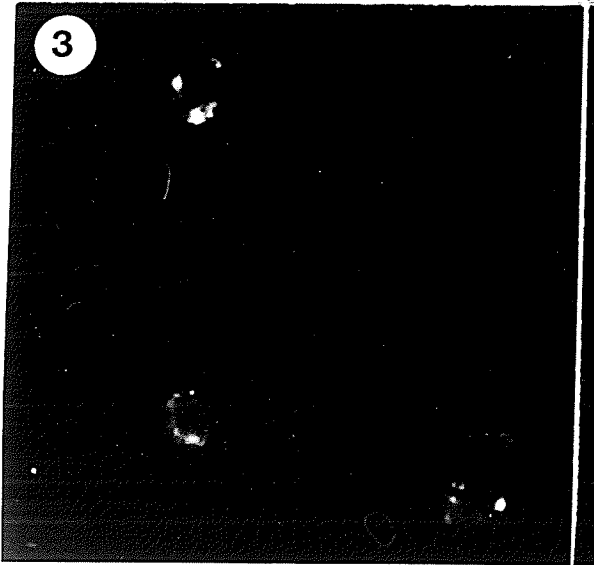
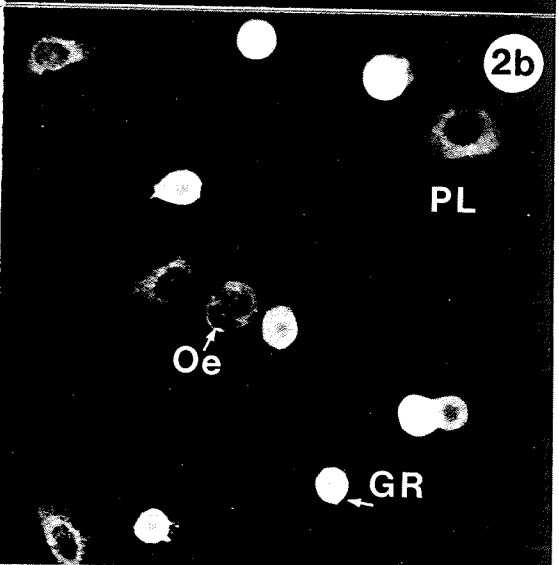
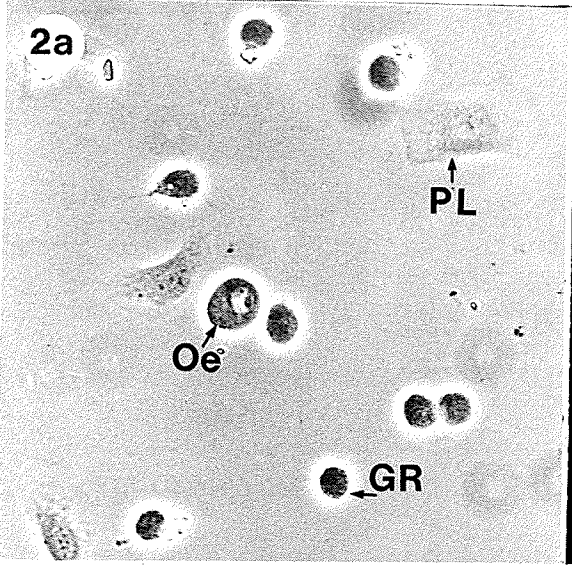
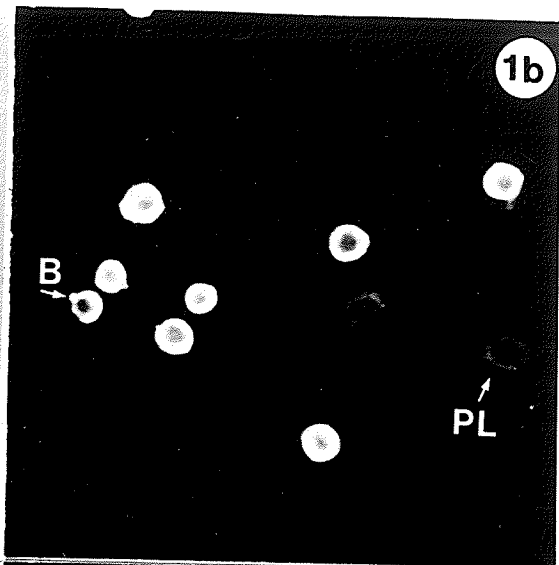
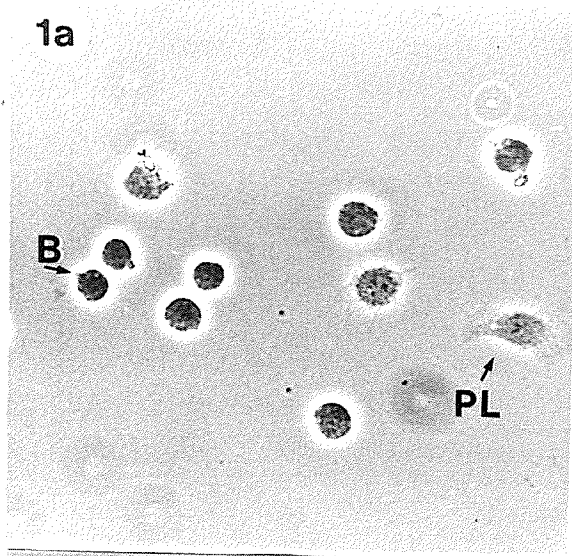
Figures 1-4. Fixed preparations of F-ConA and F-WGA stained hemocytes from control and experimental groups. Phase contrast and fluorescence optics x600.

Figure 1a,b. F-ConA stained hemocyte from control larvae; arrow indicates bleb (B) on GR. Note non-specific staining on GR.

Figure 2a,b. F-WGA stained hemocytes from control larvae. Note Oe, PL and GR.

Figure 3. F-ConA stained hemocytes from axenically-infected larvae.

Figure 4. F-WGA stained hemocytes from axenically-infected larvae.



RESULTS

Hemocytes from control and BSS-injected larvae

Virtually all GR's from control and BSS-injected larvae showed a strong positive fluorescence when stained with F-ConA (Fig. 1a,b). The pattern of fluorescence staining was continuous around the periphery of most GR's; areas of localized fluorescence or patching (Bourguignon and Bourguignon, 1984) were present on a small proportion of cells. Blebs, or spherical cell surface protrusions, also stained positively, while PL's showed poor specificity for F-ConA. Non-specific, background fluorescence was evident around the nucleus of most PL's, and a few small fluorescing granules were sometimes present. Results are summarized in Table I.

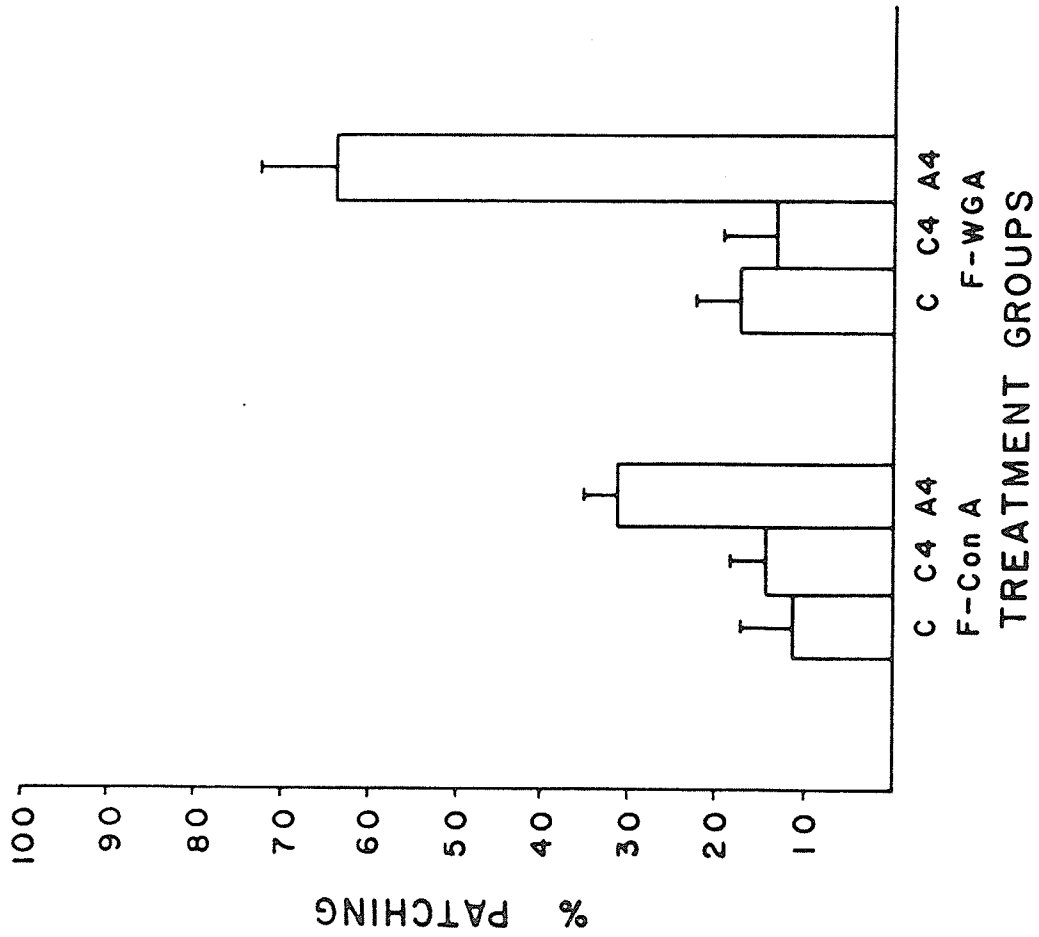
Hemocytes from control and BSS-injected larvae showed a similar specificity for F-WGA. GR's stained intensely and continuously around the cell periphery (Fig. 2a,b), and a few GR's had discrete patches. PL's, by contrast, stained non-specifically. The peripheral cytoplasm was devoid of fluorescence, and the perinuclear region stained diffusely and had a few fluorescing granules. F-DBA, however, did not bind specifically to either GR's or PL's, although the latter demonstrated a few fluorescent perinuclear granules.

Hemocytes from axenically-infected larvae

Specificity of PL's from axenically-infected larvae for either F-ConA or F-WGA was similar to that of previous groups. GR's, however, showed a marked increase in patching of receptors for both F-ConA and F-WGA (Figs. 3 and 4, respectively). The relative frequencies of patching on hemocytes from control, BSS-injected, and axenically-injected larvae are indicated in Fig. 5. Patching frequencies for F-ConA and F-WGA receptors on hemocytes from infected larvae were both significantly higher than in control or BSS-injected larvae. Furthermore, the patching frequency of F-WGA receptors was significantly greater than that of F-ConA receptors on hemocytes from infected larvae. Differences between hemocytes of control and BSS-injected larvae were not significant.

Aside from alterations in patching frequency, there were also morphological differences between F-ConA and F-WGA patches. F-ConA staining of GR's was distributed over the entire cell surface, whereas F-WGA stained GR's had smaller patches localized around the periphery of the cell. In addition, F-WGA stained GR's from infected larvae stained less intensely than GR's in the same treatment group stained with F-ConA. A greater proportion of GR's in infected larvae showed a low affinity for F-ConA and F-WGA than those in other groups, but this was not quantified.

Figure 5. Frequency of patching of ConA and WGA receptors on GR's from control (C), sham-injected (C4) and axenically-infected (Ax4) larvae. Five replicates/group and 100 cells/replicate were counted. Bars indicate standard error.



DISCUSSION

Based on the binding specificities of the lectins used in these experiments, GR's of G. mellonella have at least the following terminal carbohydrate moieties on the cell surface: N-acetyl-D-glucosamine (GlcNAc), -D-glucose (D-Glc), and/or -D-mannose (D-Man). In contrast to Plodia sp. hemocytes, these glycosyl components are usually distributed continuously over the surface of GR's, and normally only a small portion are patched. Aside from weakly-fluorescing granules in the perinuclear zone of PL's, GR's and PL's apparently lack accessible N-acetyl-D-galactosamine determinants. It is also possible that such components were present but were sterically hindered from binding (Kabat, 1976). The presence of GlcNAc on GR's is consistent with one of the roles of hemocytes; that is, hemocytes have functions during wound responses and cuticle repair (Wigglesworth, 1979), and GlcNAc is a precursor of chitin (Hughes, 1976).

The increase in patching on GR's was the result of nematode infection, and not wounding, as shown in Fig. 5. It is not known if patching resulted from activation of GR's during unsuccessful attempts at encapsulation, or if this is a manifestation of nematode secretions. The former is the most likely possibility, since Chain and Anderson (1981) have shown hemocyte activation by wounding, and the magnitude of this cellular response is probably greater than that of

encapsulation. In addition, Yoshino (1981) has shown that hemocytes from schistosome-susceptible gastropods show a higher frequency of F-ConA capping than resistant gastropods. A simple way to test this would be to inject U.V.-killed S. feltiae and examine lectin binding.

There are several models to account for patching and capping phenomena, involving either ligand-dependant or ligand-independant processes (Bourguignon and Bourguignon, 1984). There are also several ways in which nematode infections might have induced patching. For example, if patching was ligand-dependant, nematodes may have produced factors which bound multivalently to surface receptors, thereby causing aggregation of receptors. Alternatively, nematodes may have induced production of certain factors, such as hemagglutinins, which could have bound to surface receptors. Since this probably would have interfered with the binding of lectins to those same receptors, this is unlikely.

In ligand-independant processes, patching may have been induced by factors affecting transmembrane linkage between receptors and cytoskeletal elements. Membrane-microfilament associations are well known (Sundqvist and Ehrnst, 1976). Nematode-induced disruption of microfilaments may have caused patching, as Cytochalasin B and D induce capping in rabbit lymphocytes (Godman et al., 1980). However, the opposite effect occurs in mouse lymphocytes (De Groot, 1981). Alternately, nematode-impairment of the microtubular cytoskeleton may also have induced receptor redistribution since microtubule disrupting agents such as colchicine and vinblastin stimulate patching.

The formation of stable contacts between particles and the surface of mammalian phagocytes is believed to involve patching of relevant receptors (Silverstein et al., 1977). However, the decrease in phagocytosis and increase in patching observed in my study, are not necessarily related phenomena. As well, noticeable inhibition of phagocytosis occurred only at 8hrs PI, well after patching was noted. However, the main significance of receptor patching in PL's from infected animals is that nematodes do cause PL cell membrane alterations, and this has implications not only for mechanisms of non-self recognition (Ratner and Vinson, 1983b), but also for mechanisms of cell movement (Geiger, 1983) and cell-cell adhesion (Evans and Jones, 1974). These findings further indicate that the relationship between G. mellonella and S. feltiae is perhaps more complex than originally thought, and that S. feltiae induce alterations in hemocyte cell surface which may be related to cellular immunocompetency.

Chapter 3: Hemocyte Morphology and Motility

INTRODUCTION

Insect hemocytes mediate three main cellular immune responses: phagocytosis, nodule formation, and encapsulation (Ratcliffe and Rowley, 1979). The latter two responses, and possibly all three, are contingent on the ability of hemocytes to change shape (Gotz and Boman, 1985; Ratcliffe and Gagen, 1977) and to chemotactically migrate (Ratner and Vinson, 1983; Vey and Vago, 1971). Since the entomophagous nematode S. feltiae is able to circumvent or inhibit host immune mechanisms, analysis of the ultrastructure, spreading morphology, and locomotory behaviour of a primary component, the hemocyte, may provide new insights into the role of hemocytes in insect immunity.

Internal ultrastructure of hemocytes from normal, control, and nematode-infected wax moth larvae was examined by transmission electron microscopy (TEM). Spreading morphology of hemocytes from control and nematode-treated larvae was examined on a glass substrate by scanning electron microscopy (SEM). Since glass is not a natural substrate, spreading morphology of control hemocytes was also examined on basement membrane Matrigel TM, which is a more biological surface. As well, mode and rate of locomotion in vitro on a glass substrate was assessed using video time-lapse microscopy.

MATERIALS AND METHODS

Hemocyte preparation

Early seventh instar larvae of G. mellonella, reared as previously described, were used for all experiments. For TEM, hemocytes were bled from an amputated thoracic proleg directly into cold (4°C) modified Karnowsky's fixative in 0.1M sodium cacodylate buffer (pH 7.2) (Huebner and Anderson, 1972), and immediately centrifuged at 1000g for 1min. Hemocyte pellets were fixed for 1hr at 4°C, resuspended, centrifuged, and washed twice for 15min each at 4°C in 0.1M sodium cacodylate buffer, and postfixed in 1% osmium tetroxide at 4°C for 15min. Hemocyte pellets were rapidly dehydrated in a graded ethanol series (70, 80, 95, 100%) at -20°C, followed by four 30min changes in 100% ethanol at room temperature. Pellets were cleared in absolute ethanol/acetone (1:1) and acetone (15min ea.) and infiltrated overnight in a mixture of acetone and a final embedding medium of epon-araldite. Silver thin sections of embedded hemocyte pellets were cut with glass knives on a Reichert ultramicrotome, placed on 200 mesh copper grids, and stained in uranyl acetate and lead citrate (Reynolds, 1963). Sections were examined on A.E.I. 801 or 6B transmission electron microscopes operated at 60KV.

Hemocytes for SEM were collected with standard bleeding techniques. Hemocytes were allowed to settle for 2, 5, and 20min at

22°C on either glass coverslips or coverslips coated with a thin layer of BMM. BMM was obtained from Collaborative Research, Inc., and contained laminin, collagen type IV, heparin sulfate proteoglycan, and entactin. Hemocytes attached to coverslips were gently washed with BSS, and fixed in a drop of modified Karnovsky's fixative for 30min. Coverslips were then washed in 0.1M sodium cacodylate buffer (pH 7.2), and adherent cells were post-fixed in osmium tetroxide as described above. Cells were washed twice in buffer, dehydrated through a graded series of cold (-20°C) ethanol, and cleared as described above. Coverslips were then critical point dried in a Sorval critical point drier using acetone as the final solvent, mounted on stubs, and gold coated in a Balzer sputter coater. Stubs were examined in a Cambridge Stereoscan EM at a tilt angle of 20°. Photomicrographs were taken on Pan-X (ISO 32) 35mm film.

Video microscopy

Hemocytes observed during video time-lapse microscopy were routinely collected from surface-sterilized G. mellonella larvae. All procedures were conducted in a laminar air-flow bench under aseptic conditions. Eighty μ l of hemolymph from each larva were diluted into 0.5mls of cold GIM (4°C) with PTU. Care was taken to insure adequate mixing of hemolymph, and the dilute hemolymph (200 μ l) was immediately transferred onto a round coverslip that formed the

upper surface of a Sykes-Moore culture chamber (Sykes et al., 1959). Cells settled for 5min at room temperature (22°C), after which the coverslip was assembled into a culture chamber. This was filled with 2.3mls of GIM (22°C) without PTU, and gently flushed with an additional 1ml of GIM. Care was taken not to exert pressure during filling and flushing. Time-lapse videorecording was begun at 10min after initial bleeding, and time in culture from that point on was referred to as elapsed time (ET).

Sykes-Moore chambers with a vertical working distance of 2.5mm (kindly supplied by Dr. S. Caveney, Dept. of Zoology, University of Western Ontario) were used for observation of hemocyte cultures with a Zeiss Photo II microscope equipped with Nomarski differential interference contrast optics. Filming was done using a 40X planapo oil immersion objective lens (N.A.=1.0) and a 1.25 optivar. The video-recording system consisted of a Dage-M.T.I. series 68 MKII camera with a 1" Newvicon tube, a Panasonic model WJ-810 time/date generator and a 3/4" Sony TVO-9000 time-lapse VCR. Live or taped images were viewed on an Electrohome model EYM-1719 16" B/W monitor. Time-lapse video recording was done on 48hr time-lapse over 4hrs ET with one field recorded every 0.67sec. Playback was at normal speed, and observations were made at 0min ET and every 15min till 4hrs ET.

During the initial 15min ET, PL's migrating away from cell clusters (exomigrating) were used for measurements; thereafter, both contact-free and exomigrating cells were observed in approximately

equal numbers. PL's from hemocyte clusters larger than 50um dia. were not examined, nor were PL's from clusters which appeared to be densely packed. The centre of the nucleus of each cell being tracked was marked on a clear acetate sheet overlain directly onto the video monitor. The distance between the center of the nucleus of the same cell at successive 15min intervals ET was converted to the actual field-distance in um travelled by each hemocyte. The same PL was usually observed for a maximum of 1hr ET, after which it usually wandered out of the field and new hemocytes wandered into it.

Measurements were not made on hemocytes that remained in the same position and showed no lamellar extension during the entire recording period; this was to insure that the number of non-motile cells in each culture did not bias results, and to prevent the measurement of GR's, which are non-motile, mistakenly identified as PL's. Numbers of non-motile cells were not counted as this could not be accurately assessed. At least 5 time-lapse recordings of different hemocyte cultures were used for each treatment group, and between 40-50 PL's were observed over each 15min interval ET in each group. One-way analysis of variance was used to determine significance ($p=0.05$) (Zar, 1974) between control and experimental groups at 1, 2, 3 and 4hrs ET.

Geometric distortion of video images can result from camera tubes and from curvature of video monitor screens (Inoue, 1986). To test the degree of possible geometric error in our system, an image of

a micrometer slide was recorded at the same magnification that time-lapse observations were made at, and the interval between 10um markings was measured at various positions on the video screen. Intervals only varied between 1.3 to 1.4cm in width, so geometric distortion was not a source of significant error.

Treatment groups

For TEM, hemocytes from normal (uninjected), sham-injected (10ul sterile BSS), and xenic nematode-infected (15-20 nematodes in 10ul sterile BSS) larvae were used. Hemocytes from the latter two groups were collected 4hrs post-treatment.

Hemocytes examined by SEM were collected from sham-injected larvae, and larvae infected 4hrs previously with 15-20 xenic or axenic in 10ul sterile BSS (XPI4 and AxPI4, respectively).

Several different treatment groups were used for video time-lapse microscopy. Hemocytes from larvae sham-injected 4hrs previously constituted the control group, and experimental groups included hemocytes from larvae injected 4 or 12hrs previously with a standard dose of xenic (XPI4 and XPI12, respectively) or axenic (AxPI4 and AxPI12, respectively) nematodes. Other experimental groups included hemocytes from untreated larvae and either exsheathed xenic or axenic nematodes incubated in the culture chamber during time-lapse recording (XNiC and AxNiC, respectively.)

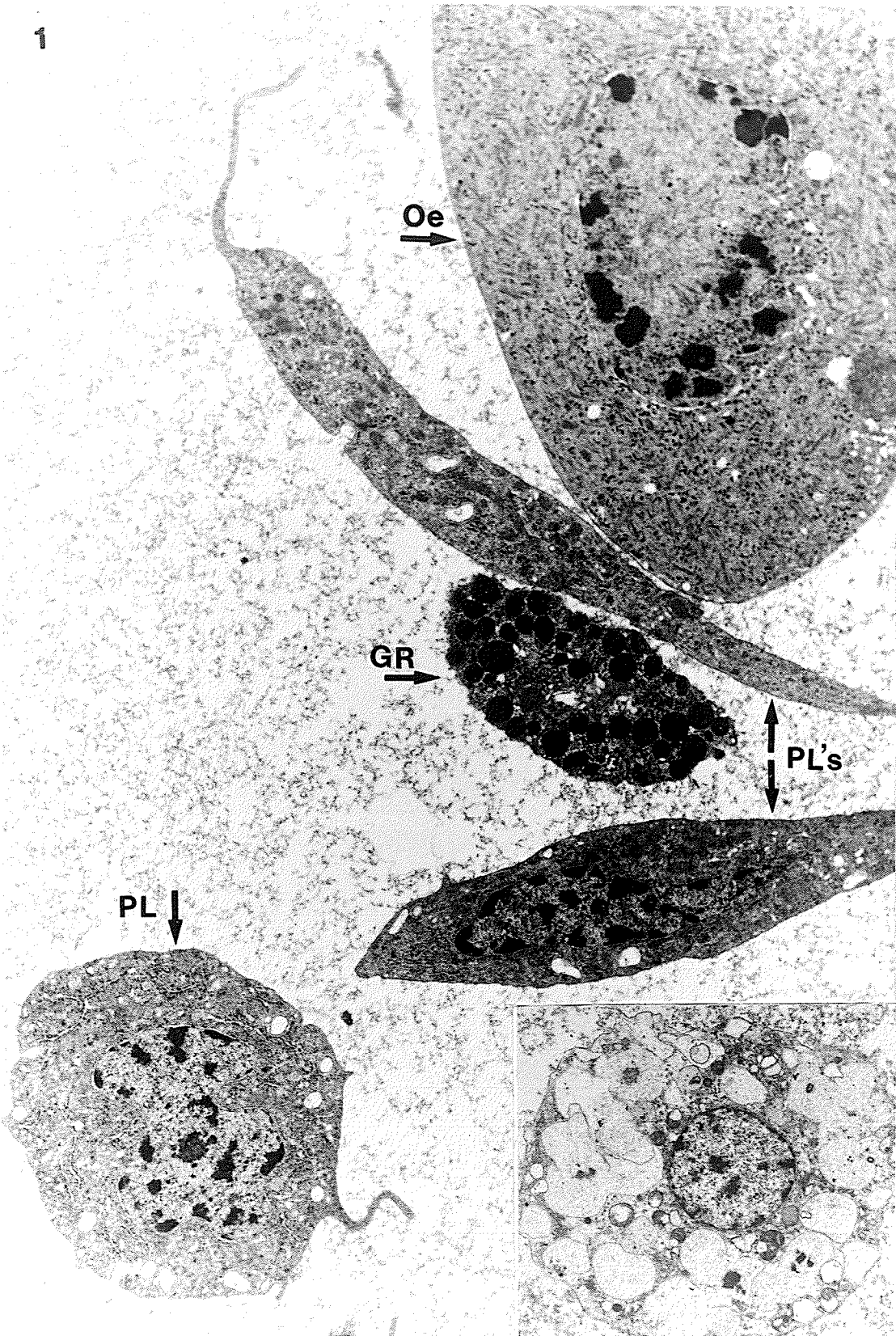
RESULTS

Internal Ultrastructure

Normal hemocytes observed by TEM exhibited basic morphologies similar to those described by Neuwirth (1973). Four hemocyte types were present in pellet preparations: oenocytoides (Oe's); spherulocytes (SP's); GR's; and PL's. Oe's were large and oval in shape, with a non-extending periphery (Fig. 1). There were few membranous cytoplasmic organelles, although numerous free ribosomes, vacuoles, and microtubules were present. The nucleus was roughly spherical and centrally located, and microtubules were evident in the nucleoplasm. SP's, by contrast, were smaller and distinguished by numerous large cytoplasmic spherules which contained a homogeneous granular material (inset). SP's were often ruptured, and the contents of spherules were externalized. The nucleus of SP's was usually small and eccentric. GR's were spherical to oval, and contained numerous cytoplasmic inclusions; among these were granules which appeared to be packed with a regularly arrayed fibrous material (Fig. 1). The cell membrane of GR's frequently had filopodial extensions and clathrin-coated pits (Fig. 2). The fourth major cell type, PL's, were the most numerous, and were either spindle-shaped or round (Fig. 1). Mitochondria, RER, golgi, free ribosomes and numerous cytoplasmic vacuoles were present.

Figure 1. TEM of principle hemocyte types: oenocytoide (Oe), plasmacytes (PL's), granulocyte (GR), and spherulocyte (inset). x6,300 (inset x7,200).

1



The cell membrane typically showed numerous infoldings and filopodial extensions, as well as round, outward bulges or "blebs" (Ratcliffe and Rowley, 1979). The nucleus was usually irregular in shape (Fig. 1).

Hemocytes from both sham-injected and nematode-injected larvae were not markedly different from normal hemocytes, with the exception of GR's. Most GR's from treated larvae indicated obvious, distended RER (Fig. 3). As well, numerous multi-vesicular bodies (MVB's) were evident in many GR's (Fig. 4), and these were similar to the MVB's described by Ratcliffe and Rowley (1979). Bacteria, such as X. nematophilus, were not seen in cytoplasmic inclusions of either PL's or GR's of nematode-infected larvae.

Normal Morphology of Spreading GR's

Glass substrate

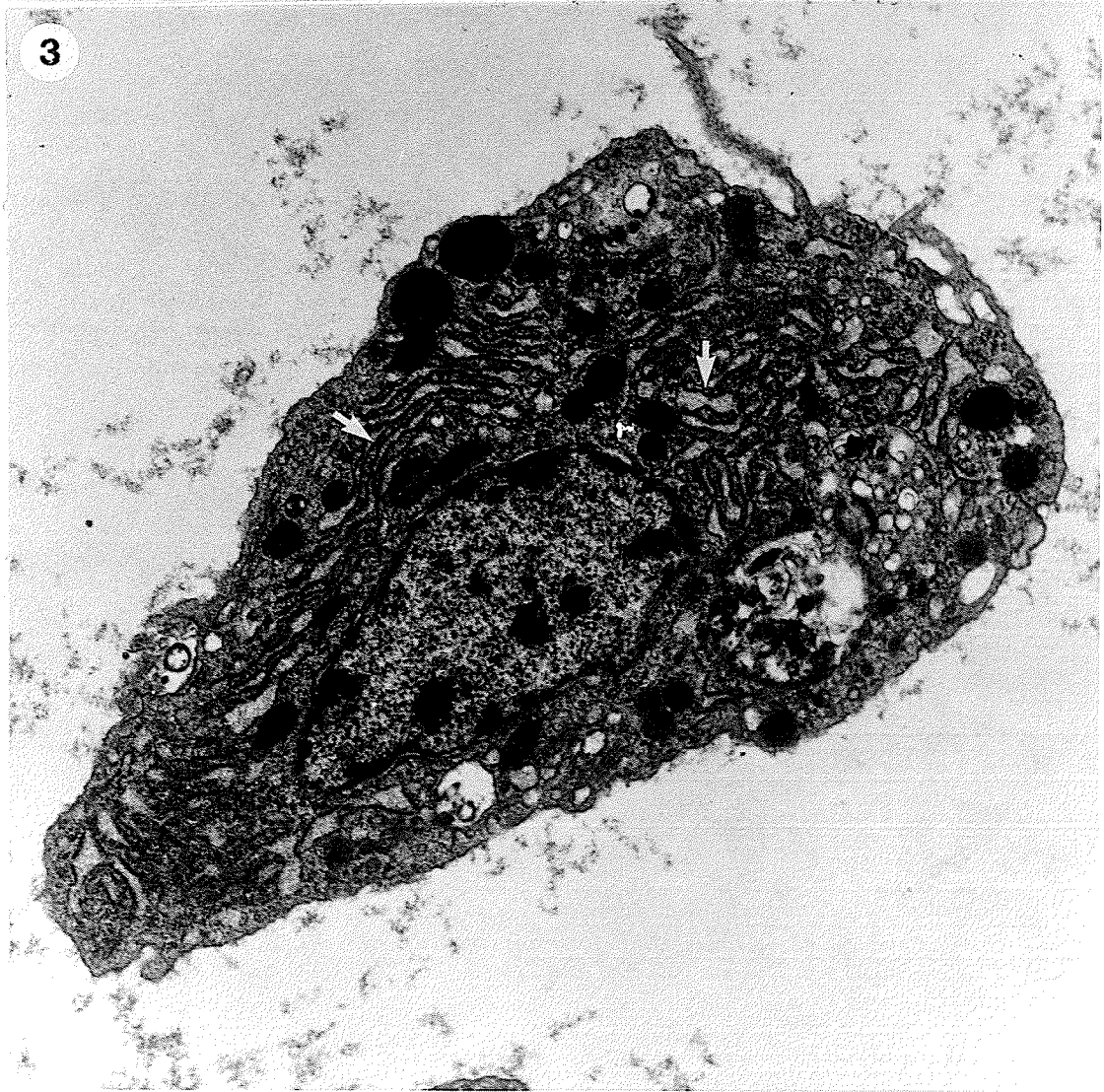
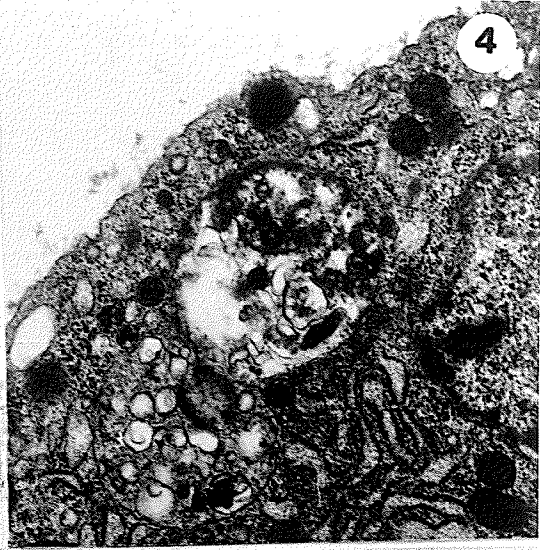
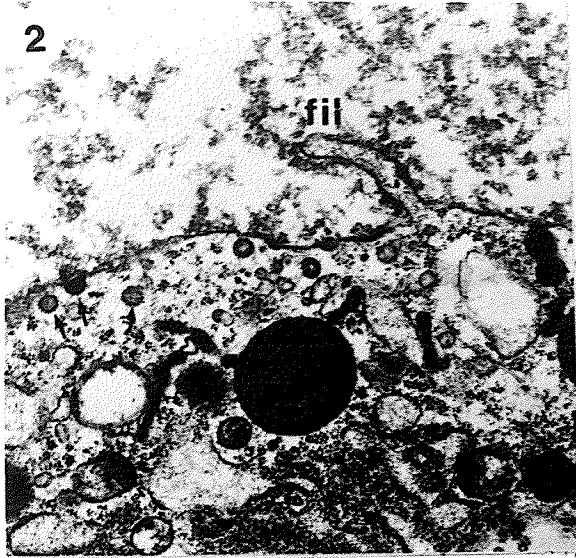
After 2min incubation in GIM, GR's on glass substrates were rounded, with only a few short processes attaching the cell to the surface (Fig. 5). These were similar to the attachment micro-extensions described on human MRC-5 cells (Witkowski and Brighton, 1972), and numerous, minute surface projections (presumably forming filopodia) were also present on the visible surface of these GR's, while others had developed filopodia (Fig. 6). Numerous filopodia

Figures 2-4. TEM's of hemocytes from control and xenically-infected larvae.

Figure 2. GR from control larvae showing a filopodium (fil) and coated pits (arrows). x22,500.

Figure 3. GR from control larvae showing distended RER (arrows) and numerous cytoplasmic inclusions. x17,300.

Figure 4. Higher magnification of Fig. 3 showing MVB. x21,650.



were present on most GR's after incubation for 5min or more (Fig. 7), and these varied somewhat in morphology (Fig. 8). The two main types of filopodia were: long, slender cytoplasmic extensions (type I); and short, flat processes (type II), which were fewer in number (Fig. 9). Type I filopodia usually terminated distally in bulbous vesicles at or near the tip, while type II filopodia terminated variably. After 20min incubation, most GR's had extensive arrays of filopodia, and the central mass of these cells was flattened (Fig. 10). Type I filopodia often extended a distance equal to the diameter of the cell.

BMM substrate

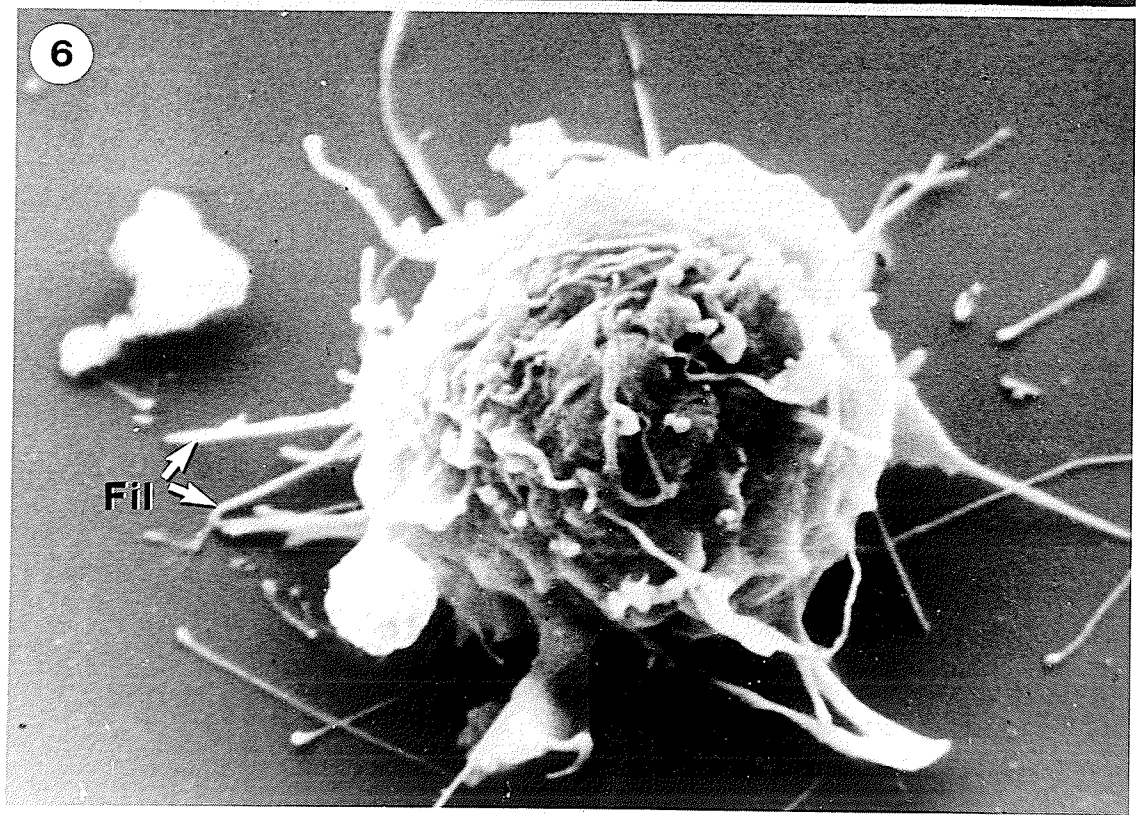
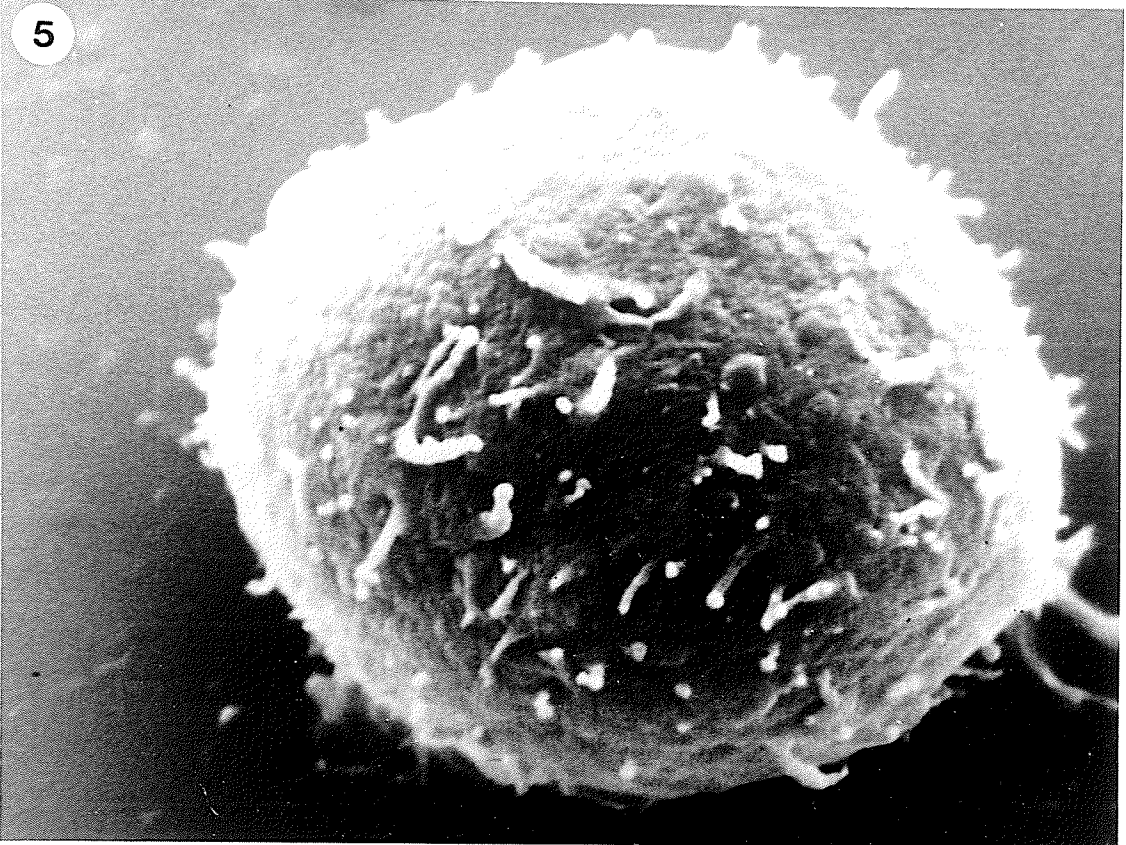
Initially, early stages of GR spreading on BMM differed only slightly from those spreading on glass (Fig. 11). However, after 20min incubation, most GR's differed in several respects: there were fewer type I filopodia, rarely any type II filopodia, and less flattening of GR's attached to BMM (Fig. 12); the surface of such cells showed intense rippling and numerous small projections.

Normal Morphology of Spreading PL's

PL's often appeared spindle-shaped, with a rounded central mass and small, flat cytoplasmic extensions at the sites of cell attachment after 2min incubation (Fig. 13) and these constituted early spreading

Figure 5. SEM of normal GR after 2min incubation on glass substrate. Note short, numerous filopodia. x9,500.

Figure 6. SEM of normal GR after 2min incubation on glass. Filopodia (fil) are longer and cell surface is more folded. x7,700.



Figures 7-9. SEM of normal GR's on glass substrate.

Figure 7. GR after 5min incubation. x7,600.

Figure 8. GR after 5min incubation. Types I (1) and II (2) filopodia are present. x5,300.

Figure 9. Higher magnification of types I and II filopodia. Note distal termination (arrow). x10,600.

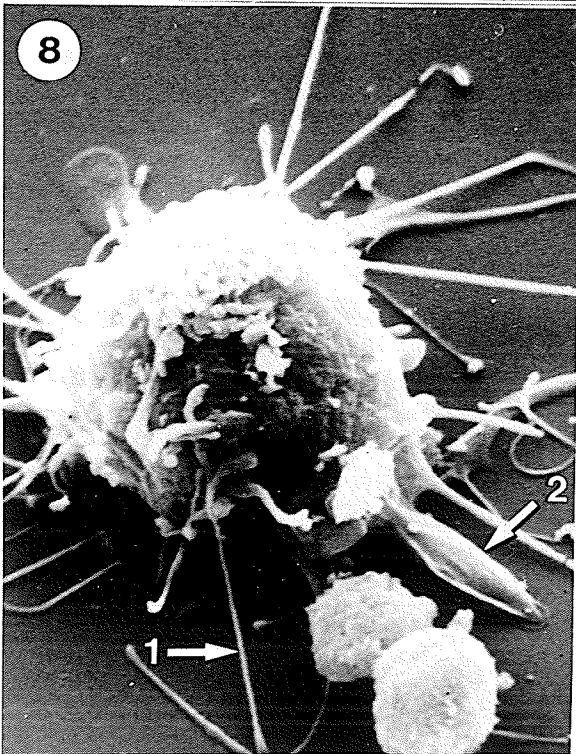
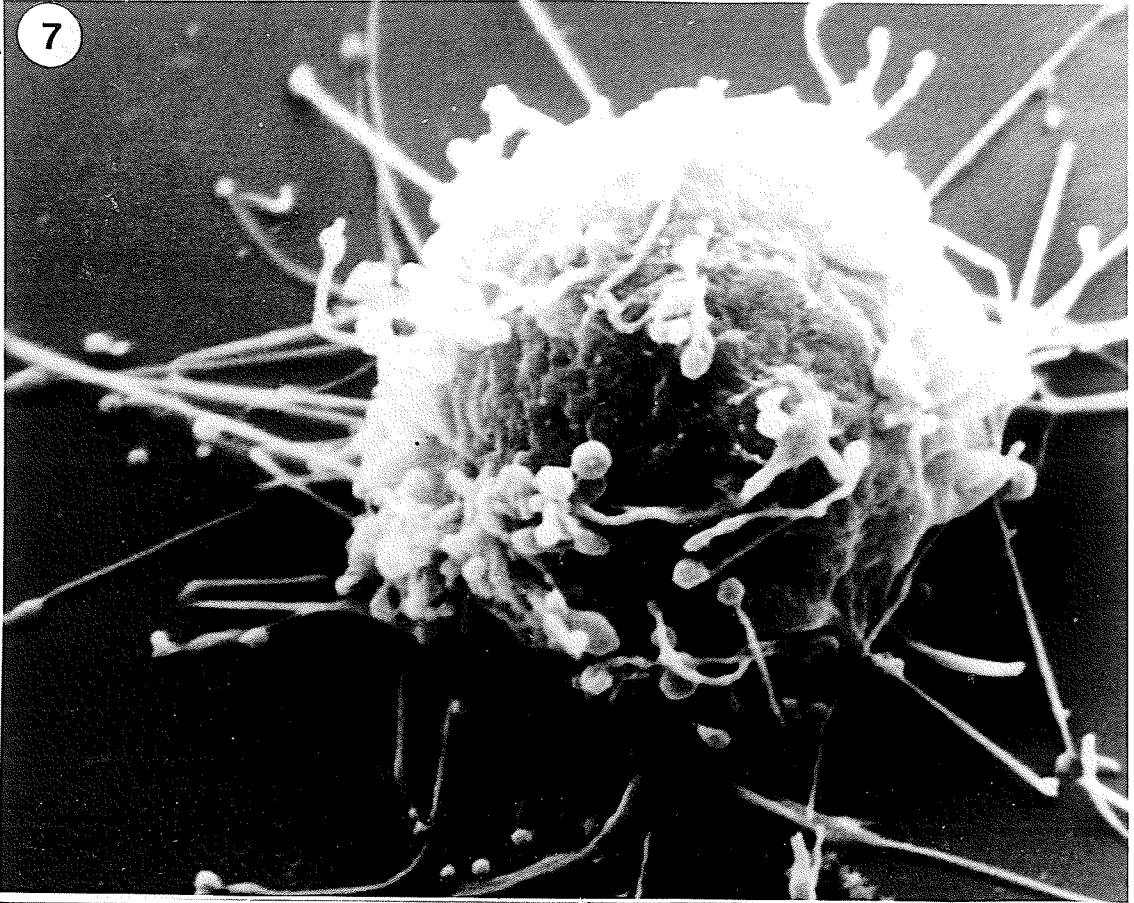


Figure 10. SEM of normal GR after 20min incubation on glass substrate. Note flattened cell and elongated filopodia. x3,500.

10

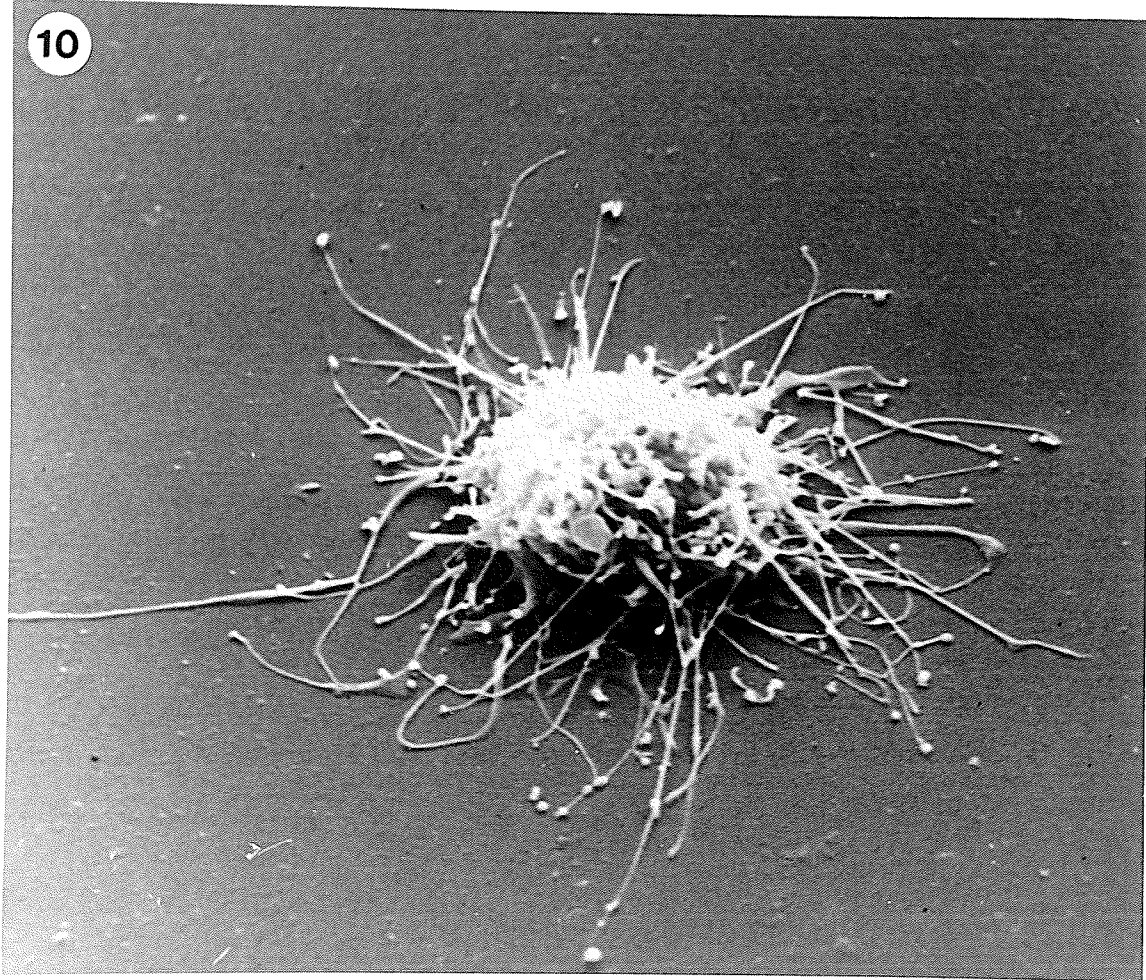


Figure 11. SEM of normal GR after 2min incubation on BMM. Note relatively smooth cell surface. x9,500.

Figure 12. GR after 20min incubation on BMM. Note relatively few filopodia and lack of flattening. x7,600.

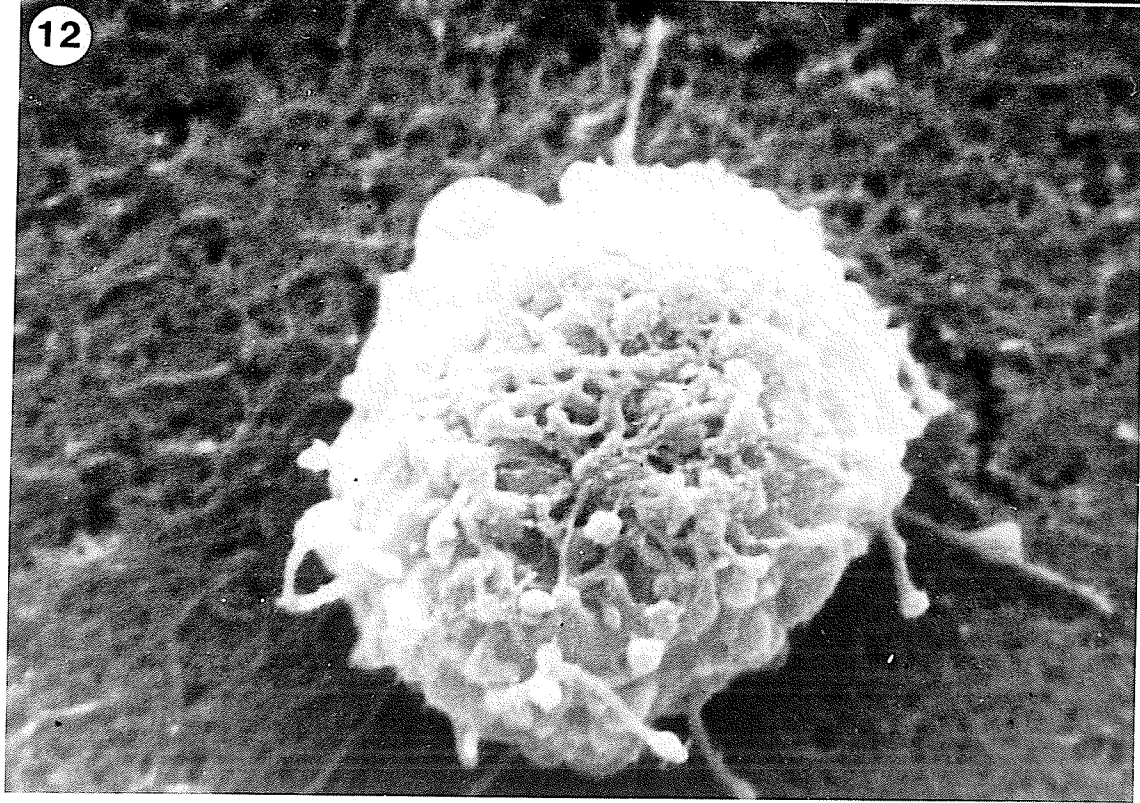
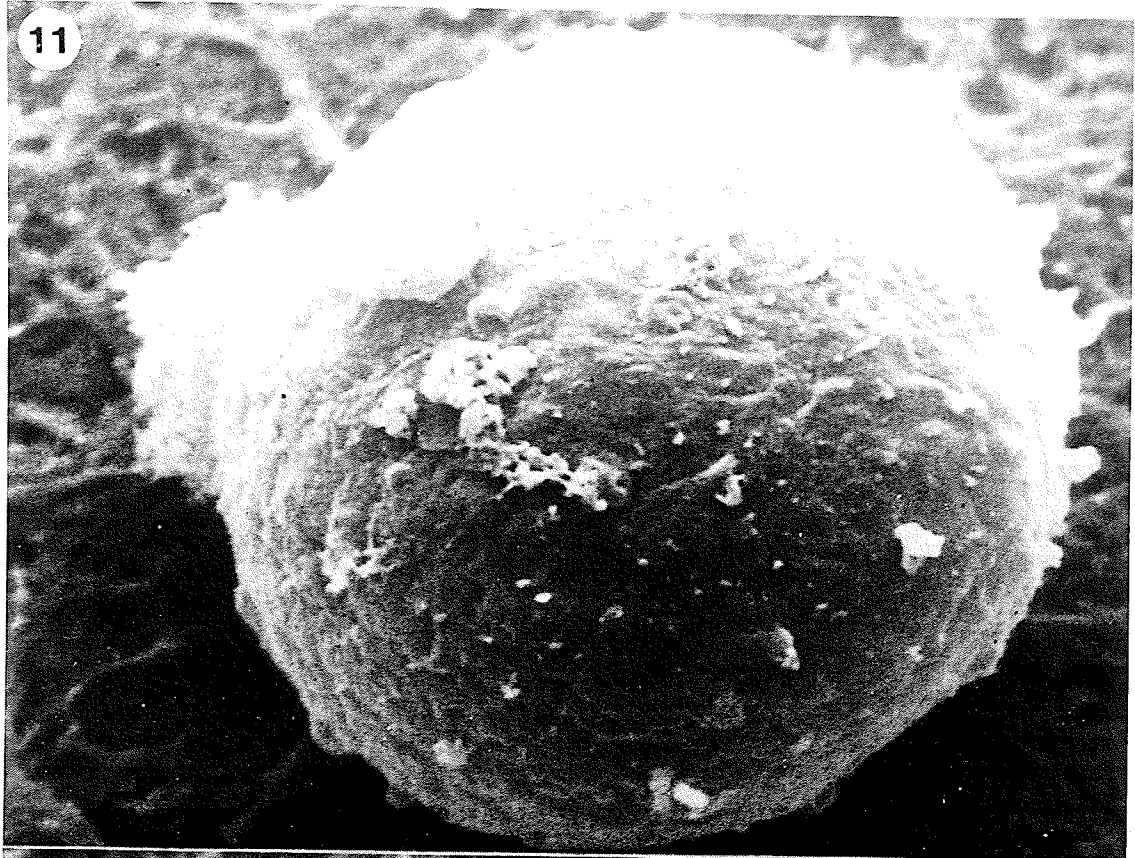
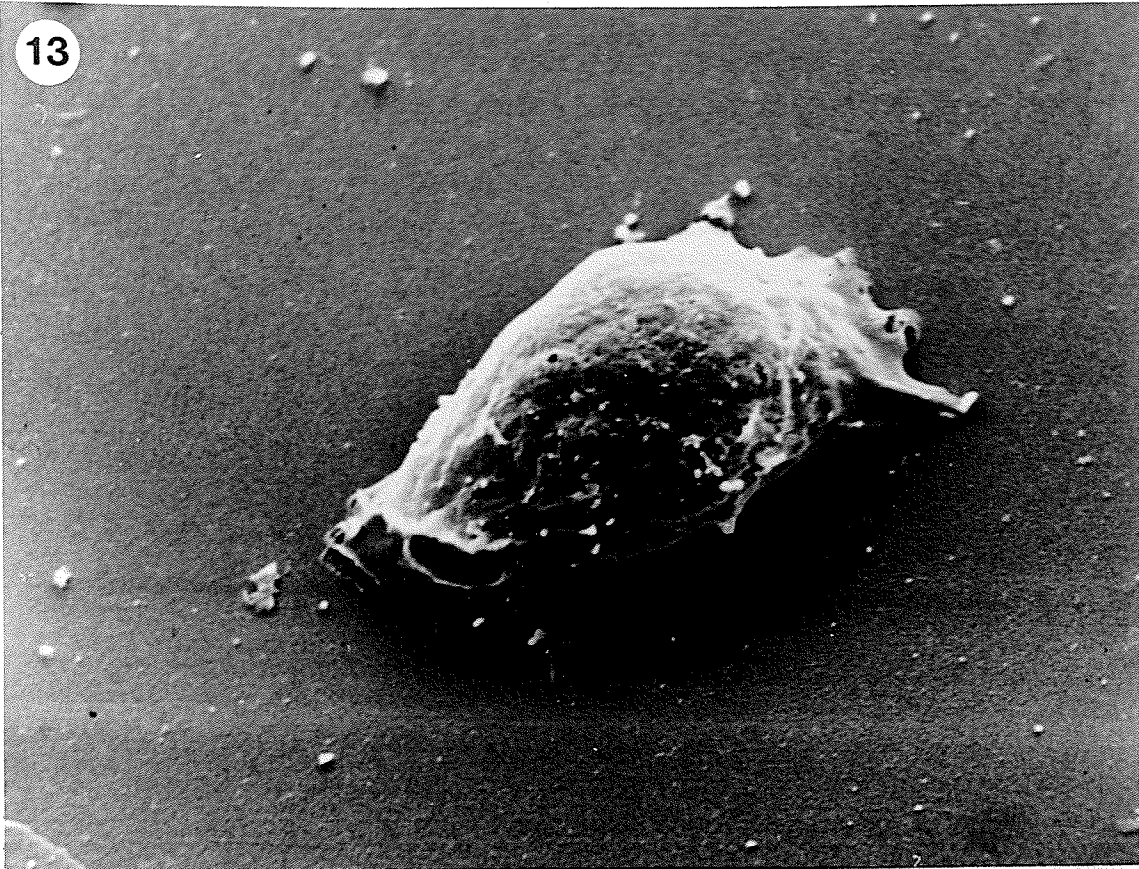


Figure 13. SEM of PL after 2min incubation on glass substrate.
Note spindle-shape. x3,100.

Figure 14. SEM of PL after 2min incubation on glass. Note
flattening of cell mass and ruffling of lamellopodium
(arrows). x3,300.

13



14

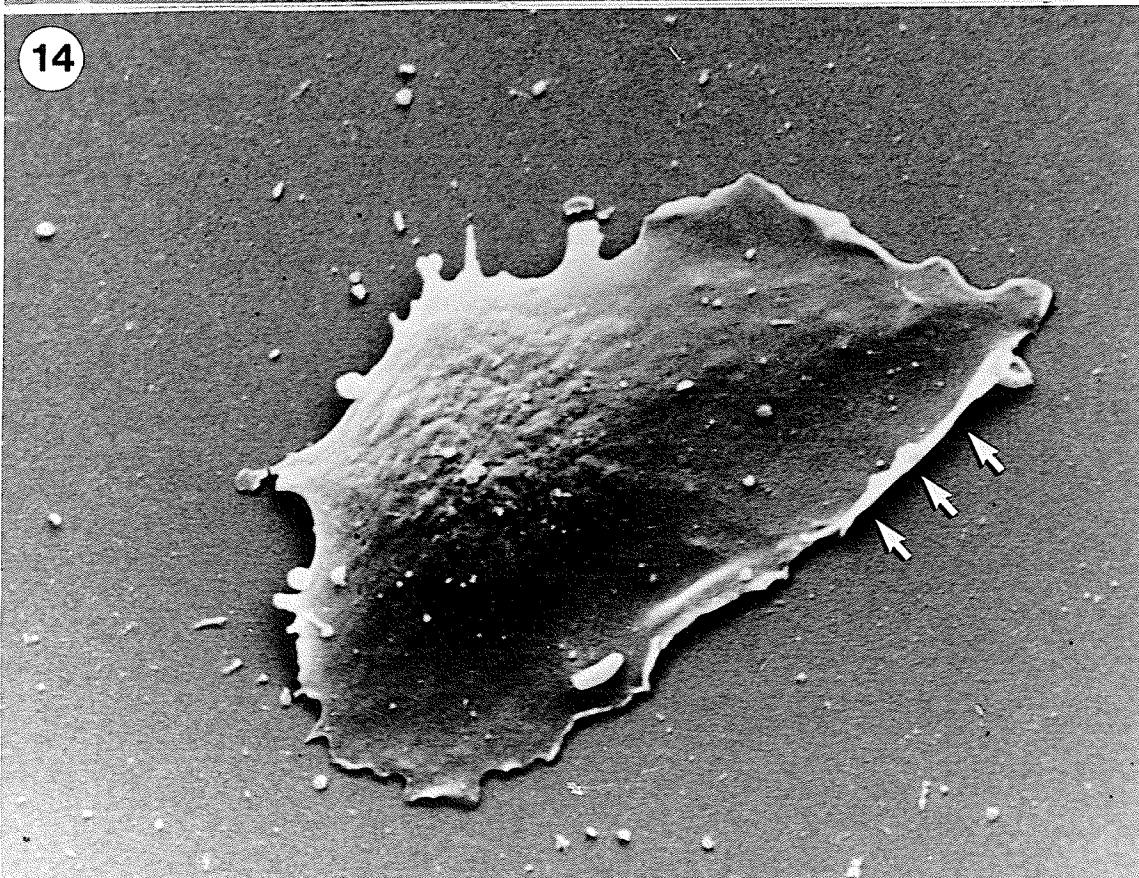
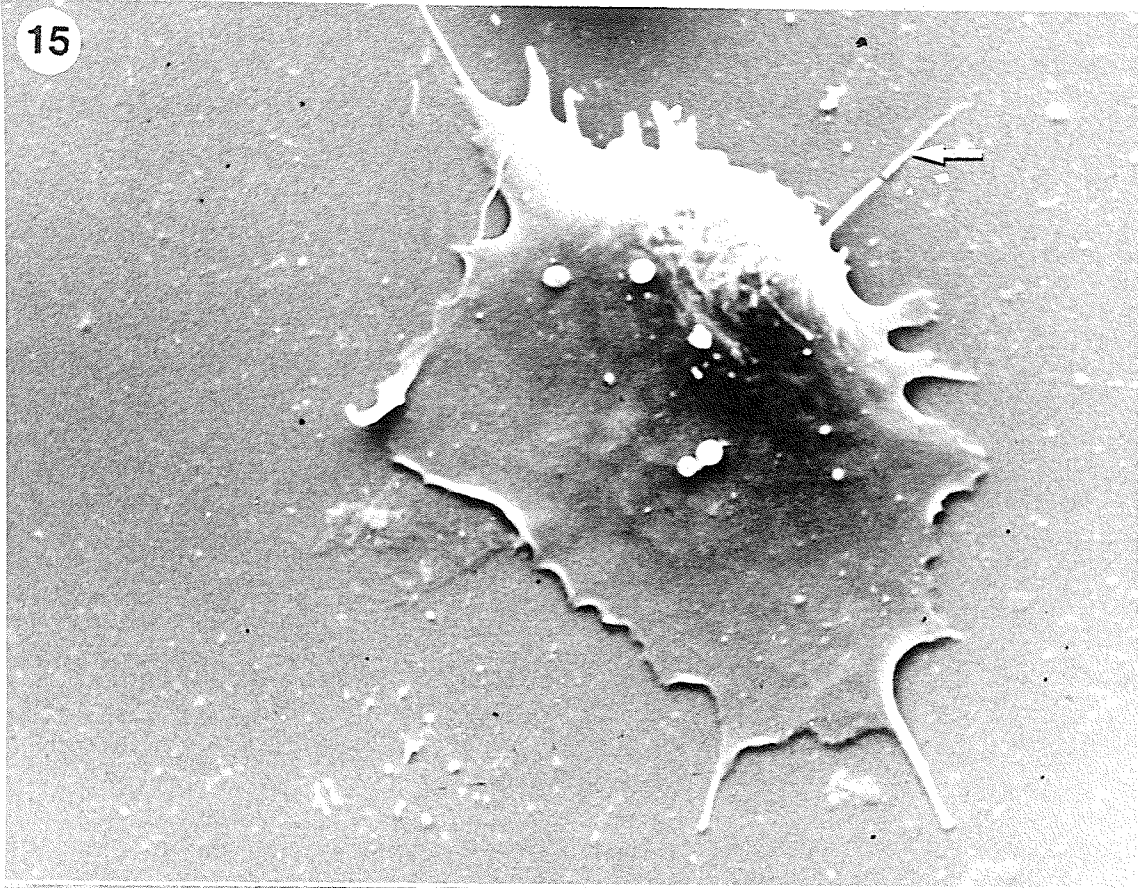


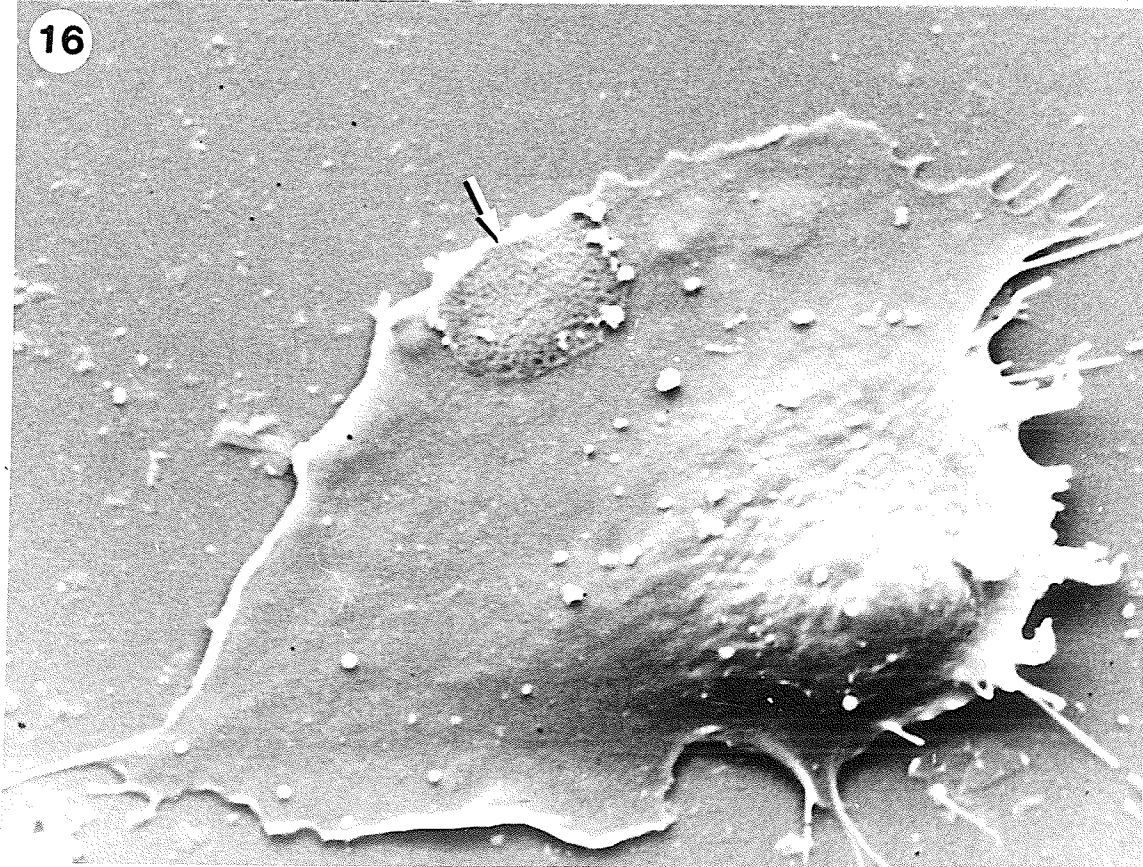
Figure 15. PL after 2min incubation on glass. Posterior retraction fibre is visible (arrow). Breakage of fibre is due to processing. x3,300.

Figure 16. Intermediate spreading PL on glass. Lamellopodial extension is accompanied by flattening of cell mass. Arrow indicates where cell membrane has been torn away. x3,500.

15



16



stages. In PL's in transition between early and intermediate spreading, the initial amount of spreading varied, and some PL's exhibited developing lamellae and a flattened central mass (Fig. 14). Ruffling at the leading edge of the lamellopodia was usually evident, as were finer cytoplasmic extensions or 'retraction fibres' (Davies and Preston, 1985) at the posterior edge of the cell, opposite the advancing lamellopodium (Fig. 15). PL's with more extensive lamellae and increased flattening of the cell mass were identified as intermediate spreading forms (Fig. 16).

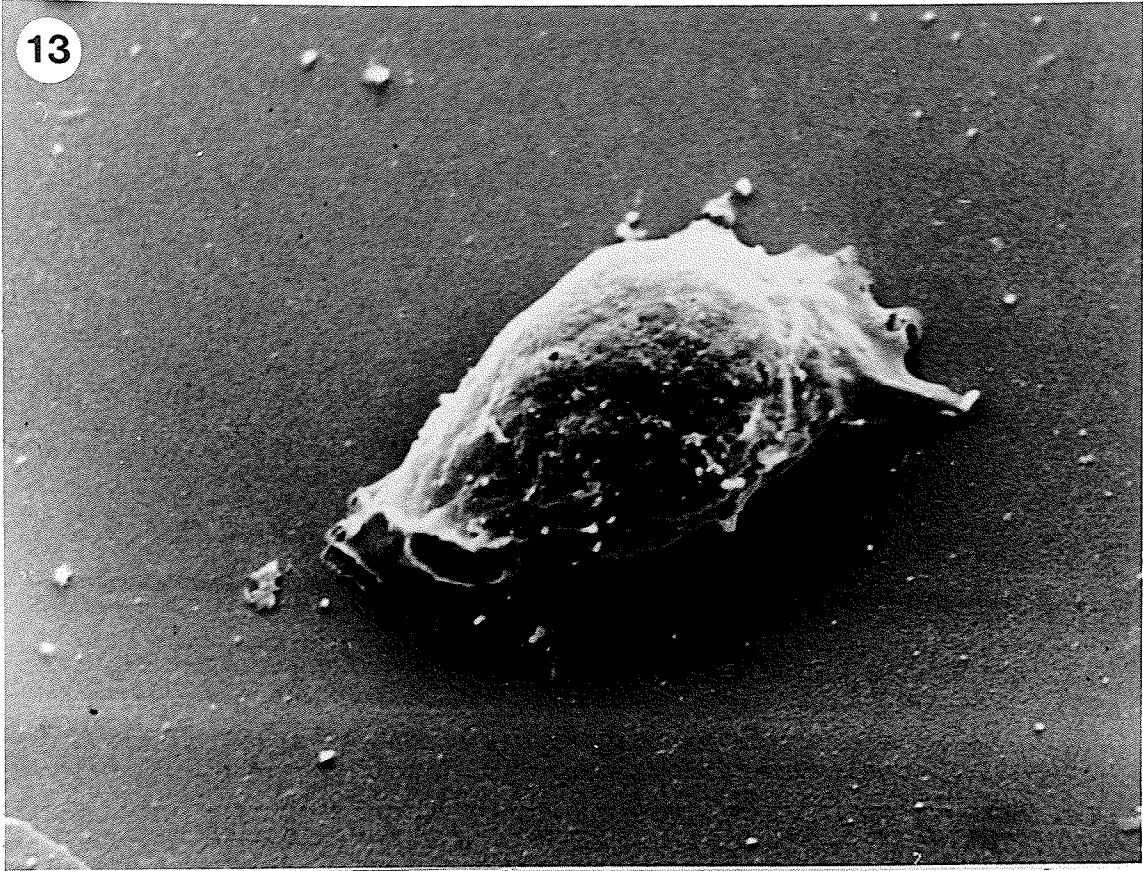
After 5min incubation, most PL's exhibited greater lamellar extension and an increased flattening of the central mass (Fig. 17). Lamellae usually extended along a wide arc, forming a leading edge which was broadly polarized. Filopodia were frequently present at the leading edge of such cells, and the dorsal cell surface was devoid of protrusions or elaborations, with the exception of some slight rippling of the cell membrane over the nucleus. The posterior pole of intermediate spreading PL's varied in shape (Figs. 18, 19).

After 5min and 20min incubation, PL's undergoing polarized spreading were evident. These were differentiated from the previous stage on the basis of longitudinal spreading and the orientation of the leading edge of the cell along one or more definite axes. Late intermediate/early polarized spreading PL's were as indicated in Fig. 20. An anterior-posterior axis was present, and lamellopodia were defined at both ends. In a slightly later stage of polarized

Figure 13. SEM of PL after 2min incubation on glass substrate. Note spindle-shape. x3,100.

Figure 14. SEM of PL after 2min incubation on glass. Note flattening of cell mass and ruffling of lamellopodium (arrows). x3,300.

13



14

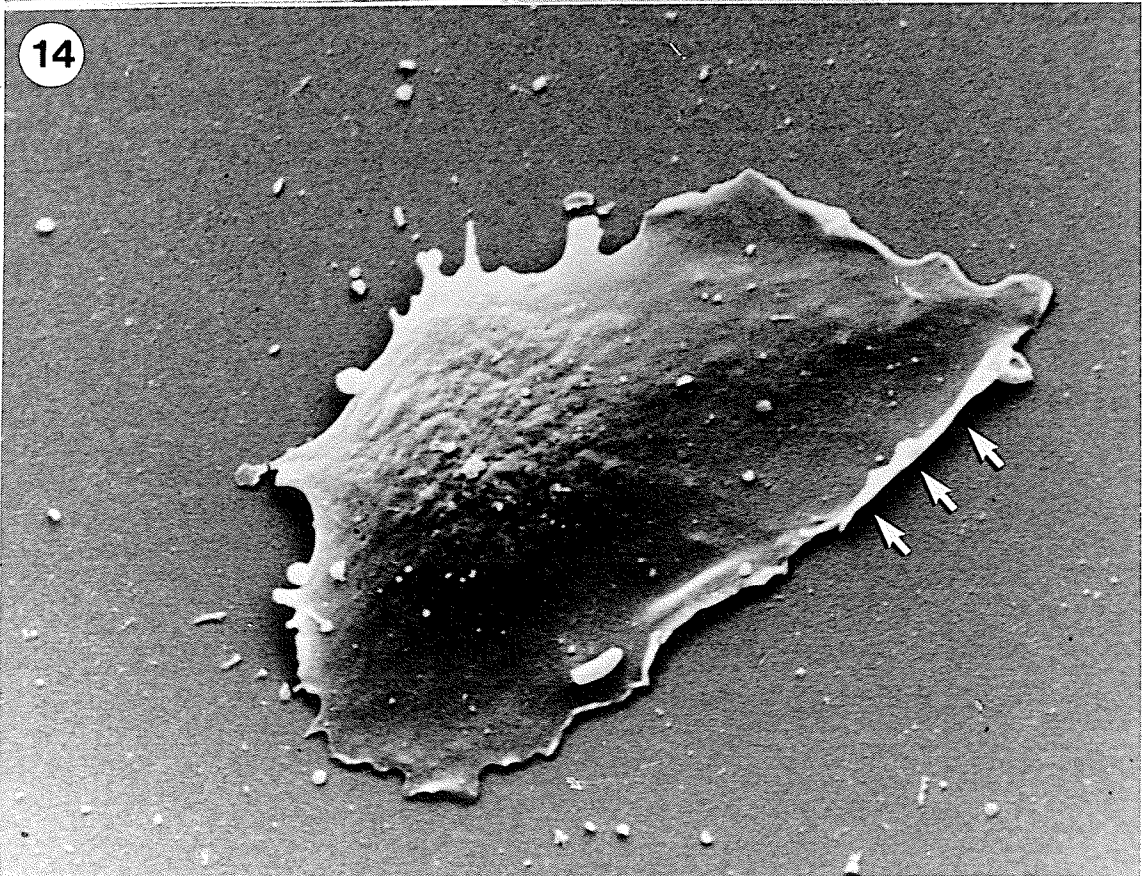
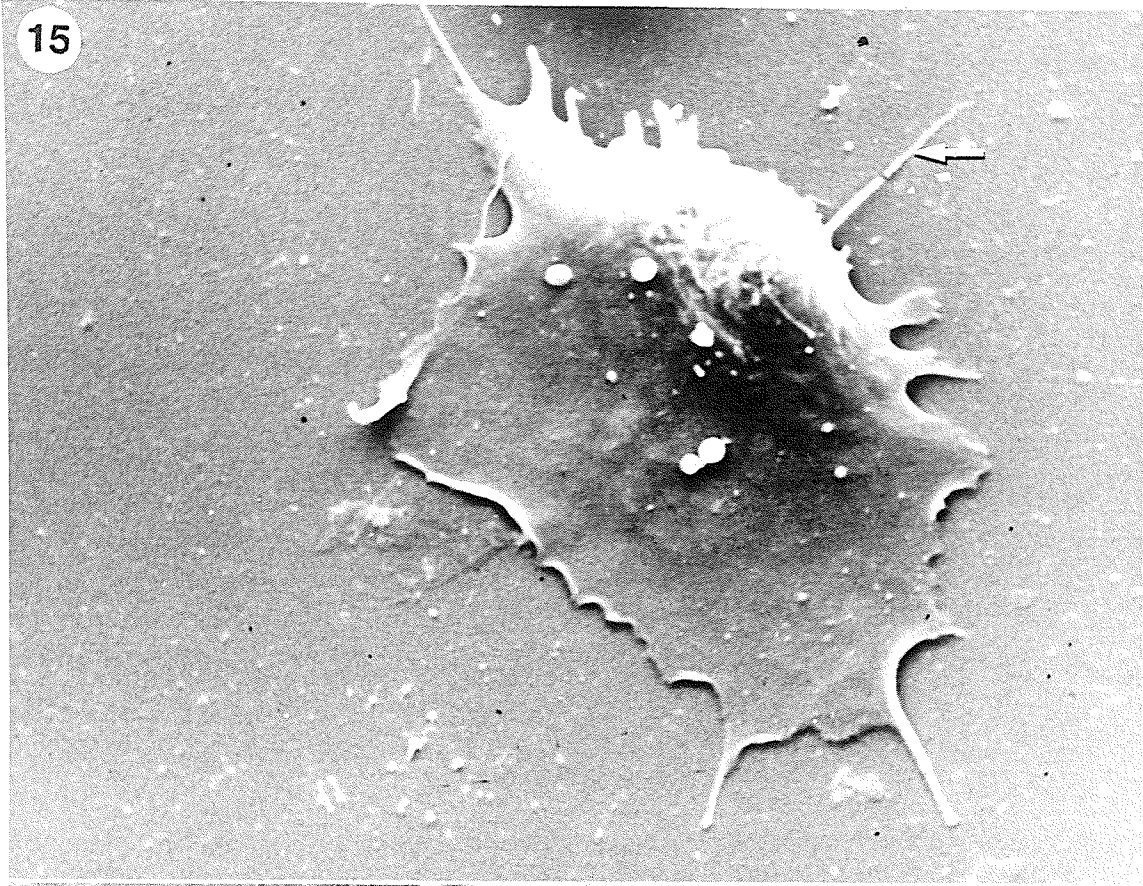


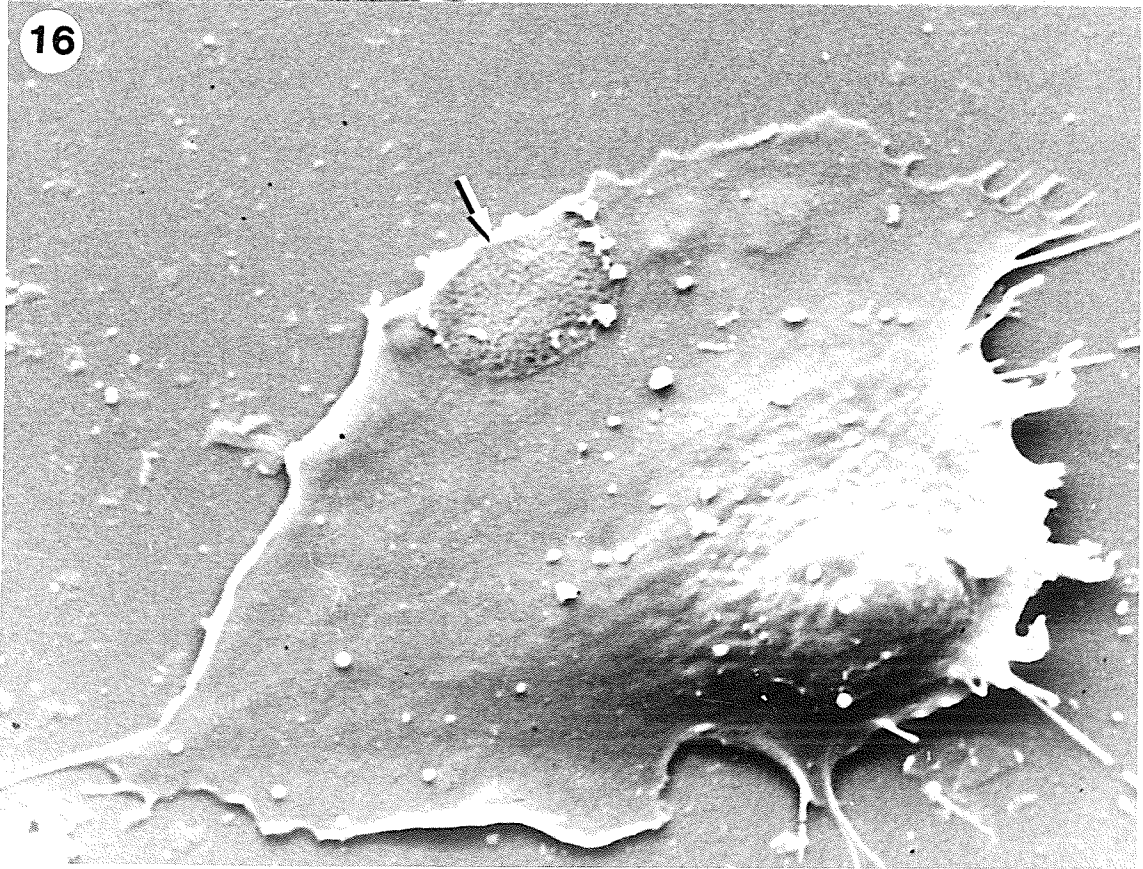
Figure 15. PL after 2min incubation on glass. Posterior retraction fibre is visible (arrow). Breakage of fibre is due to processing. x3,300.

Figure 16. Intermediate spreading PL on glass. Lamellopodial extension is accompanied by flattening of cell mass. Arrow indicates where cell membrane has been torn away. x3,500.

15



16

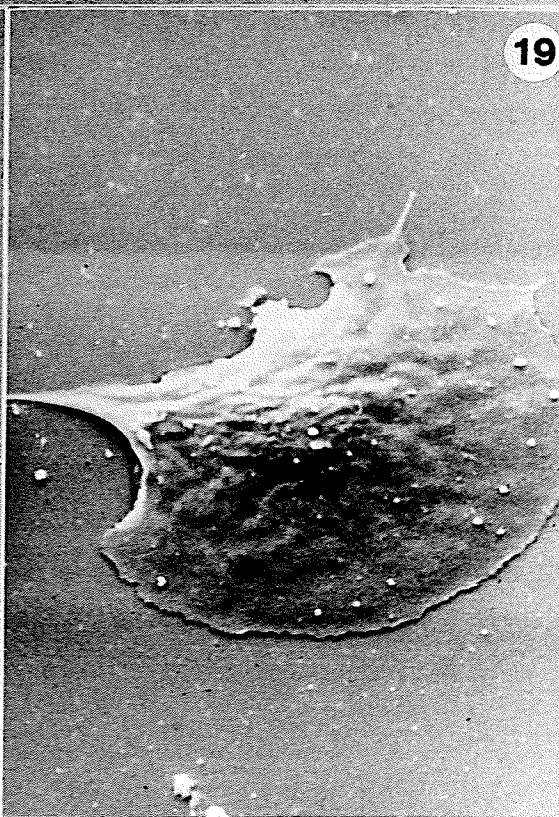
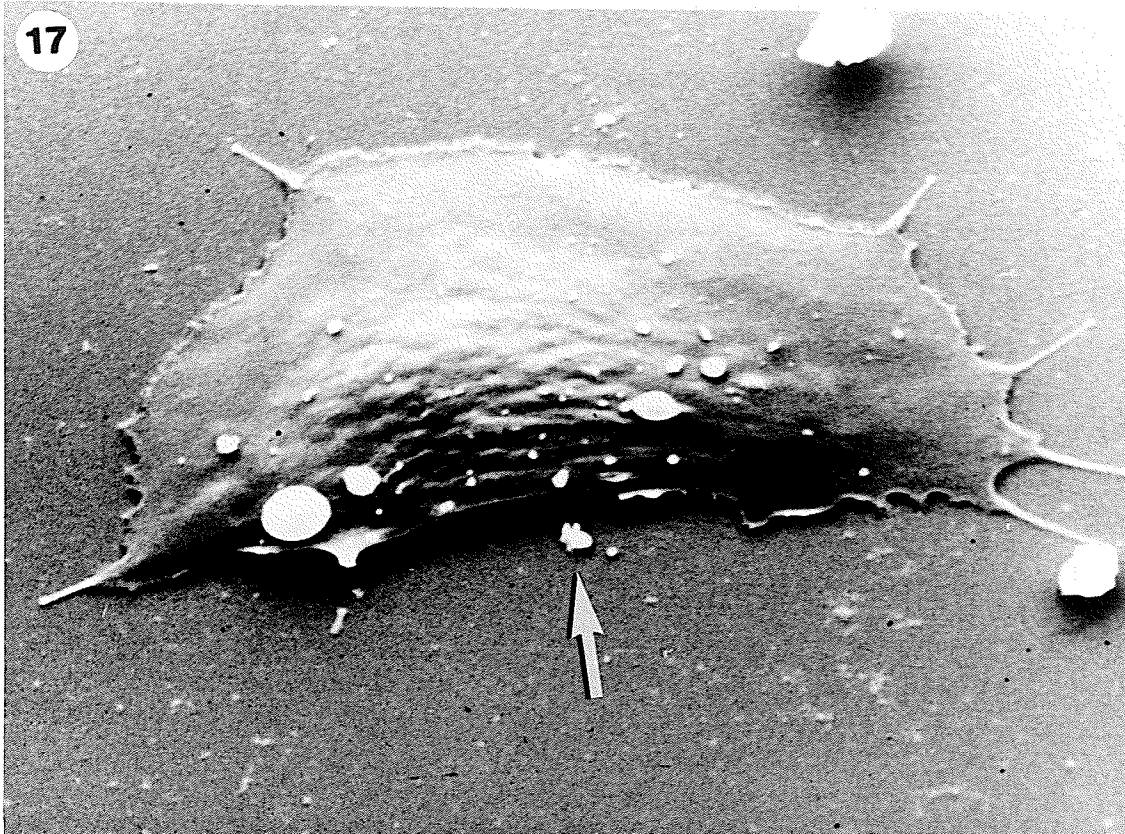


Figures 17-19. SEM of PL's after 5min incubation on glass substrate.

Figure 17. Intermediate spreading PL. White spheres are lipid droplets. Cell mass has retracted anteriorly (direction indicated by arrow). x3,500.

Figure 18. Intermediate spreading PL. x2,100.

Figure 19. Intermediate spreading PL. x2,600.



spreading, PL's extended over a greater distance on the substrate (Fig. 21), and in the case of the PL, showed a prominent lamellopodium at one end of the cell, resulting in a unipolarized configuration. The cell mass was displaced more to the anterior pole, and the posterior end of the cell was narrower than the anterior end. Some PL's were also seen which had apparently undergone retraction of the trailing end of the cell (Fig. 22). The longitudinal axis was greatly decreased, while the anterior lamellopodium was quite broad.

Bipolar PL's, in which the poles of the cell were at opposite ends of the longitudinal axis and were approximately equal in width, were present after 5 and 10min incubation (Fig. 23). Usually, both poles were convex, although some bipolar PL's had either 1 convex and 1 concave pole, or both poles were concave. Also, a number of PL's with multiple or indistinguishable polarities were evident (Figs. 24-27). These cells probably represented PL's at various stages of transformation between intermediate spreading stages and polarized spreading.

After 20min, many PL's assumed a rounded, flat shape, with only a slight increase in thickness in the area of the nucleus (Fig. 28). The dorsal cell surface usually showed little elaboration of the cell membrane, although ruffling at the cell periphery was sometimes present. Some PL's had filopodia, which may have indicated that spreading was not complete (Fig. 29). Usually, there were more polarized than non-polarized PL's in coverslip preparations, and no non-polarized PL's were seen at 2min incubation.

Figure 20. SEM of early unipolarized PL on glass substrate. x3,800.

Figure 21. SEM of unipolarized PL on glass substrate. Arrow indicates longitudinal axis and direction of movement. x3,800.

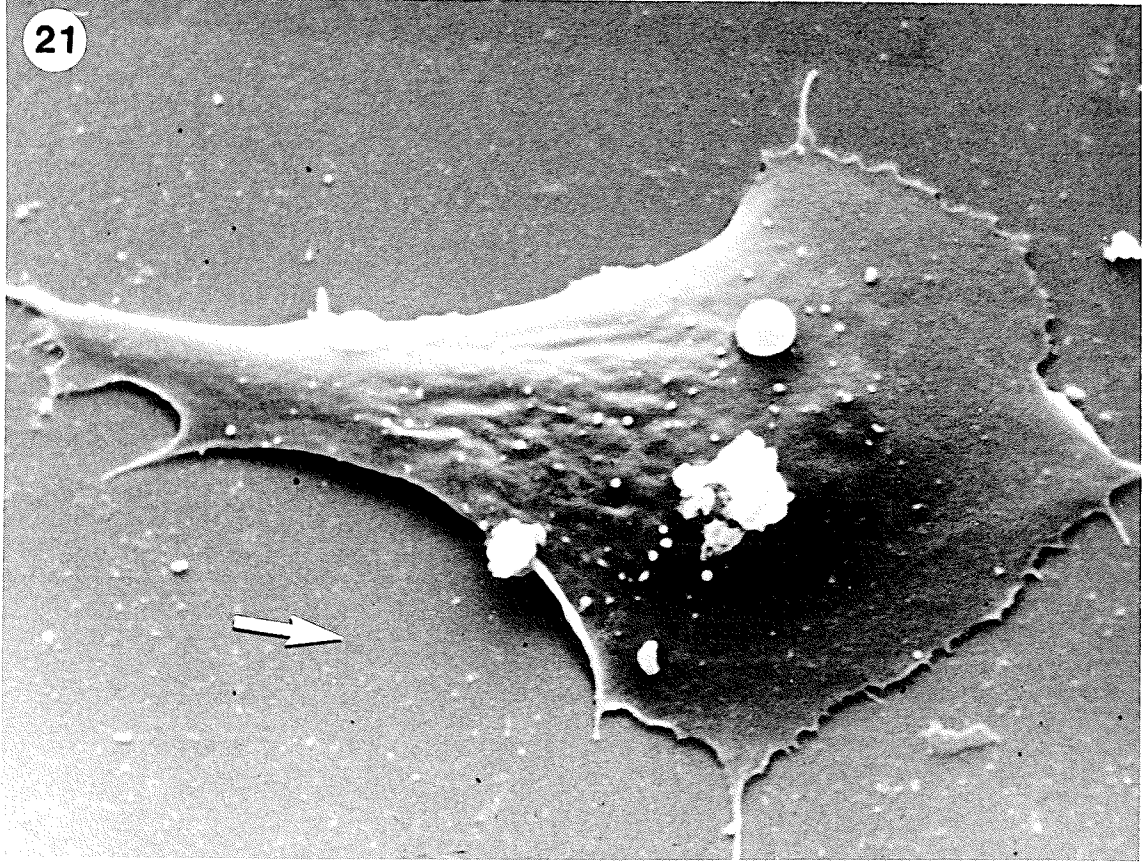
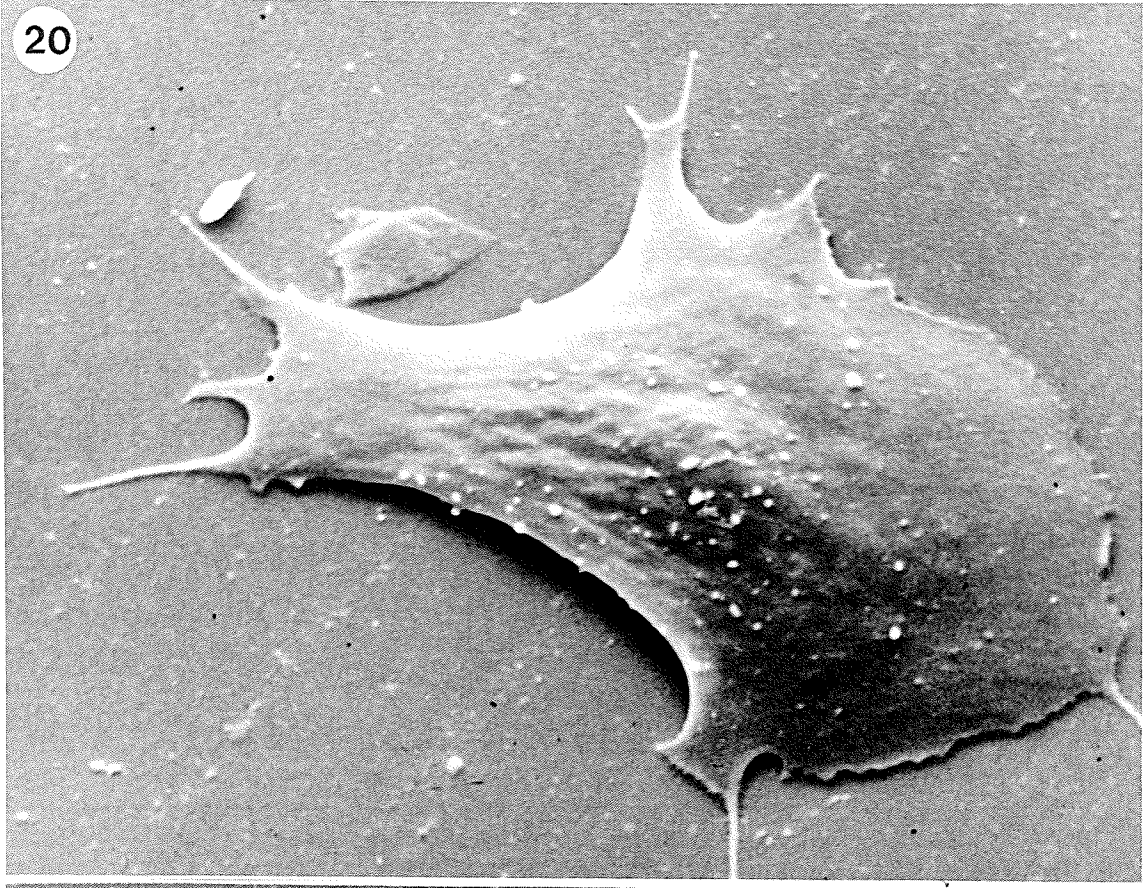
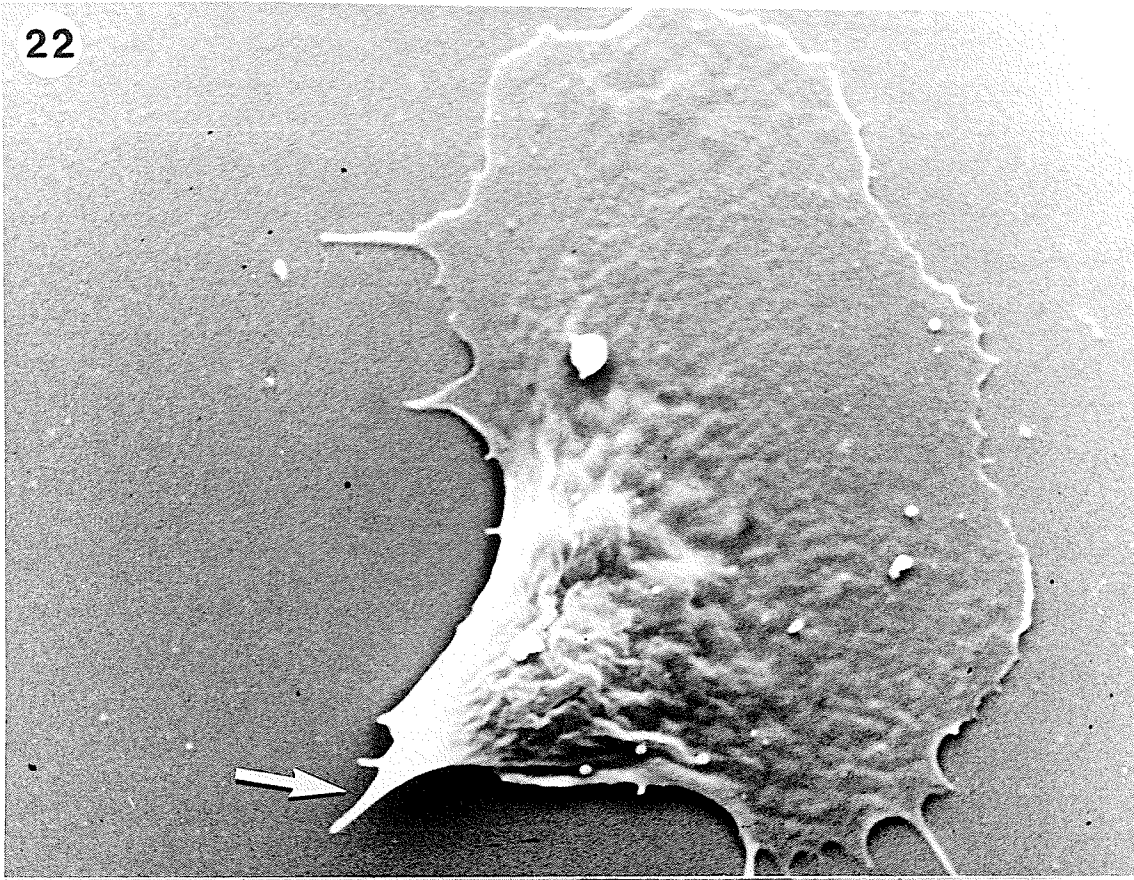


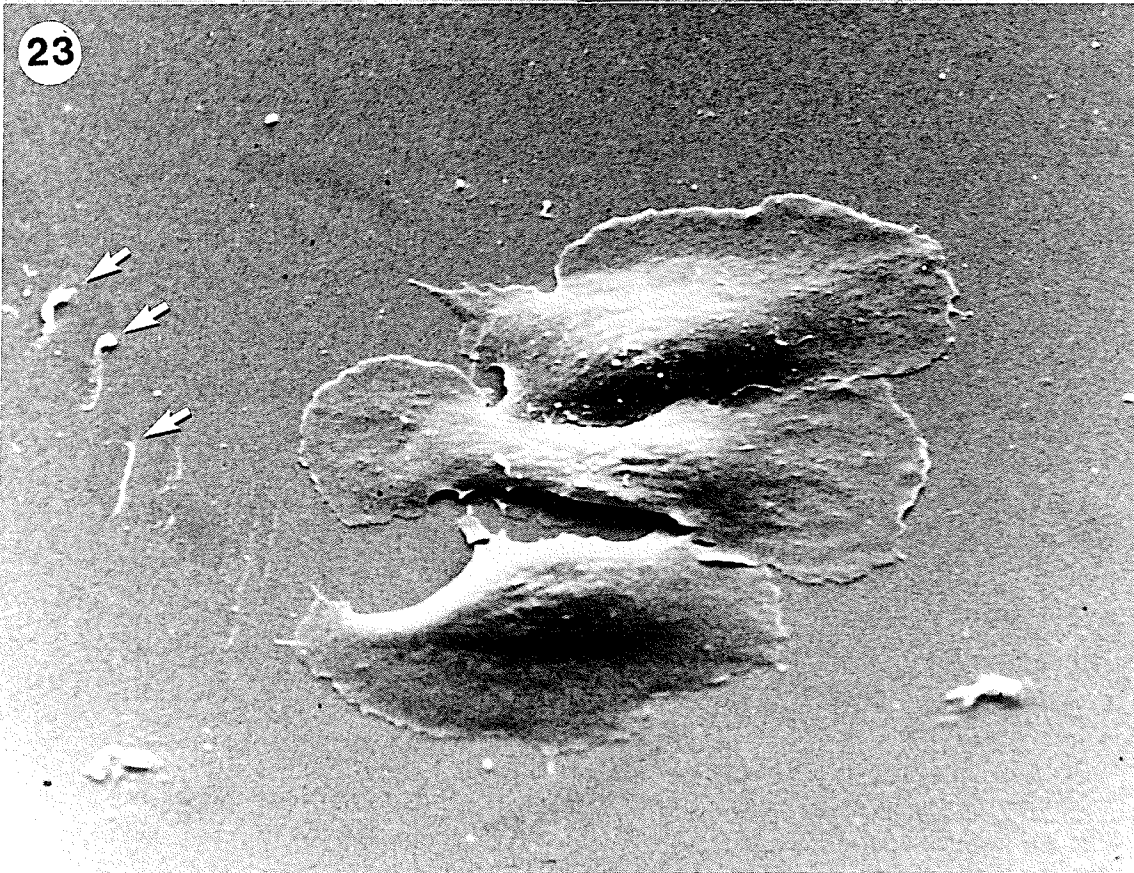
Figure 22. SEM of unipolarized PL on glass substrate. Arrow indicates retracted posterior end. $\times 3,300$.

Figure 23. SEM of bipolarized PL (middle) between intermediate spreading stages. Arrows indicate portions of trailing end of bottom PL left on substrate during locomotion. $\times 1,800$.

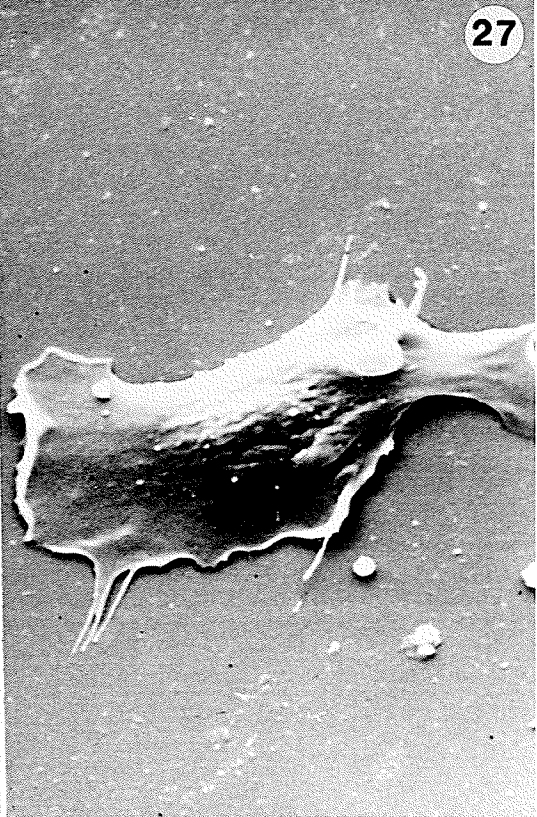
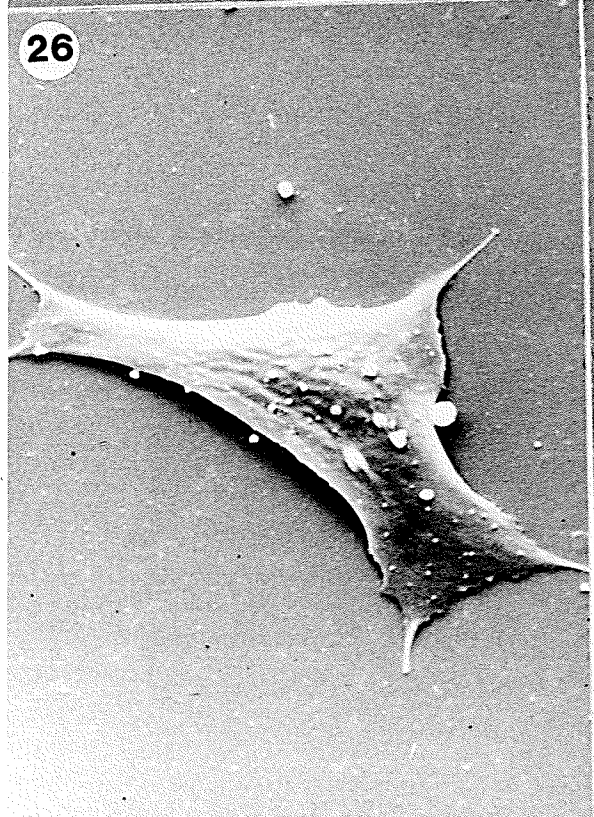
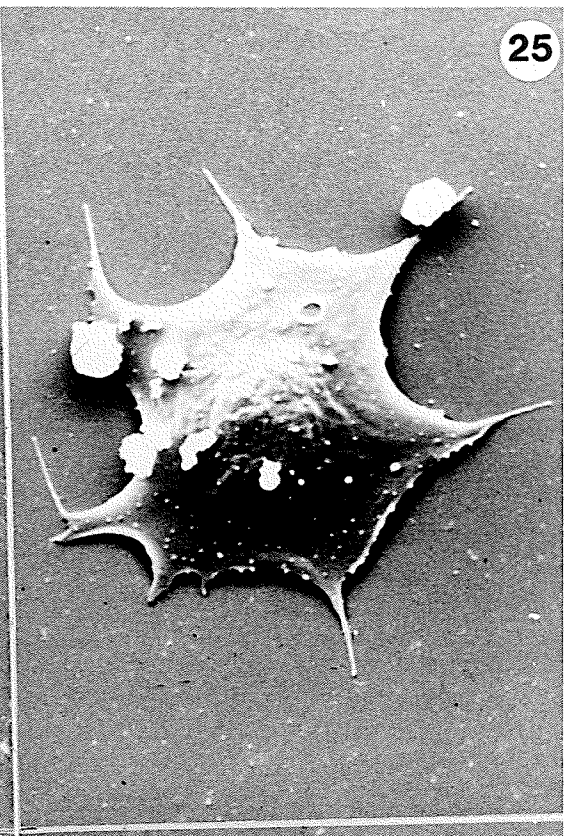
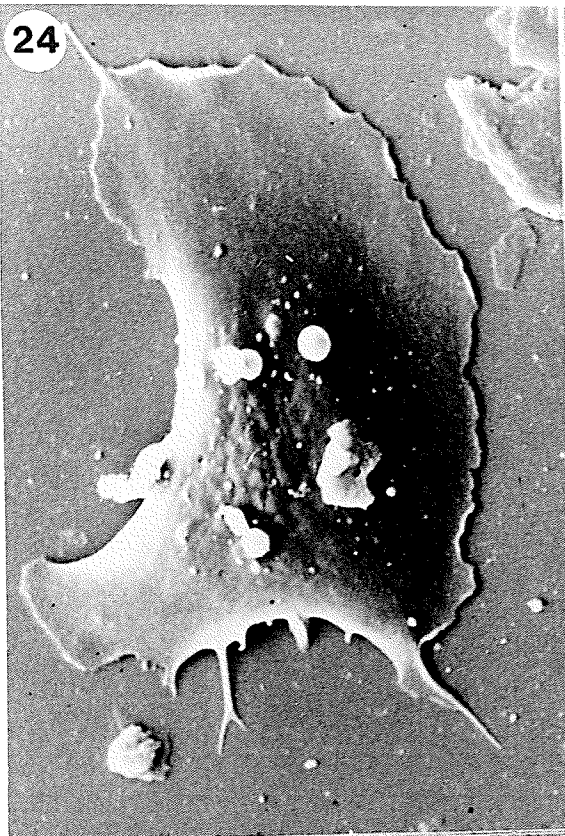
22



23



Figures 24-27. SEM's of PL's on glass substrate. Note variety of forms. x2,400.



BMM substrate

The spreading stages of normal PL's on BMM varied dramatically from those observed on glass substrates. Some very early stages of spreading examined after 2min incubation were similar to early stages on glass (Fig. 30); however, most early spreading stage PL's had numerous, long filopodial extensions developing from the leading edge of lamellae (Fig. 31). These filopodia terminated in bulbous vesicles, similar to those of GR's spreading on glass. In addition, the cell membrane over the central mass appeared highly ruffled, and showed prominent blebbing. During subsequent development, lamellae became more extensive, and long filopodia and elaboration of the cell membrane over the central mass persisted (Fig. 32). After 5min incubation, PL's generally exhibited lamellar extension at all points along the cell periphery, and long filopodia and elaboration of the dorsal surface persisted (Fig. 33). Definite polarization was not detected. After 20min incubation, persistent filopodia marked all PL's, and prominent ruffling persisted over the nucleus, while lamellae were devoid of surface detail (Fig. 34).

Spreading Morphology in Experimental Groups

Hemocytes from sham-injected and axenically-infected larvae (AxPI4) were similar at all spreading stages on glass substrates.

Figure 28. SEM of fully spread, non-polarized PL on glass substrate. Note absence of filopodia and slight ruffling. x3,300.

Figure 29. SEM of fully spread, non-polarized PL on glass substrate. Arrows indicate filipodia. x3,300.

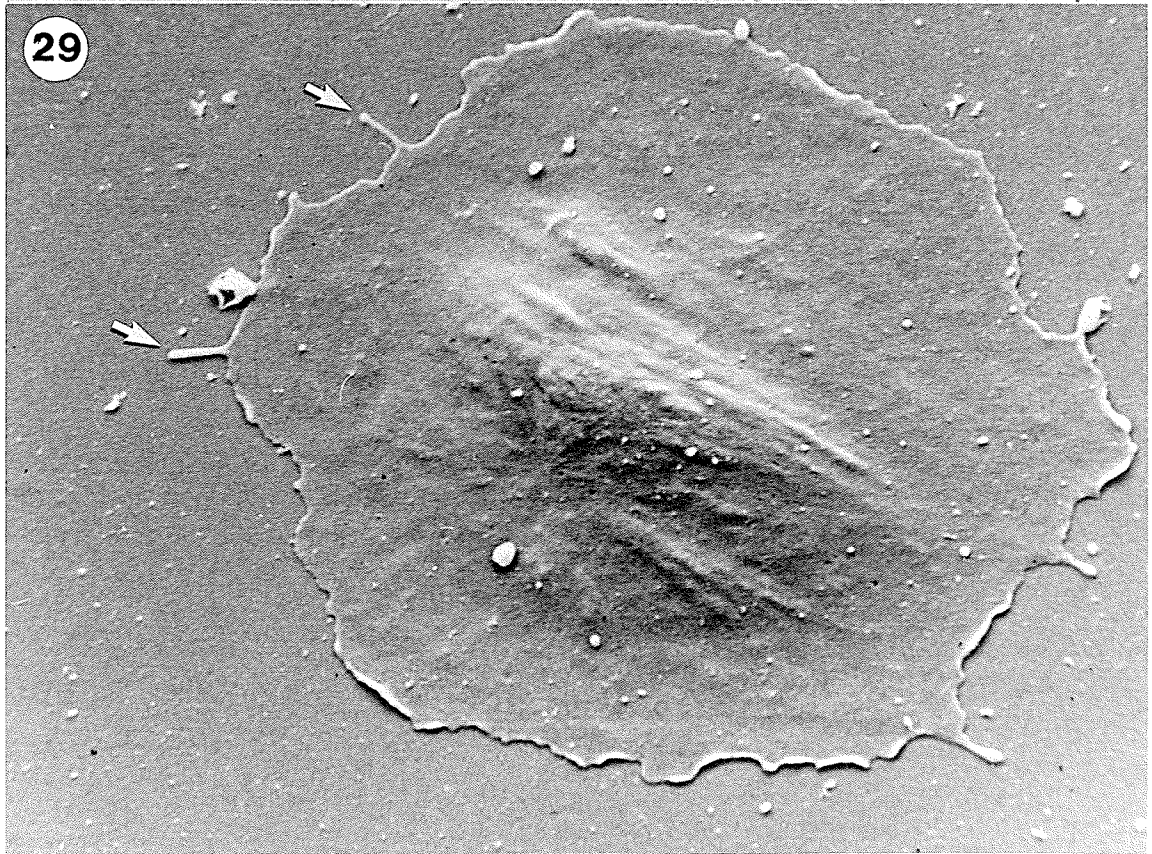
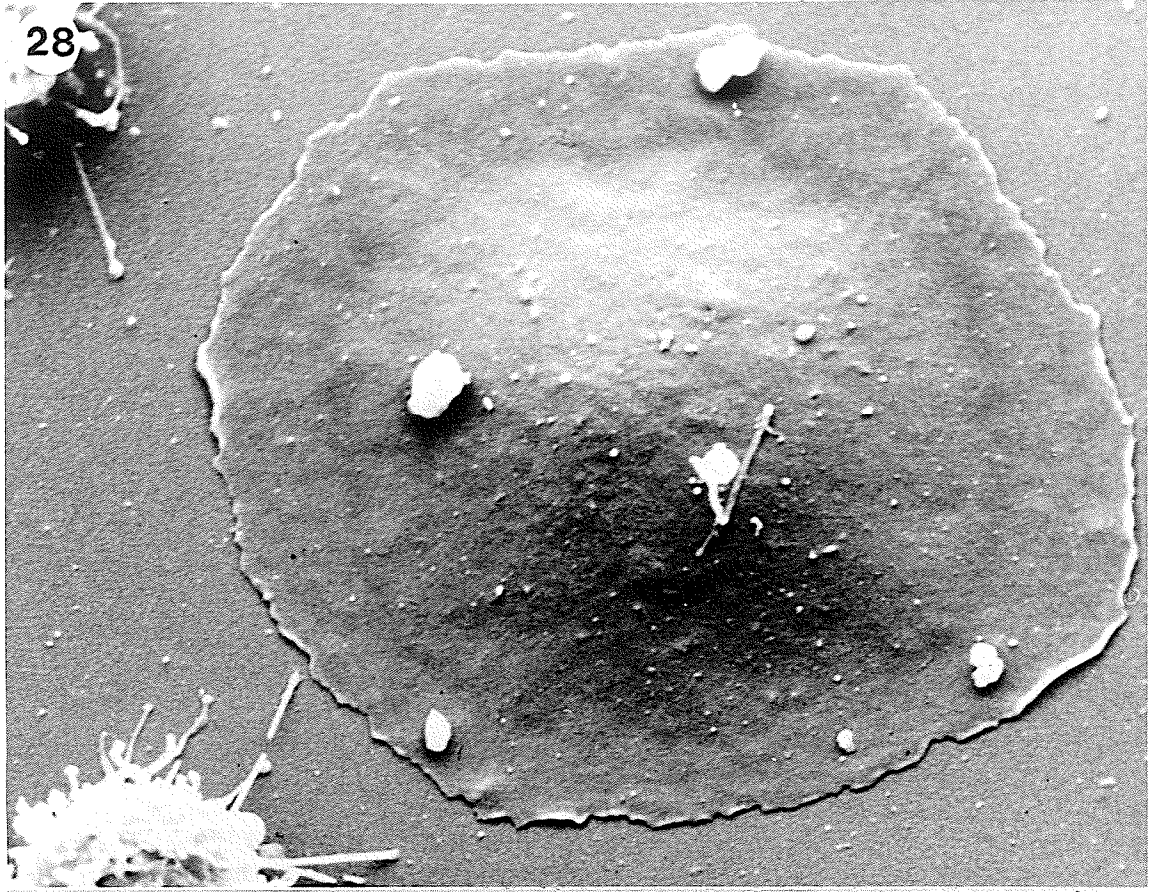


Figure 30. SEM of early spreading stage PL on BMM. Arrow indicates bleb. Tear is due to shrinkage of cell during processing. x7,900.

30

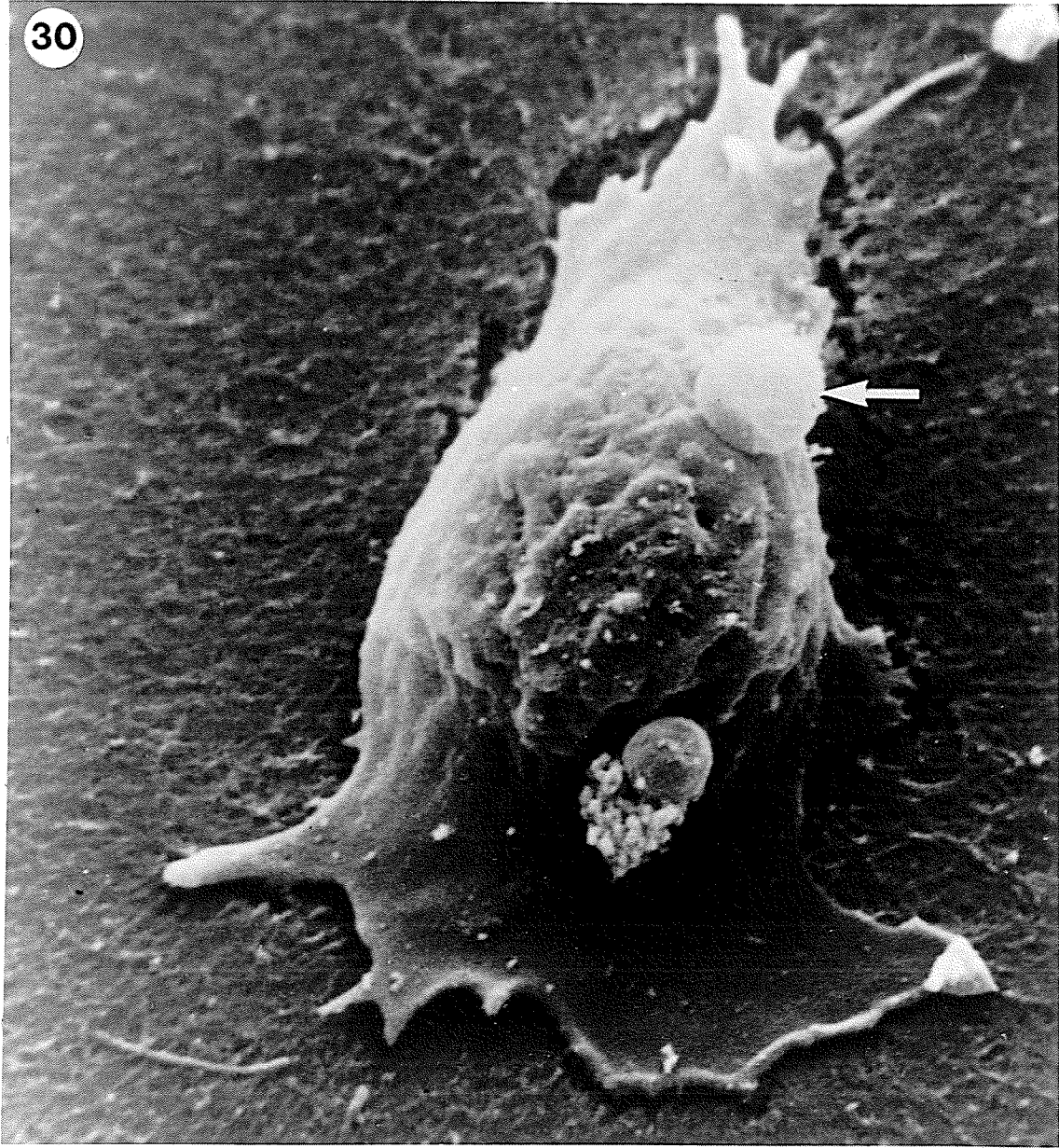


Figure 31. SEM of early intermediate stage PL on BMM. Note long filopodia and folding of cell membrane over cell mass. x5,300.

31

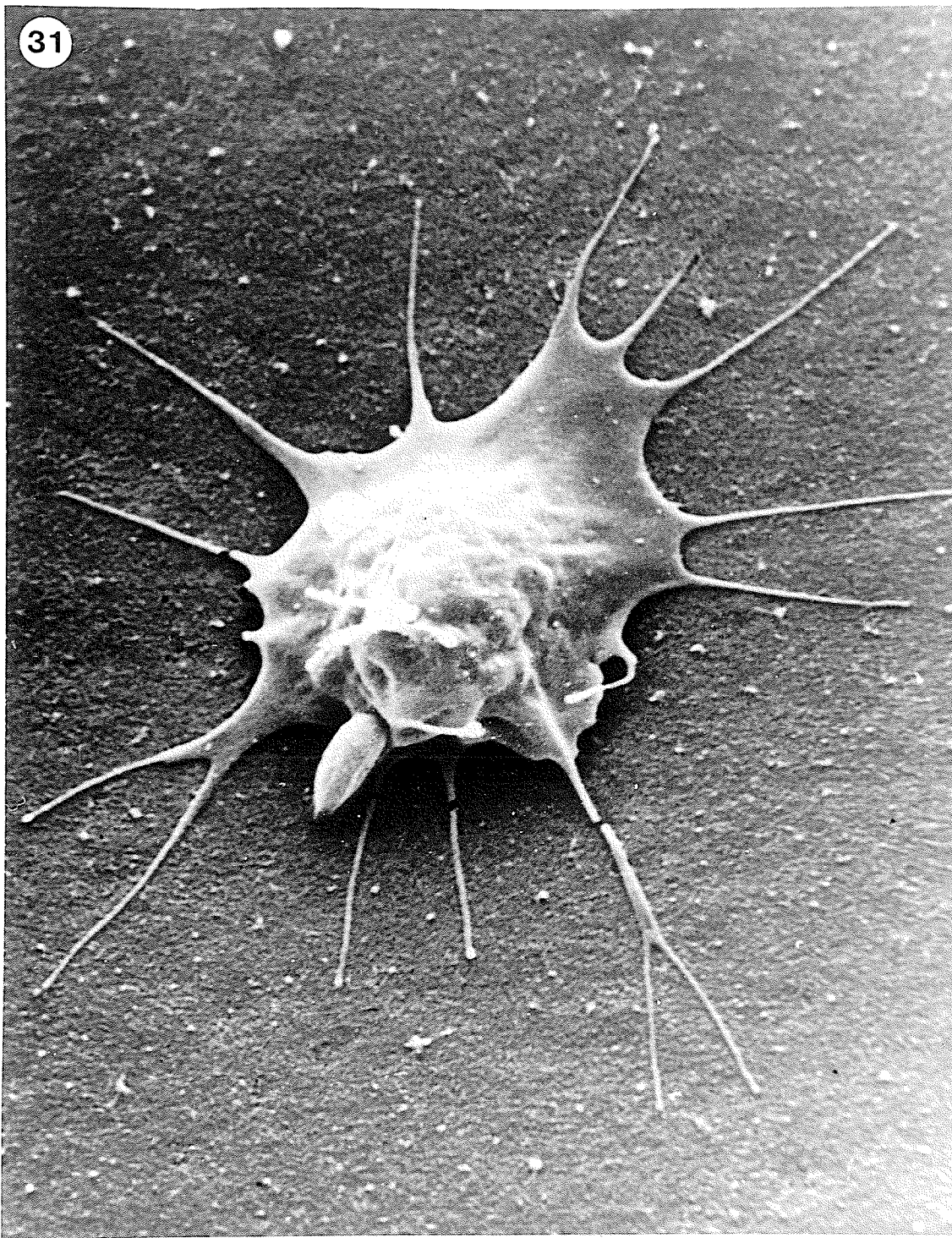
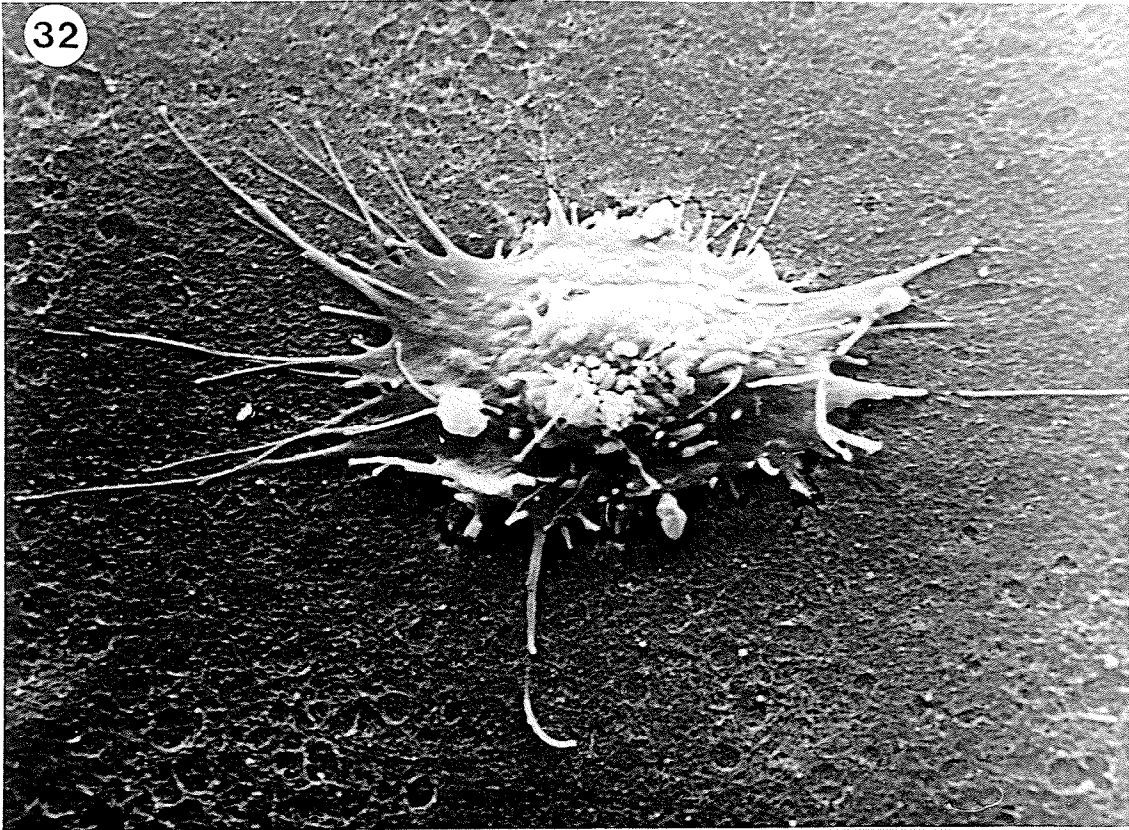


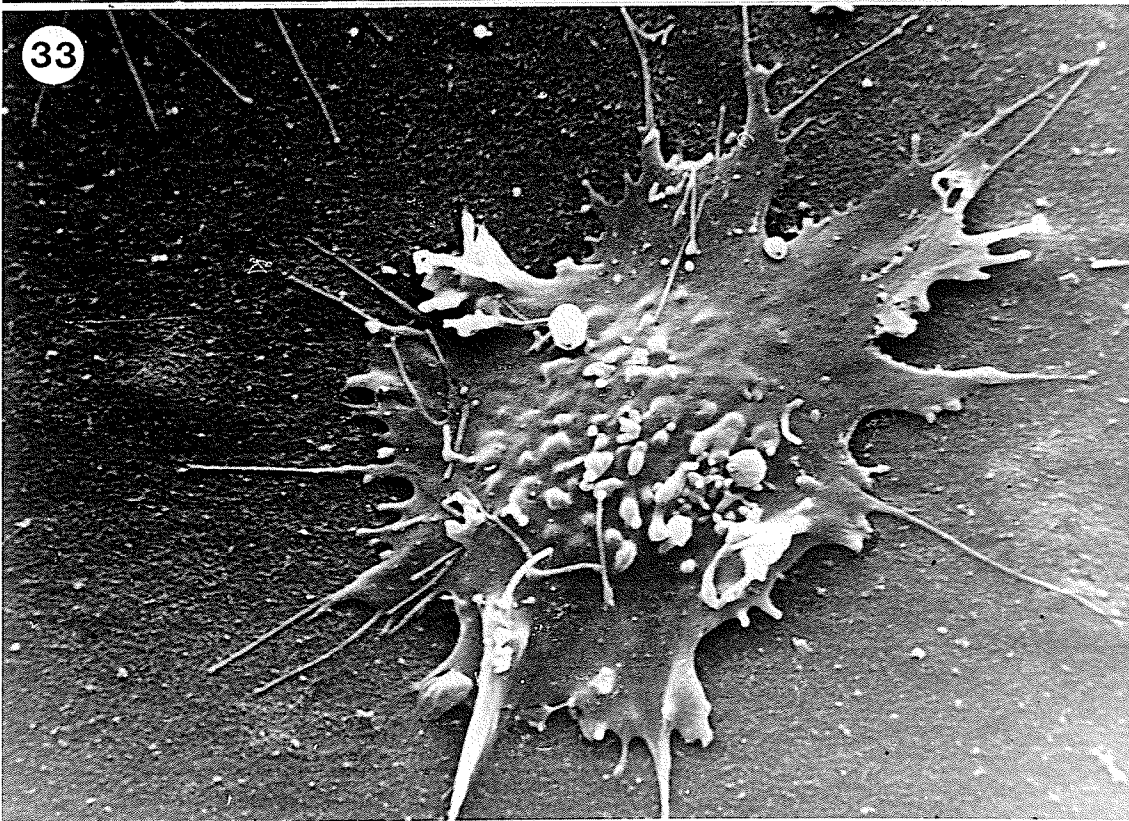
Figure 32. SEM of PL after 2min incubation on BMM. Note folded cell membrane and numerous filopodia. x3,200.

Figure 33. SEM of PL after 5min incubation on BMM. x3,200.

32



33



Hemocytes from xenically-infected larvae (XPI4) varied in spreading morphology from both of the previous groups. GR's, after 2 and 5min of incubation, were not unusual in appearance. At 20min after incubation, GR's from the XPI4 group did not show the same profusion of type I filopodia as other groups (Fig. 35), but the cell membrane of such GR's still exhibited considerable surface modification. PL's from the XPI4 group also showed abnormalities in spreading morphology on glass. Extreme flattening of intermediate (Fig. 36) and polarized spreading stages of PL's (Fig. 37) was evident. Other PL's appeared to be poorly attached to the substrate (Fig. 38).

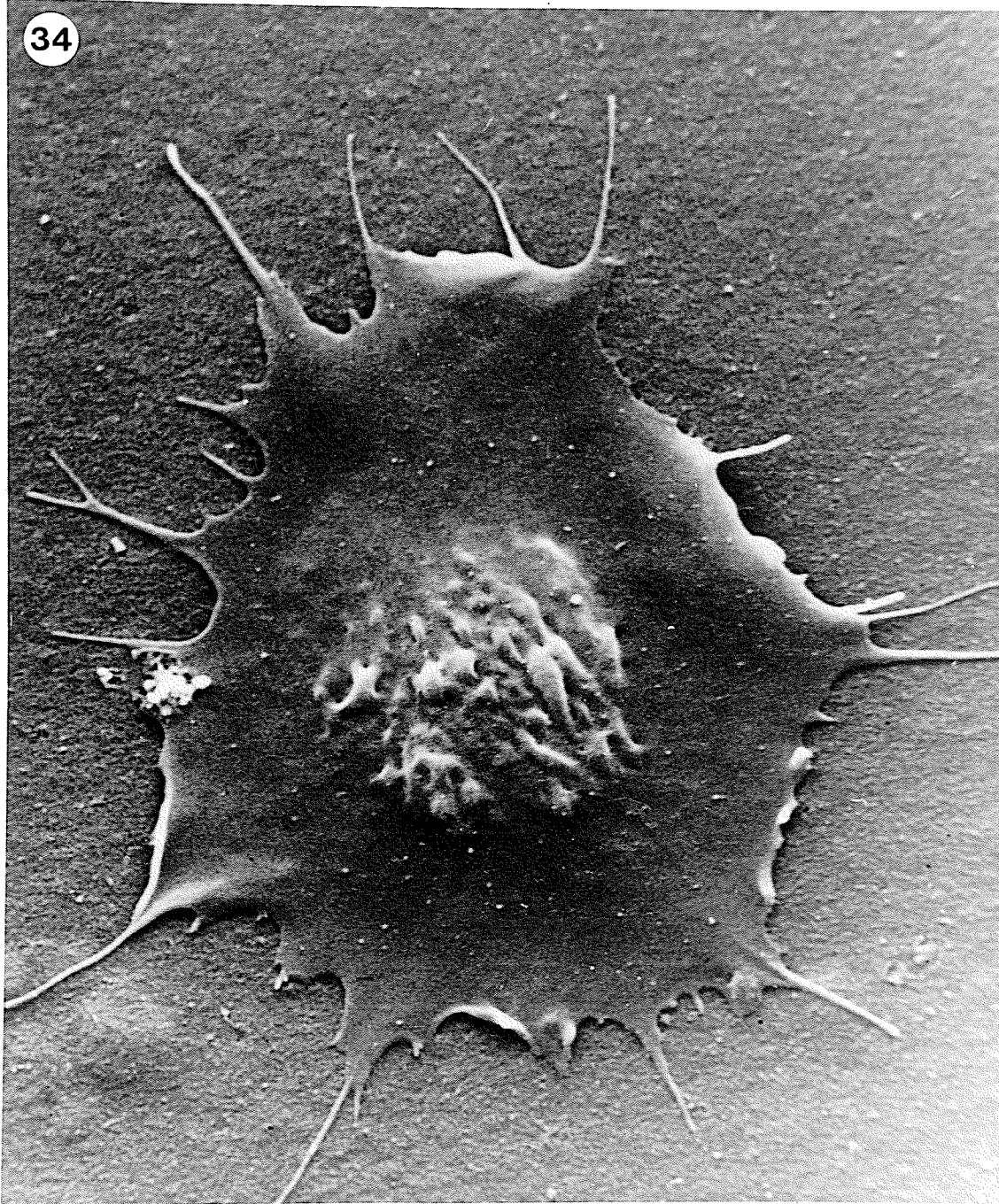
Behaviour of Locomotory PL's In Vitro

Normal cells

Within 1min ET, the first PL's began sending out filopodial and lamellar extensions (Fig. 39a), while most others remained rounded. After 3min ET, lamellopodia were well developed in many PL's, and a mixture of early spreading and intermediate spreading forms were visible (Fig. 39b). Intermediate spreading PL's exhibited ruffling of the cell membrane at the anterior cell periphery which was usually indicative of locomotory activity. By 7min ET, obvious exomigration of PL's occurred, and separation between apposed PL's was evident (Fig. 39c). At this point, most PL's retained intermediate stage

Figure 34. SEM of PL after 20min incubation on BMM. x3,900.

34



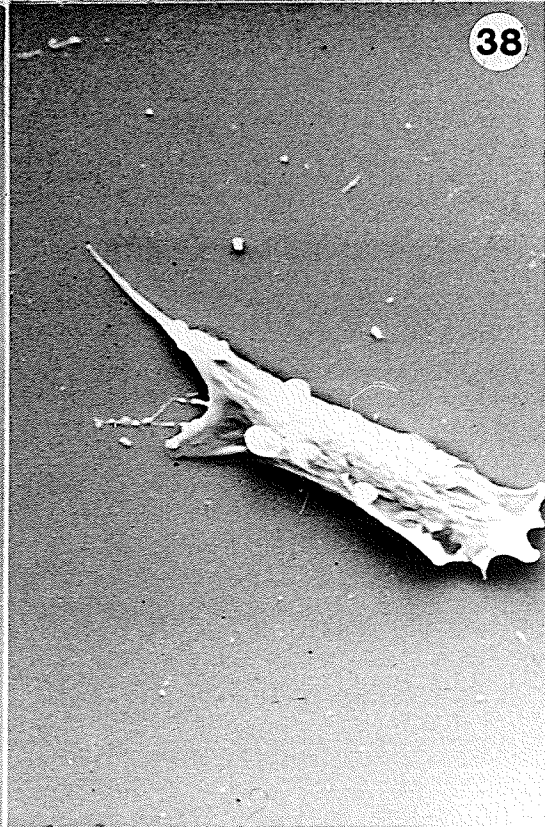
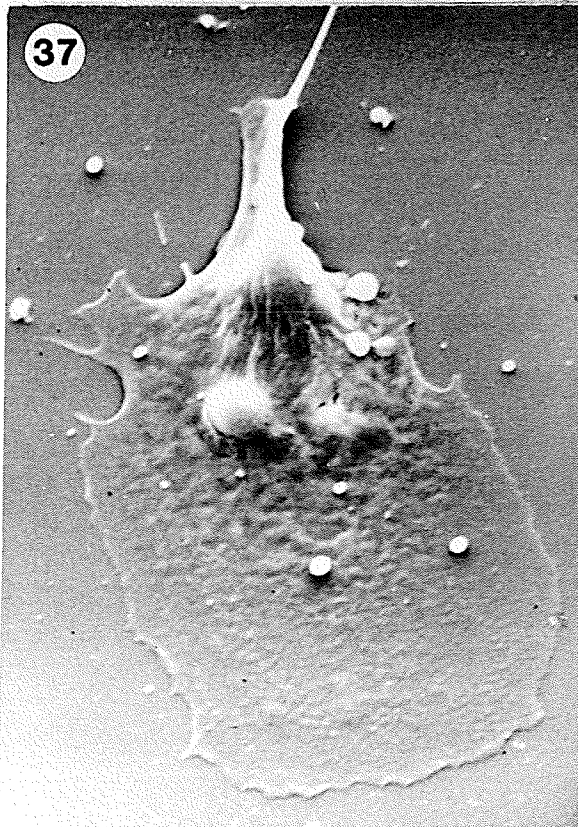
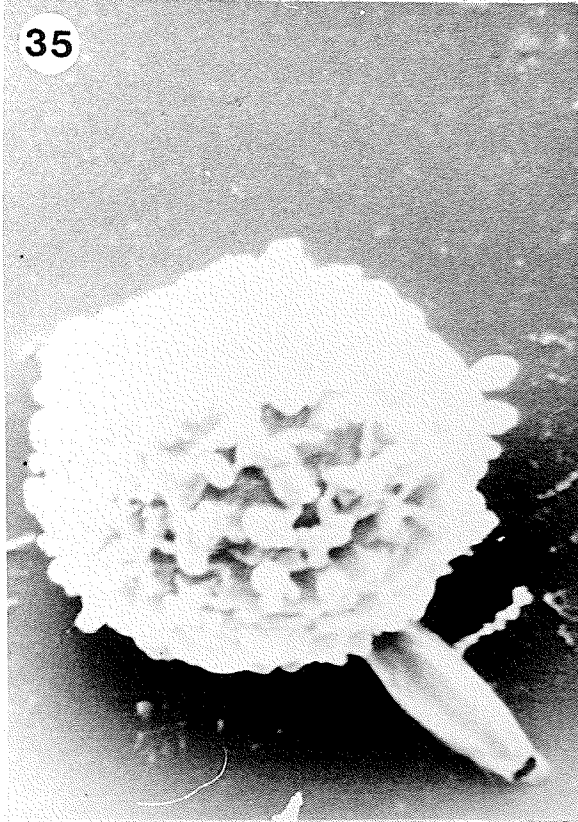
Figures 35-38. SEM of hemocytes from xenically-infected larvae.
Glass substrate.

Figure 35. GR after 20min incubation. Note lack of type I
filopodia. x5,800.

Figure 36. Intermediate spreading stage PL. Note extreme
flattening of lamellopodium. x2,300.

Figure 37. Unipolarized spreading stage PL. Note flattening of
lamellopodium. x2,300.

Figure 38. Poorly attached PL. x2,200.



spreading morphologies, as lamellopodia were broad and not confined to one axis. While not shown in this field, polarized spreading forms were sometimes present in other time-lapse cultures by this interval ET. By 10min ET, most PL's had assumed intermediate spreading morphologies, and continued to migrate away from cell clusters (Fig. 39d). GR's exhibited obvious filopodial extensions. In successive intervals ET, PL's usually retained intermediate spreading morphologies, and GR's indicated slight spreading or flattening of the cell mass (Fig. 39e,f). At 18min ET, some PL's changed direction of movement, and also changed the orientation of the anterior lamellopodium (Fig. 39f).

In the sequence depicted in Fig. 40a-f, PL's from the top of the field continued to exomigrate, and most cells were in the intermediate spreading form. The series of events during PL-GR contact are shown in Fig. 40c-f. First, the PL and GR made peripheral contact (Fig. 40c); in Fig. 40d, the PL lamellopodium ruffled and the cell mass moved forward relative to the leading edge. In Fig. 40e and f, lamellar extension occurred in the new direction of movement, initially at right angles to the original direction, and later (Fig. 40f) in approximately the same direction as in the preceding sequence. The entire sequence, from first contact to exomigration in the new direction, took approximately 15min ET. During the same interval (Fig. 40a-f), GR's (obvious by numerous cytoplasmic granules) progressed from mildly flattened states with obvious filopodia to

Figure 39a-f. Locomotory behaviour of PL's in vitro. Micrographs were taken directly from video monitor. In Fig. 39a, within the first min ET, lamellar (L) and filopodial (F) processes are visible. In Fig. 39b, recognizable intermediate spreading forms are visible (arrow), and in Fig. 39c-f, exomigration is taking place (arrows indicate direction). ET in hrs, min, and sec is indicated in first row of numerals. x450.

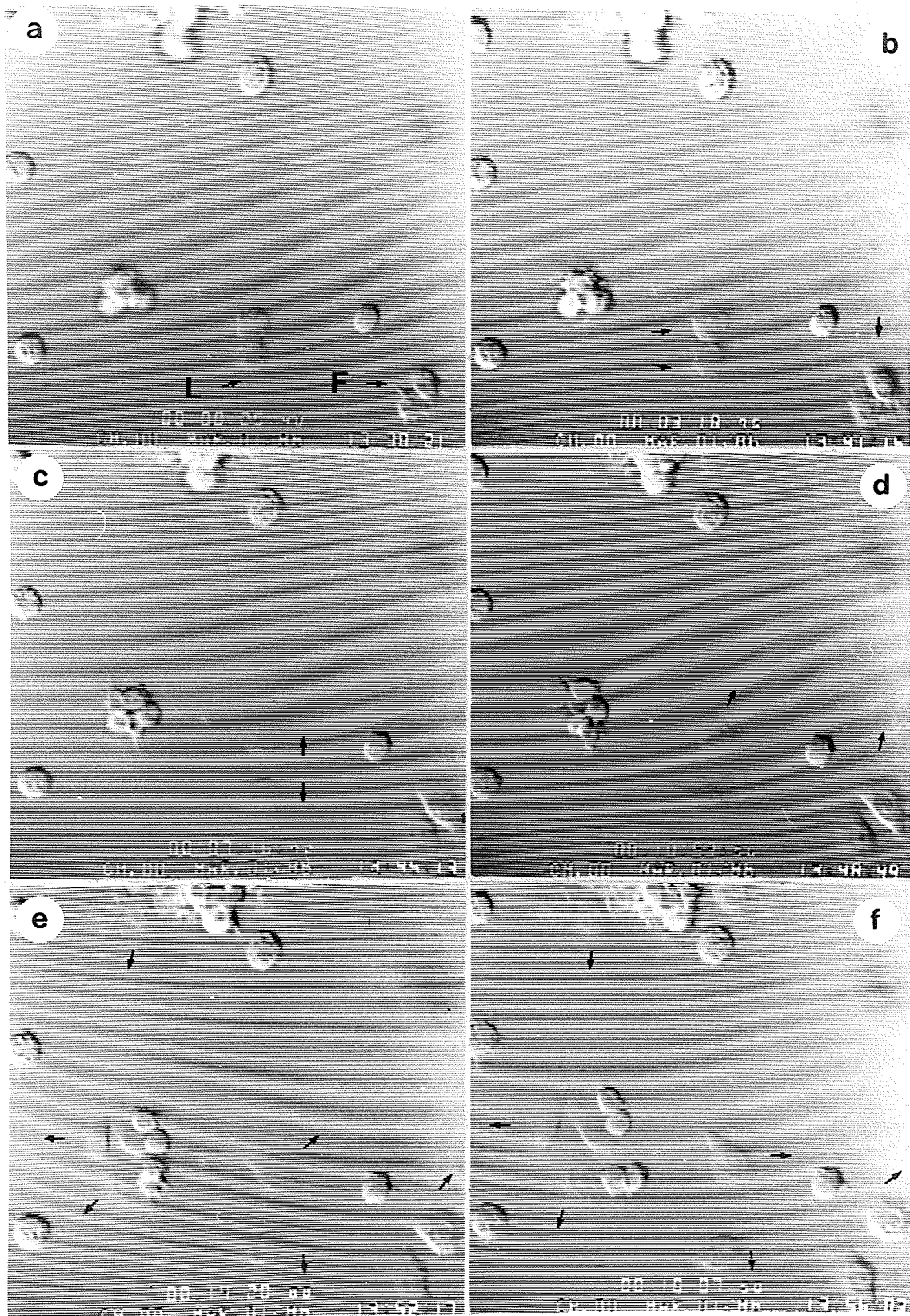
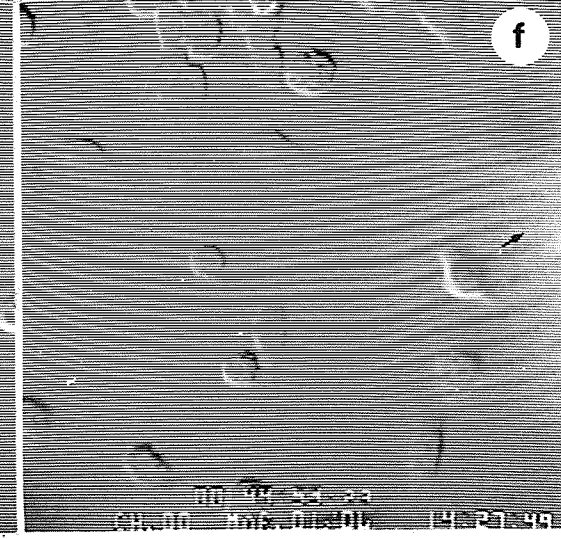
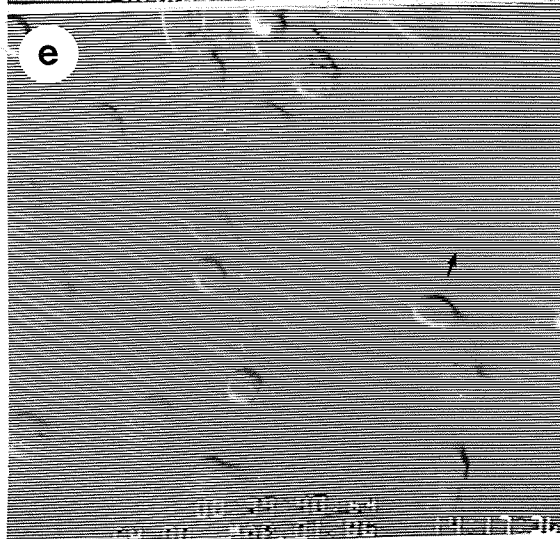
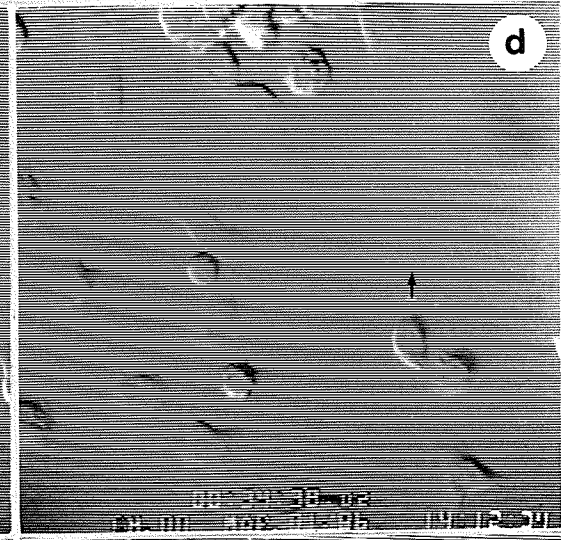
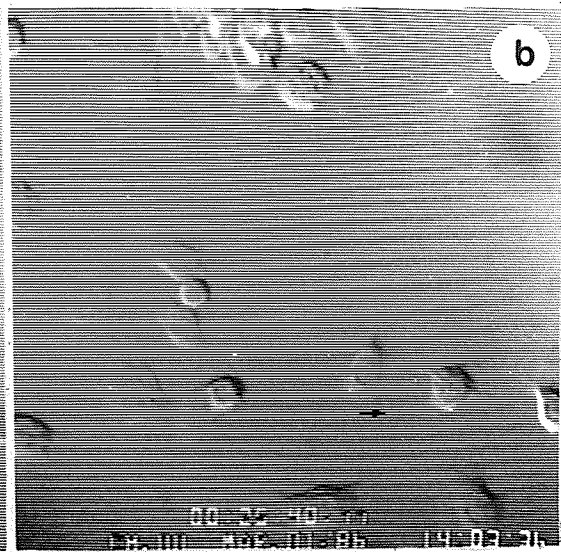
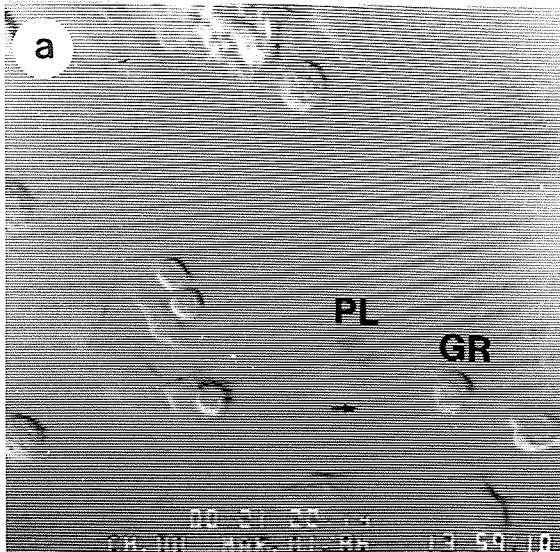


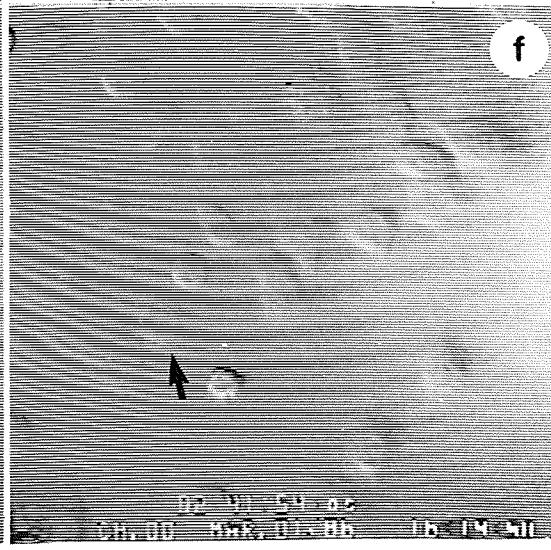
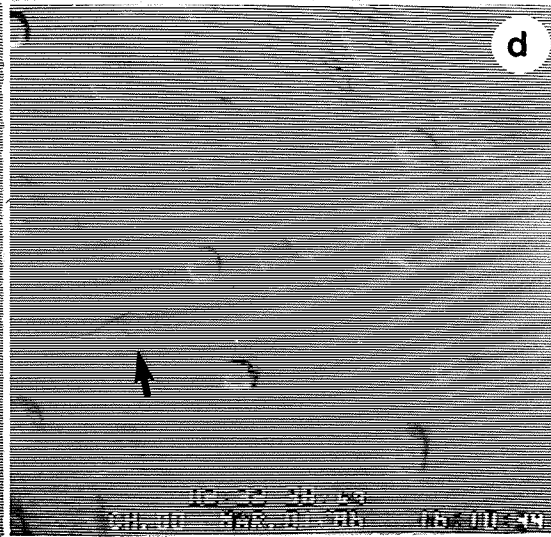
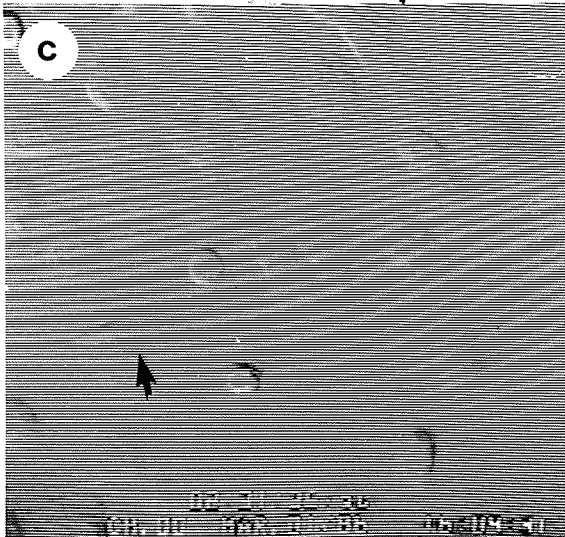
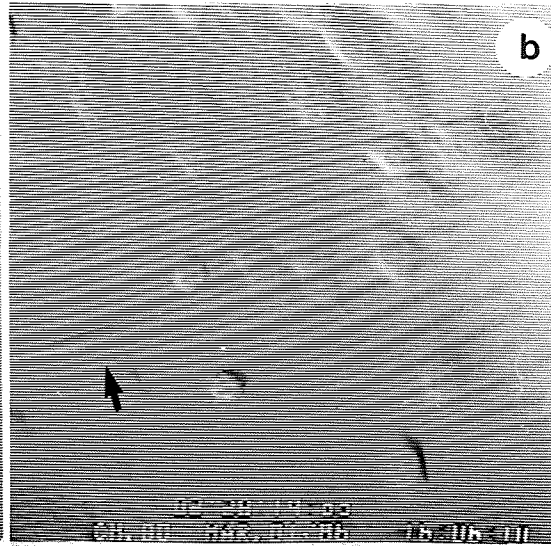
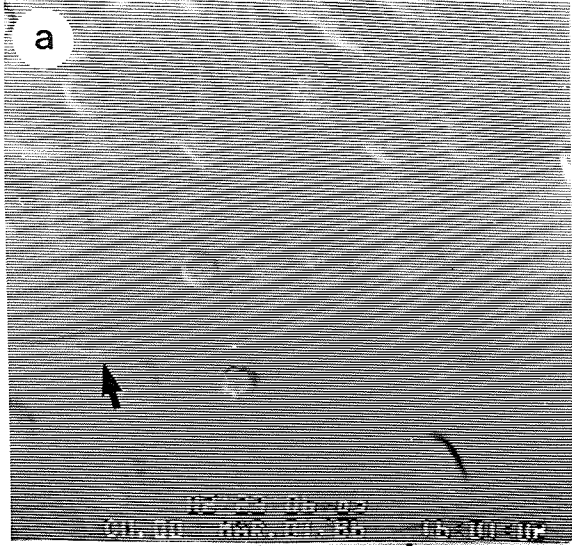
Figure 40a-f. Locomotory behaviour of PL's in vitro. This sequence illustrates PL-GR contact. Small arrows indicate direction of movement; large arrow indicates PL-GR contact. Note that most PL's are in intermediate spreading morphologies and that GR's, especially in comparison with the same cells in Fig. 39a-f, progressively flatten. x450.



extremely flat forms with few obvious filopodia. The cell periphery of these GR's appeared to have either merged between filopodia or merely obscured them.

Proportionally more PL's appeared in uni- or multipolarized morphologies during later intervals ET (Fig. 41a-f). PL's usually locomoted via intermediate spreading, while more PL's locomoted in the unipolarized state during the second 2hr interval ET than in the first 2hrs ET. The basic events of unipolarized locomotion were as follows. Extension of the leading lamella proceeded in 1 main axis, and the posterior half of the cell narrowed (Fig. 41b). Following this, the nucleus appeared to shift anteriorly, accompanied by tapering of the posterior pole of the PL (Fig. 41c). The posterior-most periphery of the PL then appeared to break, initiating posterior retraction towards the anterior pole (Fig. 41d and e). Once unipolarization started, lamellar extension and posterior tapering took at least 8min ET, while posterior retraction occurred within 5min ET after loss of contact with the substratum by the posterior end of the cell. While the time taken by other PL's to undergo each respective sequence varied, the posterior retraction invariably occurred faster than anterior extension/posterior tapering, resulting in rather abrupt net translocation of unipolarized PL's. This was in contrast to the comparatively even rate of locomotion demonstrated during intermediate spreading.

Figure 41a-f. Locomotory behaviour of PL's in vitro. Arrow indicates position of nucleus of PL undergoing unipolarized locomotion. This particular sequence was not used for measurement of rate of locomotion due to the high density of cells. x450.

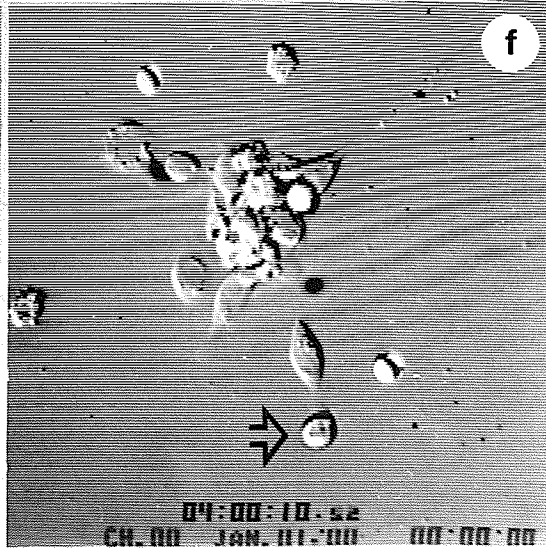
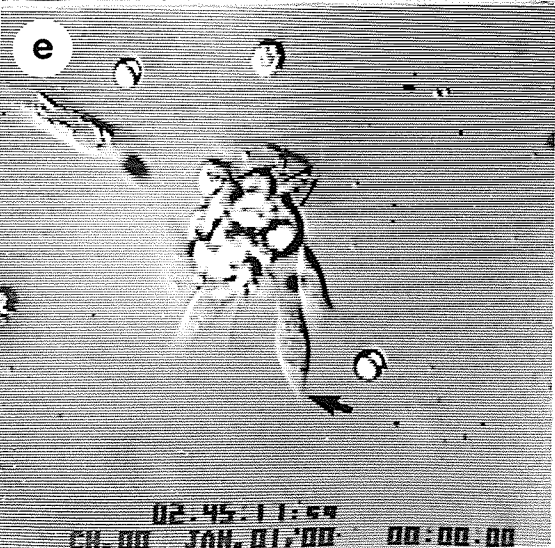
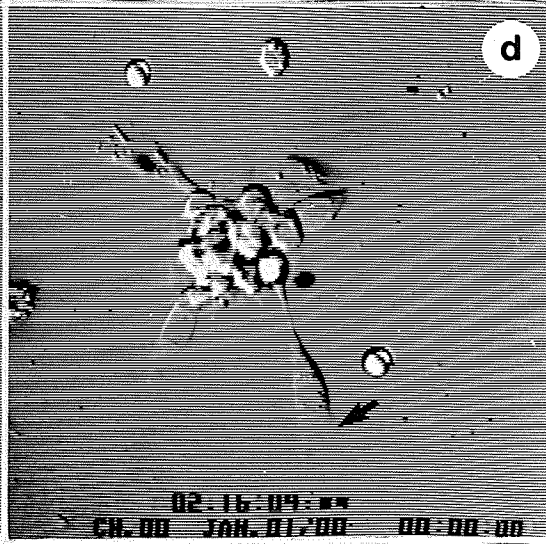
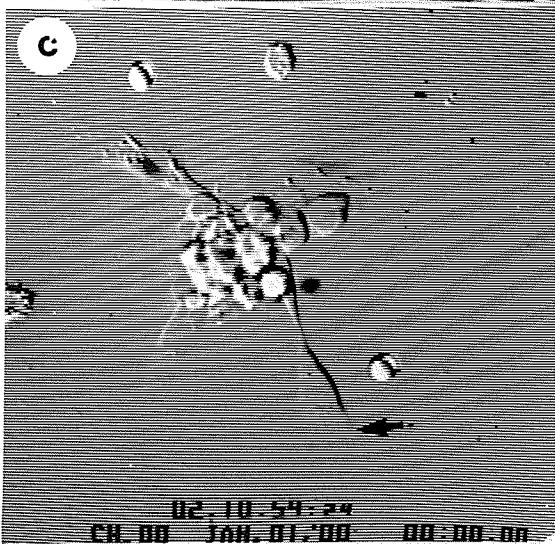
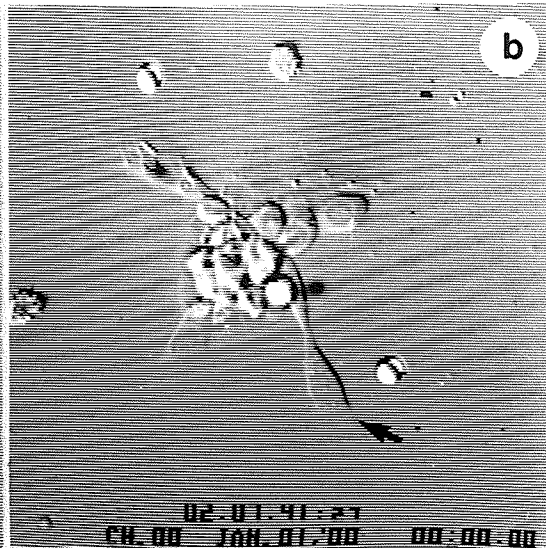
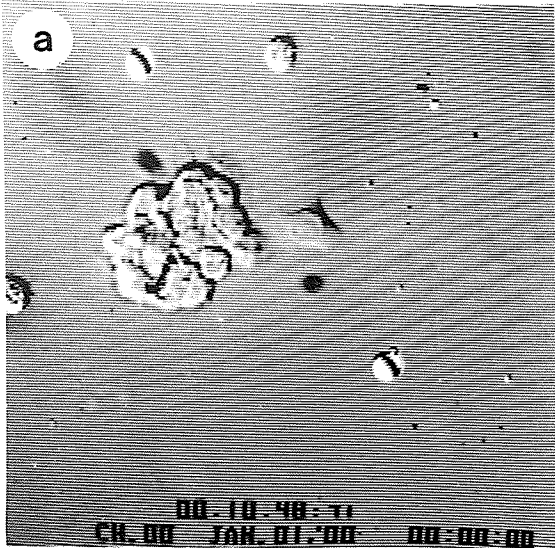


In Fig. 41f, the PL indicated had completely retracted the posterior half of the cell, and intermediate spreading had started. Also noteworthy in the preceding sequence was the relative degree of spreading of GR's, and the increasing number of PL's entering the field. As opposed to PL-GR interaction, PL-PL interaction did not usually result in contact inhibition or change in direction. PL's were capable of crawling over each other, although contact inhibition also occurred.

Treated Cells

Hemocytes from XPI4 and, to a lesser extent, from AxPI4 larvae showed alterations in locomotory activity in vitro. Major differences included: the persistence of early spreading stages, relatively fewer PL's successfully exomigrating from clumps, and inhibited contact-free migration. Fig. 42a and b shows the relative lack of spreading and poor differentiation of lamellopodia of both exomigrating and contact-free PL's from XPI4 larvae. Compared with the similar sequence of normal hemocyte spreading, relatively fewer PL's appeared to be leaving the cluster of cells in the middle of the field, and GR's were refractile and rounded. After 2hrs ET, most PL's still had not dispersed from the clump (Fig. 42c), although several PL's were undergoing unipolarized spreading away from the center of the clump. As successive pictures show, anterior extension/posterior tapering

Figure 42a-f. Locomotory behaviour of AxPI4 treatment group PL's. In Fig. 42b-e, arrows indicate leading edge of a unipolarized PL. Note failure of hemocytes to exomigrate. Arrow in Fig. 42f indicates GR which became detached and drifted to its present position. x450.



took place (Fig. 42b-d); however, posterior retraction never occurred, and PL's regressed posteriorly (Fig. 42e and f). One PL which was successful in exomigrating failed to progress much further than indicated in Fig. 42f. The contact-free PL visible in Fig. 42 appeared to change position only slightly, extending a long, thin cytoplasmic process (Fig. 42f). GR's in XPI4 and XNiC cultures often exhibited brownian motion within the cytoplasm by 3hrs ET, indicative of cell death. As well, GR's in both groups frequently detached from the substrate, and drifted out of the field. AxPI4 and AxNiC cultures were not obviously different from control cultures in these respects.

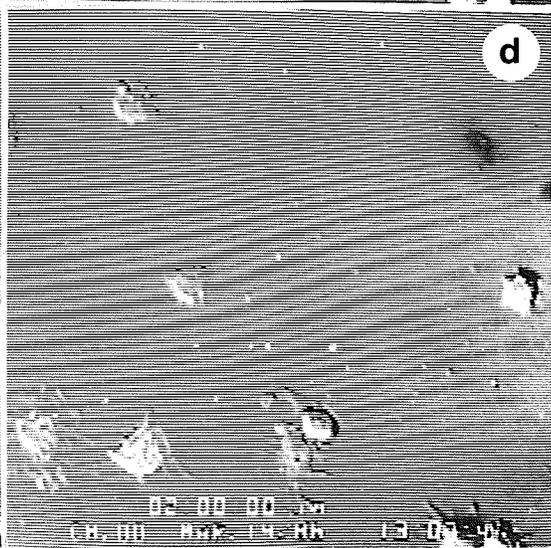
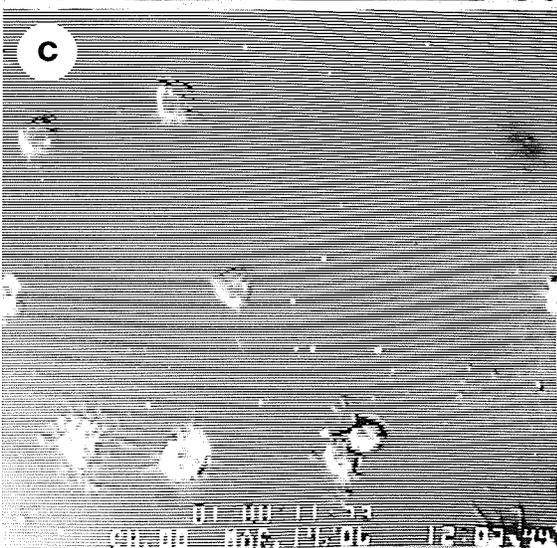
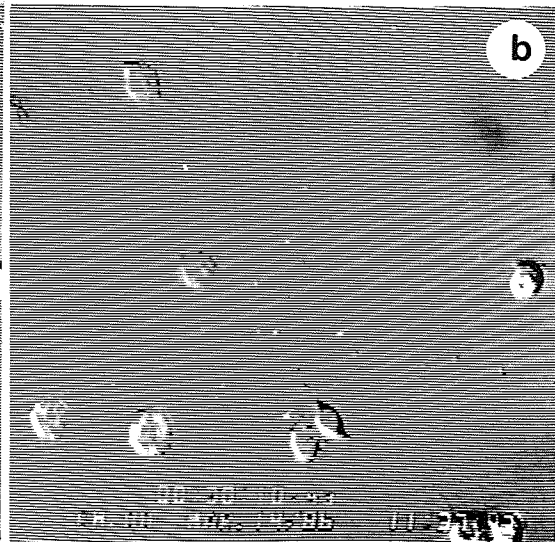
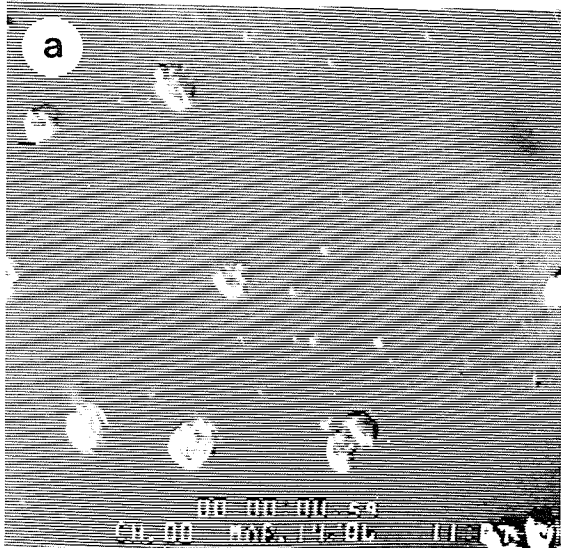
In a time-lapse sequence taken of hemocytes from an XPI12 larvae, profound alterations in GR and PL morphology and behaviour were evident (Fig. 43a-d). PL's had non-existent or poorly developed lamellae, and exhibited no directional locomotion. Both GR's and PL's appeared refractile, and most cells were obviously dead by 2hrs ET. Similar, although not as dramatic results were evident in AxPI12 cultures, and no locomotory behaviour was observed.

Rate of In Vitro Locomotion

Control group

The rate of locomotion of PL's from control larvae during each 15min interval over 4hrs ET is indicated in Fig. 44a. The average

Figure 43a-d. Locomotory behaviour of XPI12 treatment group PL's.
Note lack of movement and obvious cell death. x450.



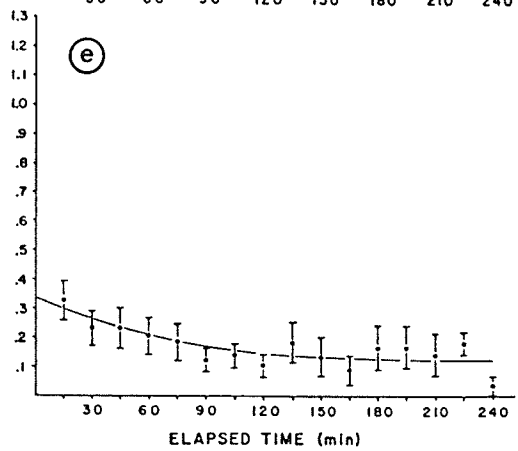
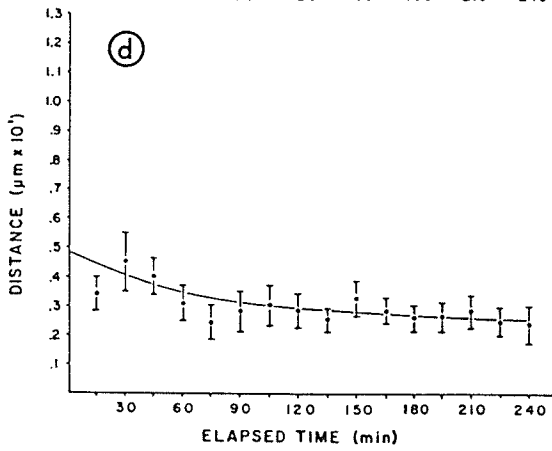
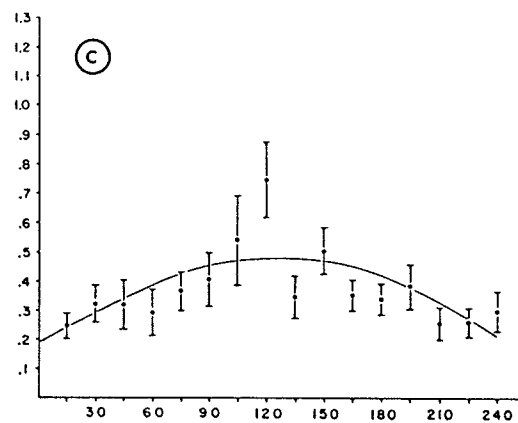
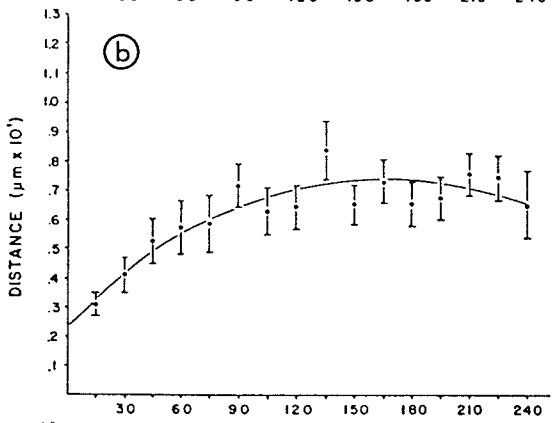
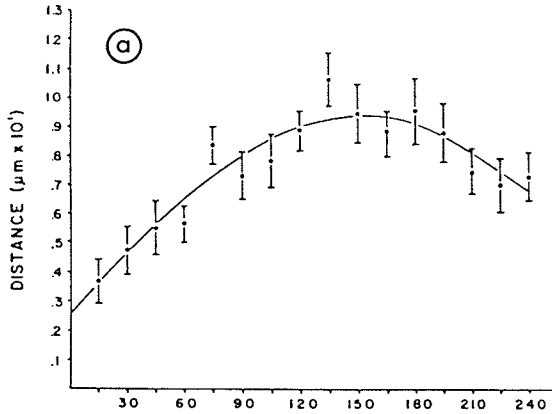
initial speed of PL's was low (approx. $3.7 \pm 0.7\mu\text{m}/15\text{mins}$), and gradually increased until, at 135mins ET, PL speed peaked at an average rate of $10.6 \pm 0.9\mu\text{m}/15\text{min}$. Thereafter, PL locomotory rate declined. The maximum speed of any single PL in control cultures was $30.8\mu\text{m}/15\text{min}$, and this occurred after 15mins ET.

Experimental groups

The overall rate of locomotion of PL's in AxNiC cultures over 4hrs ET was similar to that of control PL's (Fig. 44b). Initially, PL's moved at an average speed of $3.0 \pm 0.4\mu\text{m}/15\text{min}$. As with control PL's, AxNiC PL's peaked in average speed at 135min ET at a rate of $8.4 \pm 1.0\mu\text{m}/15\text{mins}$, whereafter locomotory rate declined. Although the average speeds of PL's from AxNiC trials appeared lower than that of control PL's, especially during the latter 2hrs ET, this was not statistically significant. The maximum speed of any single PL in AxNiC cultures was $22.3\mu\text{m}/15\text{mins}$ at 60mins ET.

The rate of locomotion of PL's from AxPI4 groups, however, was markedly different (Fig. 44c). The average initial speed of PL's was $2.5 \pm 0.5\mu\text{m}/15\text{mins}$; speed reached a maximum at 120mins ET at an average rate of $7.5 \pm 1.3\mu\text{m}/15\text{mins}$. Rate of locomotion of AxPI4 PL's was significantly different from controls at 1, 3 and 4hrs ET. High variation in speed was evident at 105mins and 120mins ET. The maximum

Figure 44a-e Rate of in vitro locomotion. Points indicate mean distance \pm S.E. at 15min intervals. Figures represent: 44a-control; 44b-AxNIC; 44c-AxPI4; 44d-XNIC; 44e-XPI4 cultures.



speed of any single PL in AxPI4 cultures was 27.7um/15mins at 150mins ET. Differences between AxPI4 and AxNiC cultures were significant at 2 and 4hrs ET.

Drastic decreases in rate of locomotion were obvious in both XNiC and XPI4 cultures (Figs. 44d and 44e, respectively). The average initial speed of XNiC PL's was 3.4 ± 0.6 um/15mins, and it peaked at 30mins ET at an average rate of 4.7 ± 1.0 um/15 min, thereafter decreasing. The maximum speed of any single PL in XNiC cultures was 17.7um/min at 75mins ET. The average initial speed of XPI4 PL's was 3.3 ± 0.7 um/min, and it decreased thereafter. The highest speed of any single PL in XPI4 cultures was 27.0um/15mins at 60mins ET. The average speeds of both XNiC and XPI4 PL's were significantly lower than control PL's at 1, 2, 3 and 4hrs Et. Differences between AxNiC and XNiC cultures were also significant at 1, 2, 3 and 4hrs ET, and differences between AxPI4 and XPI4 cultures were significant at 2, 3 and 4hrs ET.

DISCUSSION

Differences between hemocytes of sham-injected and XPI4 larvae could not be detected by TEM at a purely morphological level. The distended RER of PL's from sham-injected and XPI4 group larvae, however, were in contrast to the appearance of control (uninjected)

hemocytes whose RER was not distended, and suggested active protein synthesis (Alberts et al., 1983). Wigglesworth (1979) found that any mechanical injury to the insect integument resulted in an increase in the number of circulating hemocytes, and suggested that PL's play a role in laying down new basement membrane. Since PL's from both sham-injected and XPI4 group larvae appeared to be actively synthesizing protein, xenic S. feltiae probably did not affect hemocyte metabolism at that level. This, however, requires further experimental verification.

The general surface morphology of G. mellonella hemocytes as revealed by SEM was similar to that of other lepidopteran hemocytes (Davies and Preston, 1985), and the major stages of spreading were also similar. The extreme ruffling described in some PL's of Ephestia sp., however, was not observed in G. mellonella PL's. The rounded PL's described by Davies and Preston (1985) were also not seen in G. mellonella.

The dramatic differences between the morphology of spreading hemocytes on glass and on BMM implied that hemocytes adhering to basement membrane in vivo also spread differently than hemocytes on glass substrates. The intense ruffling on the dorsal cell surface of most PL's probably reflected the nature of adhesion between the ventral cell surface immediately under the ruffled area, and the BMM. The other differences exhibited by PL's and GR's on BMM (more filopodia on PL's, fewer on GR's, and the relative lack of distinct

polarization of PL's) may also reflect differences in hemocyte activity. Observation of PL's during in vitro locomotion on BMM was not possible since the thickness of the gel precluded obtaining a clear optical image of the cells.

Although hemocytes were shown to spread differently on BMM, the use of glass substrates for analysis of in vitro spreading and locomotion of hemocytes was nevertheless sufficient to demonstrate normal motility as well as that altered by the parasite. Furthermore, previous literature is based on experiments using glass as the substrate. Arnold (1959) observed Blaberus sp. hemocytes migrating along the inner wall of wing veins, showing that some hemocytes exhibit locomotory behaviour in vivo. Conversely, in vivo hemocyte responses have been observed in vitro. Ratcliffe and Rowley (1975) demonstrated in vitro phagocytosis, and Ratner and Vinson (1983b) demonstrated encapsulation by insect hemocytes in vitro.

Differences in SEM morphology between hemocytes from control and infected larvae suggested that S. feltiae altered PL spreading. Since many PL's from infected larvae were poorly attached to glass substrates, S. feltiae apparently inhibits adherence of hemocytes. Time-lapse observations corroborated this, as some GR's from infected larvae lost contact with the substrate (see Fig. 42f).

Video time-lapse observations of in vitro hemocyte locomotion demonstrated similarities and interesting differences with previously reported work. The basic pattern of locomotion of unipolarized PL's,

involving pseudopodial extension, attachment, and posterior retraction, was similar to that of hemocytes from other insects (Baerwald and Boush, 1970; Davies and Preston, 1985). Contact inhibition between PL's and GR's as it occurred in G. mellonella cultures has also been reported in other insects and invertebrates (Armstrong, 1977; Edds, 1977; Foley and Cheng, 1972; Partridge and Davies, 1974).

There were substantial differences between PL behaviour observed in my study and that reported by Davies and Preston (1985). Davies and Preston (1985) did not report movement of intermediate spreading stage PL's, while I found it was the predominant form of locomotion, especially within the first 2hrs ET. They also noted that ruffling did not occur at the leading edge of PL's during locomotion, while this occurred in almost all instances during locomotion of G. mellonella PL's in my experiments. In fact, this is thought to be a common phenomenon of locomoting fibroblastic cells (Abercrombie, 1970). Davies and Preston (1985) reported filopodia were associated in all cases at the leading edge of PL's, while this was not always true of G. mellonella PL's. As well, Davies and Preston (1985) reported that PL-PL contact usually (presumably) resulted in type I contact inhibition. In my experiments, PL's often crawled over each other, and only occasionally did PL-PL contact result in inhibition of movement.

Davies and Preston (1985) reported that PL locomotory activity ceased at 2hrs ET; this observation was based on data from one

exomigrating PL. I observed PL movement as late as 24hrs ET in vitro (data not shown). This and other differences were probably due to differing culture methods. I used PTU to inhibit melanization and clumping. Brewer and Vinson (1971) indicated that PTU inhibits melanization, and preliminary experiments at the start of my research showed that neither 2% EDTA nor hemolymph dilution were adequate to prevent melanization. Davies and Preston (1985), by contrast, relied on hemolymph dilution. I also used different methods for cleaning glassware, and this may have created substrate differences to which hemocytes reacted.

Clearly, S. feltiae caused a decrease in rate of locomotion of PL's, as well as alterations in spreading morphology. The fact that XPI4 and XNiC preparations showed the greatest declines in PL locomotory speed may indicate that S. feltiae has the greatest effect on all locomotion when paired with X. nematophilus. That AxPI4 preparations showed a significant decrease in PL speed from both AxNiC and control cultures may be due to the ability of S. feltiae to secrete immune inhibitors which destroy antibacterial proteins in G. mellonella (Gotz et al., 1981) and their presumed ability to produce cytotoxic secretions may have allowed normally non-pathogenic bacteria present in the hemolymph to produce septicemia. Possibly, AxNiC cultures did not show significant reductions in PL rate of locomotion due to a lower concentration of such bacteria. Alternately, AxNiC cultures may not have shown significant differences due to the absence of X. nematophilus and suboptimal conditions for nematode growth.

The data have clearly shown that the inhibition of the host response to S. feltiae is associated with an impairment of hemocyte locomotion and alterations in spreading morphology. The precise mechanism of this inhibitory action is unknown. Only with further research can this be elucidated. Since the cytoskeleton is a key element in cell locomotion (Vasiliev, 1982), analysis of the cytoskeleton of PL's is one area in need of investigation. Analysis of this aspect is presented in Chapter 4.

Chapter 4: Microtubule and Microfilament Cytoskeleton

INTRODUCTION

Hemocyte spreading and movement are involved in the process of cellular encapsulation (Gotz and Boman, 1985; Ratcliffe and Rowley, 1979). The failure of G. mellonella hemocytes to encapsulate S. feltiae is reflected by nematode-induced alterations in PL spreading and rate of migration (see Chapter 3), and this may result from impairment of the mechanism(s) governing hemocyte locomotion.

Reports in the literature show a strong link between the cytoskeleton and mammalian fibroblast motility (Abercrombie, 1980; Vasiliev, 1982; Pollard et al., 1984). Microtubules (MT's), for example, are found in almost all instances at the leading edge of locomoting fibroblast, and are probably involved in determining the sites at which stable contact formation occurs (Small et al., 1985) and in stabilization of the lateral edges of spreading cells (Vasiliev, 1982). In addition, they probably influence the microfilament system in accordance to signals from the cell center (De Brabander et al., 1977). The microfilament system consists of different actin-containing domains, including stress fibres and leading-edge networks, and is involved in force-generation and cell membrane interaction (Geiger, 1983). MT's and the microfilamentous system together form a dynamic assembly. Experiments using micro-

tubule inhibitors such as colchicine (Goldman and Knipe, 1973) or actin-binding drugs such as cytochalasin and phalloidin (Alberts et al., 1983), have shown they are instrumental in cell locomotion.

Locomotion of invertebrate hemocytes has not been extensively studied (Abercrombie, 1980), and the arrangement of MT's and F-actin in insect hemocytes has not been described. The present study examines the distribution and orientation of MT's and F-actin in PL's from normal and treated larvae, and demonstrates changes in the cytoskeleton which reflect previously observed differences in PL locomotion and spreading.

MATERIALS AND METHODS

Treatment groups

Hemocytes were examined from early 7th instar G. mellonella larvae from 3 experimental treatments. These were: (1) sham-injection with 10ul of sterile BSS; (2) injection of 10-15 axenic J3 S. feltiae in 10ul sterile BSS; and (3) injection with 10ul axenically-derived serum (collected as previously described). Insect larvae were incubated at 30°C and bled at 1, 2, 3 and 4hrs PI as previously described.

Cell preparation

Approximately 40ul of hemolymph from each larva was diluted into 0.5ml of cold (4°C) GIM with PTU; after thorough mixing, 300ul of dilute hemolymph was transferred onto clean glass coverslips ringed with grease pencil. Coverslips were then incubated at room temperature (22°C) in petriplates lined with moistened filter paper. After 5 or 20min incubation, coverslips were gently rinsed 3 times with BSS and routinely fixed in cold (-20°C) citrated acetone. Coverslips were again gently rinsed 3 times in BSS and processed for either tubulin or actin staining.

Immunocytochemical staining of tubulin

Procedures for indirect immunofluorescence staining of tubulin were modified from Osborne and Weber (1982). Fixed cell preparations were washed 3 times with 1% bovine serum albumin in pH 7.4 phosphate buffered saline (BSA/PBS), and then incubated for 1hr at 37°C in dark, humid containers. After removal of excess BSA/PBS, approximately 25ul of 1°antibody (Ab) was added to each preparation, and these were incubated for 1hr as described above. Primary Ab was removed with 3 washes of 5min each of BSA/PBS. Excess BSA/PBS was again removed, and approx. 25ul of 2°Ab conjugated with fluorescein isothiocyanate (FITC) was added to each coverslips, followed by a 1hr incubation. Cover-

slips were then washed with 3 changes of 5min each of BSA/PBS and prepared for fluorescence microscopy.

The 1°Ab was rabbit anti-sea urchin tubulin (kindly supplied by Dr. K. Fujiwara, Harvard Medical School) used at a 1:50 dilution in PBS. The 2°Ab was FITC-conjugated goat anti-rabbit IgG (Miles-Yeda Laboratories) used at a dilution of 1:16 in PBS. Controls consisted of preparations when the 1°Ab was omitted and cells were given an additional 1hr incubation in BSA/PBS, or others where 25ul of rabbit pre-immune serum was used instead of 1°Ab. Both controls were negative.

Actin localization

Fixed cells on coverslips were rinsed 3 times with PBS and stained in the dark at 25°C in 25ul of 5ug/ml rhodaminyphalloidin (kindly provided by Professor Dr. Th. Wieland, Heidelberg, FRG) in PBS for 20min. Staining was followed by three, 5min rinses in PBS. Actin and tubulin-stained cell preparations were mounted on slides with PBS/glycerin (4:1), and examined on a Zeiss Photo II microscope equipped with a Zeiss III RS epifluorescence condenser and neofluoar objectives. Photomicrographs were taken using either Kodak Tri-X Pan (ISO 400), Kodak Ektachrome daylight (ISO 400) or Ilford XPI-400 film. Black and white prints were made on Ilford Ilfospeed (glossy, single weight) F3 photographic paper.

RESULTS

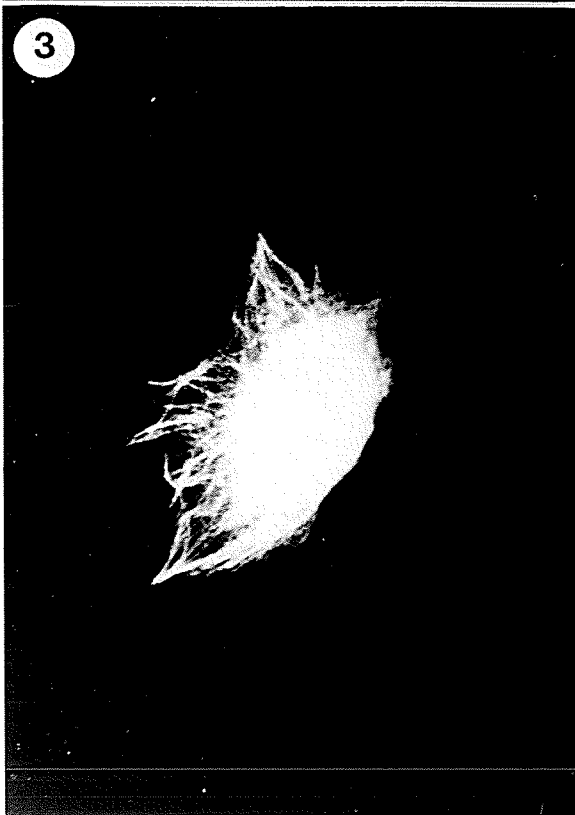
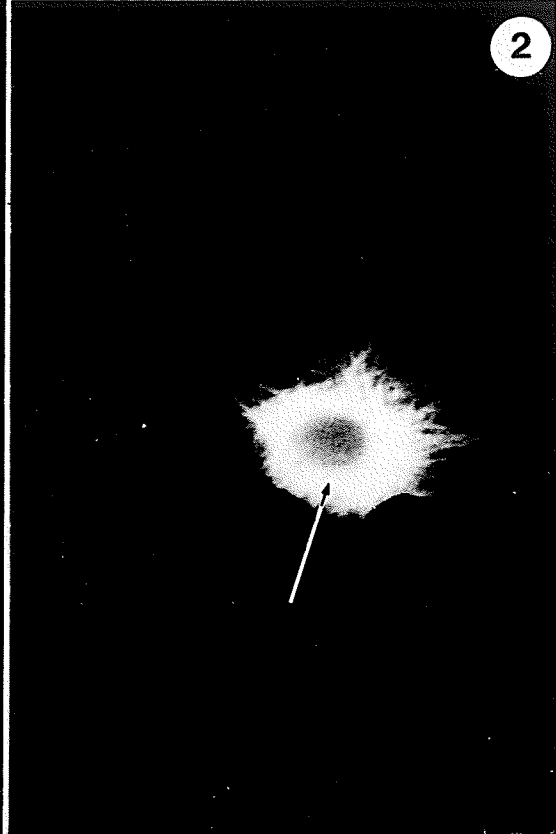
Microtubule Localization

To establish the existence and organization of the MT cytoskeleton in normal G. mellonella hemocytes, and to form a basis for comparison with hemocytes from treated larvae, PL's were examined at four different stages of settling and spreading. These stages correspond to those described during previous time-lapse observations of cultured cells and to SEM observations.

Stage 1 - early settling and spreading

PL's were rounded and had few cytoplasmic extensions besides filopodia after 5min incubation, and constituted the early spreading stage. The anti-tubulin staining pattern showed a brightly fluorescing band in the circumnuclear area (Fig. 1). In those cells where limited lamellar extensions had formed, faintly fluorescing bundles of MT's emanated from the perinuclear region and extended to the cell periphery (Fig. 2). PL's exhibiting early to intermediate spreading revealed a radially-oriented network of microtubules extending into the lamelloplasm, as well as the bright perinuclear staining (Fig. 3).

Figures 1-4. Fluorescence micrographs showing MT distribution in successive early spreading stages (Figs. 1-3) and early intermediate stage (Fig. 4). Arrow in Fig. 2 indicates perinuclear region and in Fig. 4 indicates MT's following cell periphery. x1,030.



Stage 2 - intermediate spreading

Numerous PL's in intermediate stages of spreading were found after 20min incubation. These cells had well-defined lamellopodia; perinuclear anti-tubulin staining was less prominent while the radial pattern of fluorescing MT's were more prominent, with some appearing to follow the cell periphery (Fig. 4). Through-focus observation of these cells showed that near the upper cell surface, a basket-like weave of fluorescent strands occupied the area between the nucleus and the plasma membrane (Fig. 5a). In contrast, the lower sub-nuclear area showed a brilliant zone near the nucleus where fluorescing strands emerged from the nuclear area and crossed as they extended through the cytoplasm (Fig. 5b). Finally, at the lower cell-surface, fine fluorescent strands traversed the lamellopodium in a fan-like array, and reach the cell periphery (Fig. 5c); a few strands bent back towards the nucleus from the periphery. The extent of the fluorescence pattern in lamellopodia varied, from relatively thin, diffuse fluorescent strands in some PL's (Fig. 6), to relatively straight, unbranched strands radiating through the lamellopodia in other cells (Fig. 7).

Stage 3 - polarized spreading

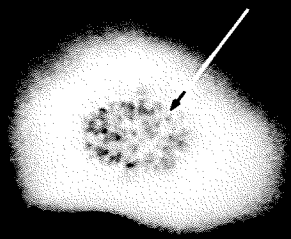
PL's which demonstrated distinct polarization in one or more directions were found after 20min incubation. Fully spread, uni-

Figures 5-7. Fluorescence micrographs showing MT distribution in intermediate spreading stage PL's.

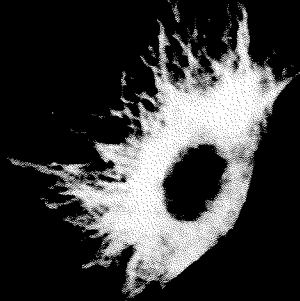
Figure 5a,b,c. MT organization at different focal planes. Arrow indicates perinuclear MT's. xl,250.

Figures 6,7. Variation of MT's in lamellae. xl,030.

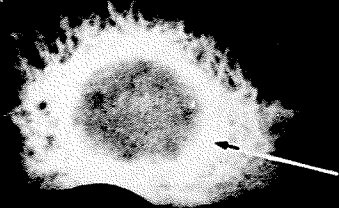
5a



6



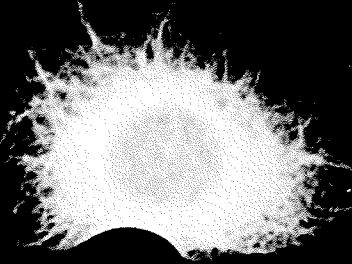
5b



7



5c



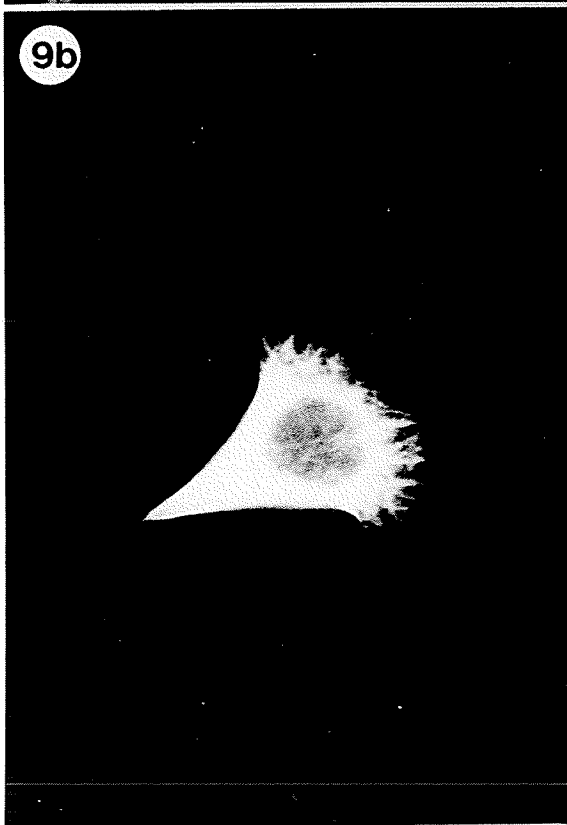
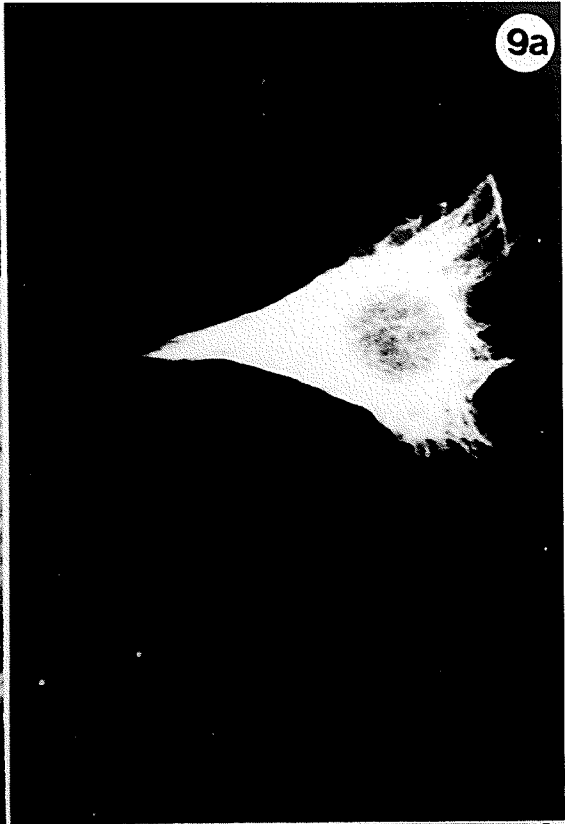
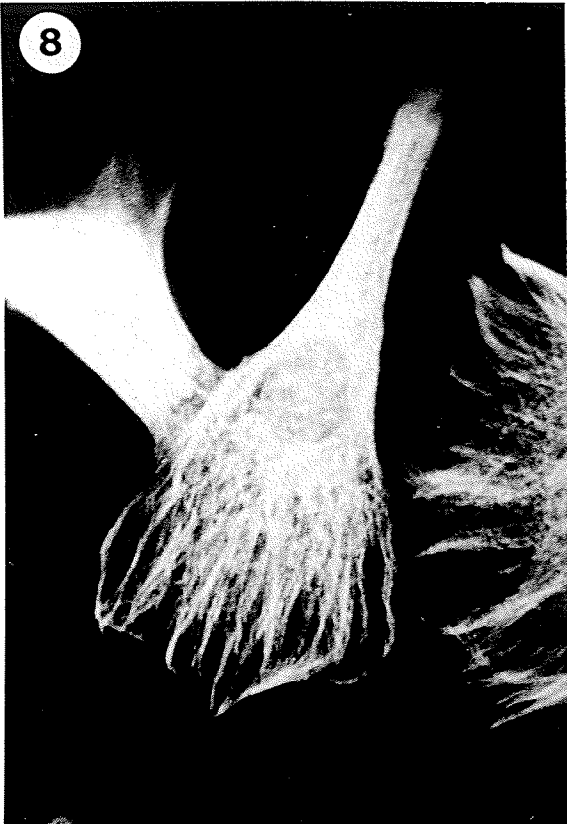
polarized PL's displayed relatively straight bundles of MT's emanating from the perinuclear region, fanning-out to the convex, anterior edge of the cell (Fig. 8). Some bundles of MT's curved and travelled along the cell periphery, while MT's were present in parallel bundles in the posterior half of such PL's. The perinuclear band was less intensely fluorescent in unipolarized cells than in previous stages.

PL's undergoing posterior retraction/anterior ruffling were also evident in many preparations. Posterior to the nucleus of these cells, individual MT bundles were not discernable since they were tightly packed and intensely fluorescent (Fig. 9a). The nucleus was displaced anteriorly, and the perinuclear region was also brightly fluorescent. During later stages of posterior retraction, the trailing end was still packed with MT's, while MT's at the anterior end diverged broadly from the perinuclear zone and traversed the lamellopodium to the extended cell periphery (Fig. 9b). During the terminal phase of retraction, the MT cytoskeleton was more easily discerned in the posterior portion of the cell, with MT's broadly dispersed through widened lamellopodium (Fig. 9c).

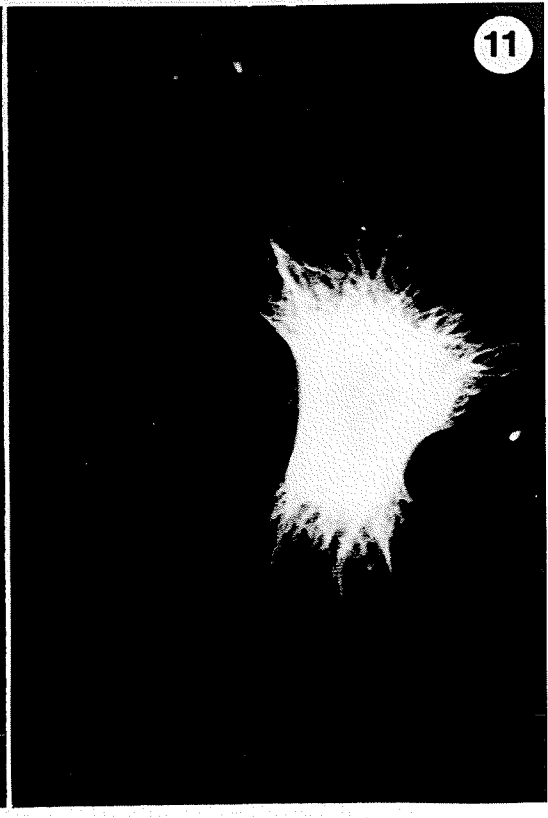
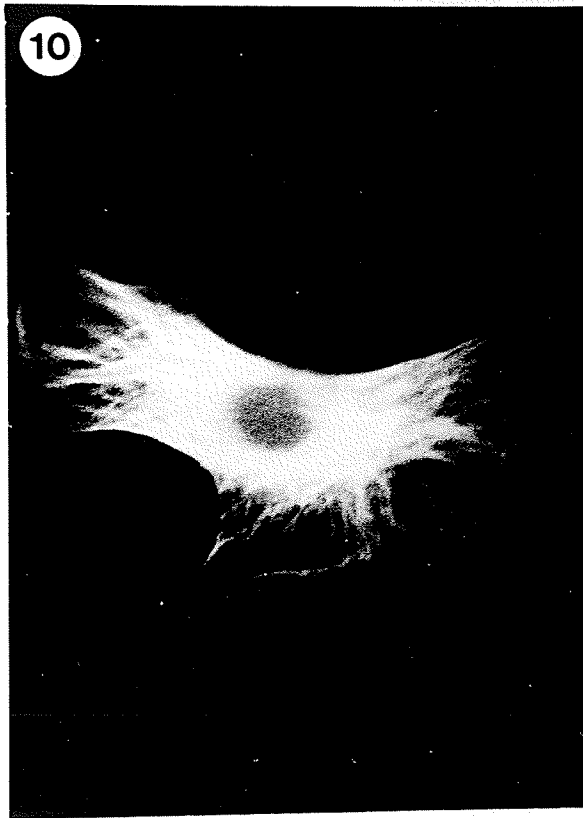
Markedly bipolar cells usually exhibited fan-shaped spreading of MT bundles from the perinuclear area into both opposing lamellopodia. In some bipolar PL's, bending of the terminal branches of MT's was pronounced, and they followed the cell periphery (Fig. 10). In less-spread cells, this was not as noticeable, and terminal MT bundles were less dispersed (Fig. 11). Also, the perinuclear band was more

Figure 8. Fluorescence micrograph showing MT distribution in a unipolarized PL. x1,450.

Figure 9a,b,c. MT distribution in unipolarized PL's at successive stages of posterior retraction. x1,030.



Figures 10,11. Fluorescence micrographs showing MT distribution
in bipolar PL's. x1,430.



intensely fluorescent, and few individual bundles of MT's were observed close to the nucleus. The peripheral distribution of MT's in bipolar cells varied, depending on whether lamellopodia were convex or concave (Figs. 12, 13).

Besides the easily classified shapes noted above, there were other variations of PL shape which displayed unusual configurations of MT's (Figs. 14, 15 and 16).

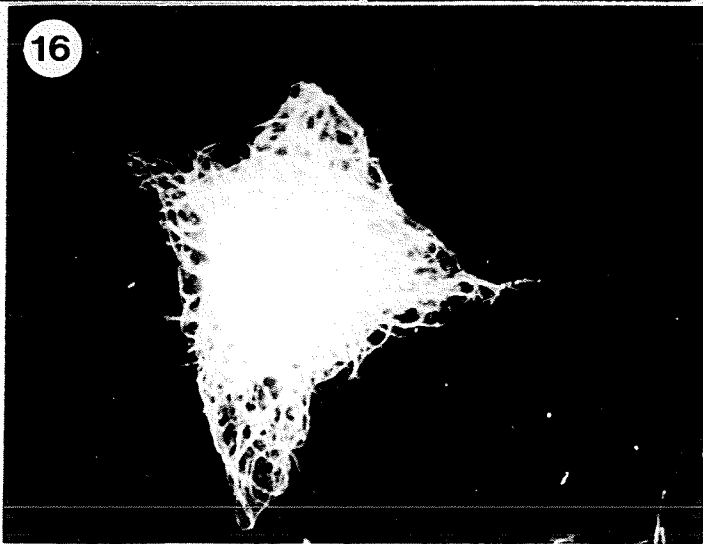
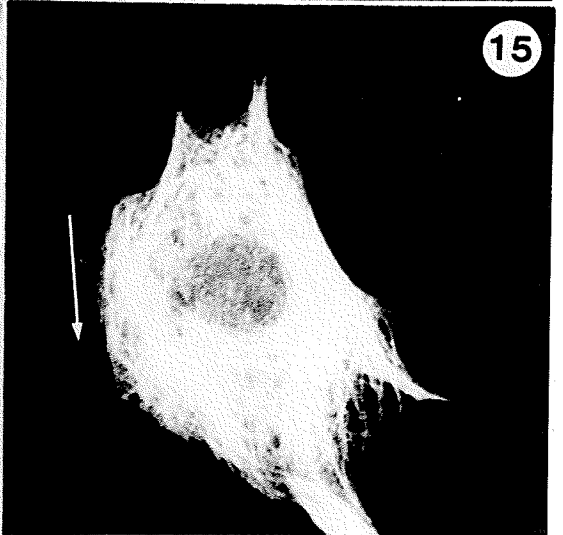
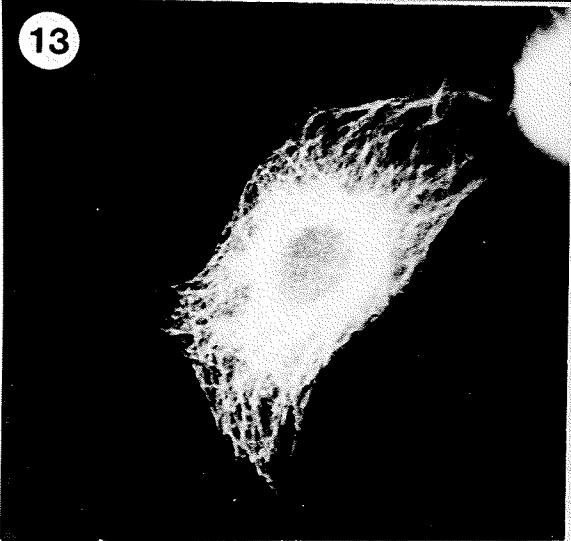
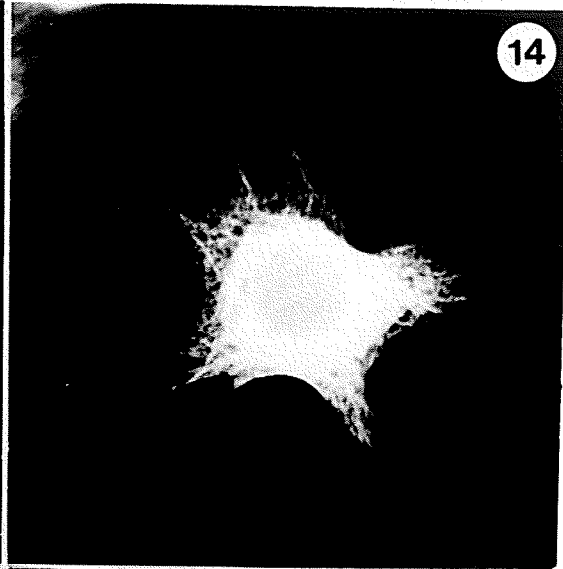
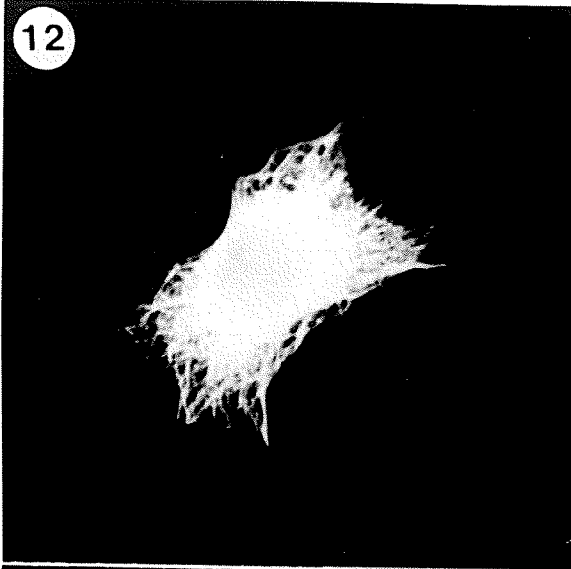
Stage 4 - fully spread, non-polarized

Most fully spread, non-polarized PL's were found in samples incubated for 20min, and displayed a typical perinuclear band of MT's, and a fine, diffuse array of MT's in the lamellopodia, radiating towards the cell periphery (Fig. 17). Some fully spread PL's showed extensive curving of terminal MT bundles (Fig. 18), while other PL's had relatively thick MT bundles which curved only slightly (Fig. 19). In only a few PL's was the MT network configured as shown in Fig. 20, where relatively few, brightly fluorescing, highly bent MT's occupied the lamelloplasm.

F-Actin Distribution

The pattern of fluorescence observed in PL's stained for F-actin with rhodaminyphalloidin was markedly different from that

- Figures 12-16. Fluorescence micrographs showing MT distribution in bi- and multipolar PL's.
- Figures 12,13. Variation of MT organization in lamellae of bipolar cells. Density and distribution varied according to cell shape. x930.
- Figures 14-16. MT distribution in multipolar PL's. Arrow in Fig. 15 indicates portion of PL lacking MT's. x930.



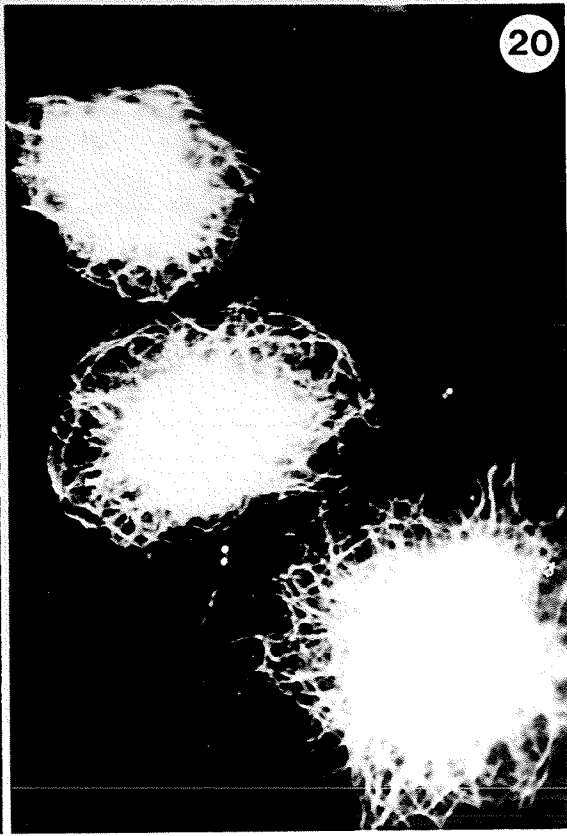
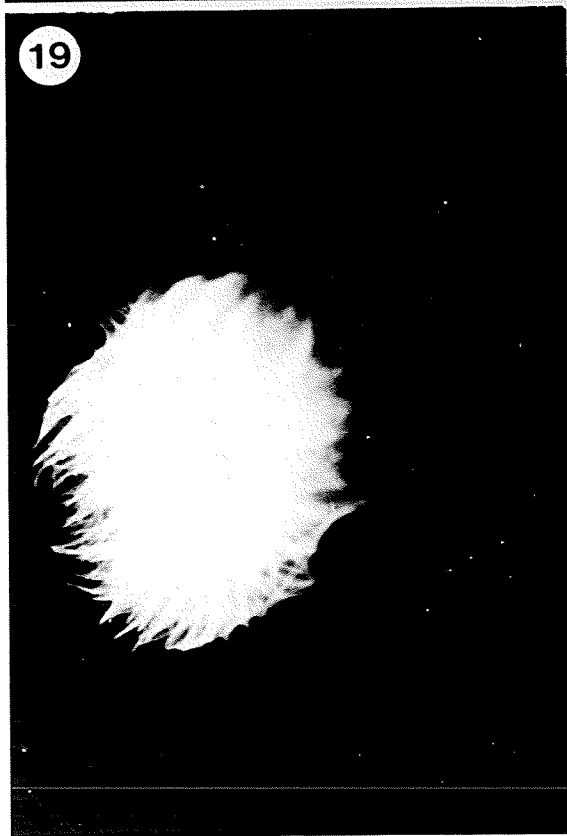
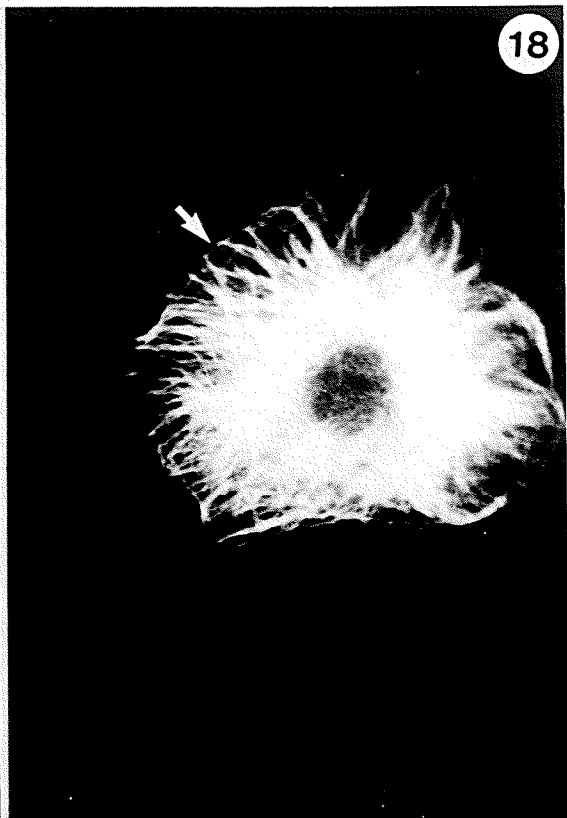
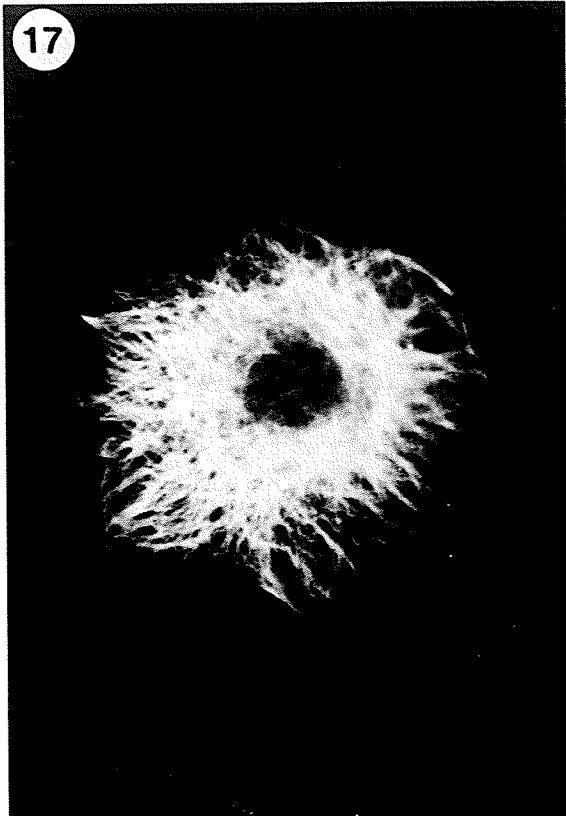
Figures 17-20. Fluorescence micrographs showing variation in MT distribution of fully spread, non-polarized PL's.

Figure 17. MT's in this PL are in fine bundles and are relatively straight at the cell periphery. x1,130.

Figure 18. MT's are in thicker bundles and bend at cell periphery. x1,130.

Figure 19. MT's in this PL are in thick, densely-packed bundles. x1,130.

Figure 20. MT's appear to be in thick, sparsely-packed, highly bent bundles, and perinuclear region is intensely fluorescent. x1,030.

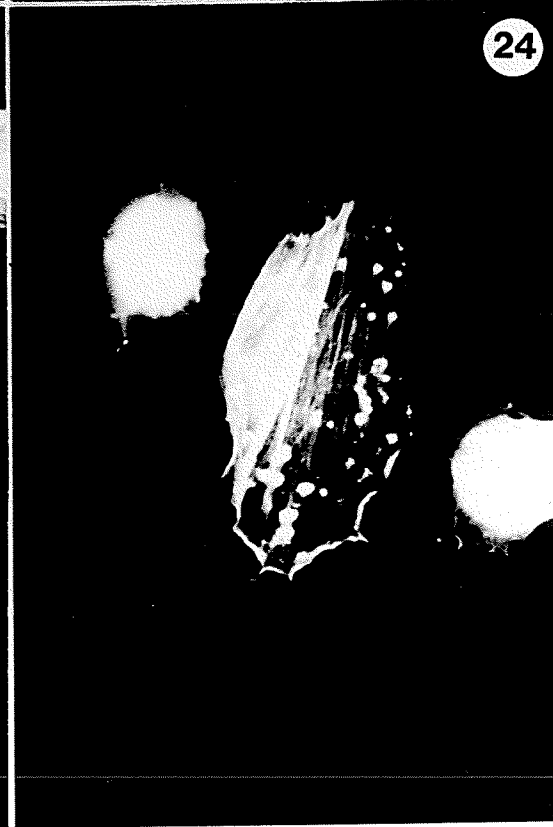
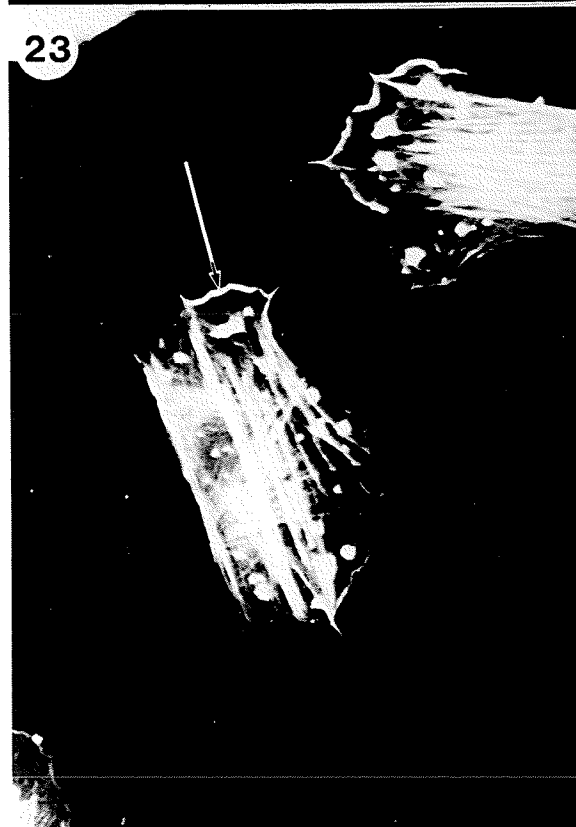
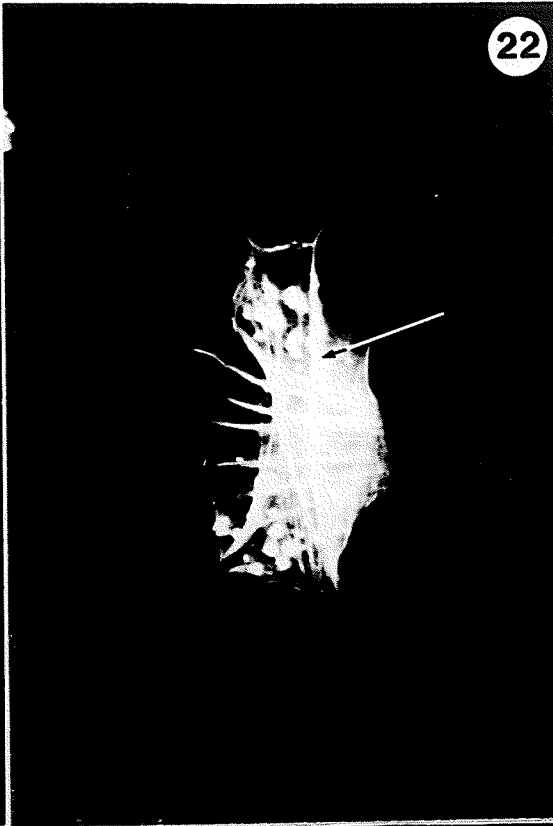
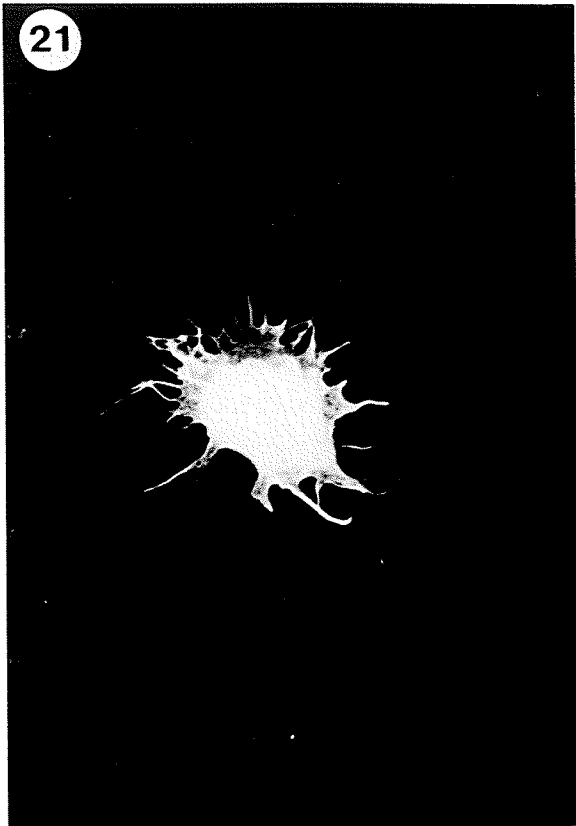


observed in anti-tubulin stained cells. Early spreading stages of PL's revealed a brightly fluorescing area around the nucleus, and a diffuse pattern of fluorescence in the cytoplasm (Fig. 21). Bright bands of fluorescence were also visible in filopodia, and appeared to terminate in the cortical lamelloplasm. In later stages of lamellopodial extension, the pattern of fluorescence was more distinctive. Large, brilliantly fluorescing bundles of F-actin extended from filopodia at the ruffled edge of the cell, and ran perpendicular to lateral bundles, often extending across the entire cell (Fig. 22). A diffuse, fuzzy network of F-actin, apparently composed of many fine actin filaments, was distributed throughout the lamelloplasm. A more intense fluorescence was evident around the nuclear region. Scattered fluorescent granules were also evident throughout the cytoplasm of almost all intermediate and later spreading stages.

In other intermediate spreading stages, the main orientation of F-actin bundles was perpendicular to the anterior pole of the cell (Fig. 23). In such PL's, F-actin comprised the subplasmalemmal zone between filopodia, and F-actin bundles in filopodia did not usually extend past this zone (Fig. 24). In other PL's, F-actin bundles crossed obliquely along the lateral axis of the cell (Fig. 25).

F-actin bundles in unipolarized PL's were mainly oriented in an anterior/posterior axis (Fig. 26). The anterior-most edge of unipolarized PL's usually had subplasmalemmal bundles of F-actin between filopodia, and a network of fine F-actin bundles in the

- Figures 21-24. Fluorescence micrographs showing F-actin distribution in PL's at early and intermediate spreading stages. x930.
- Figure 21. Early spreading stage PL showing diffuse pattern of fluorescence in lamella and F-actin bundles in filopodia.
- Figure 22. Arrow indicates lateral bundle of F-actin in intermediate PL. Note perpendicular bundles.
- Figure 23. Arrow indicates subplasmalemmal F-actin in intermediate PL.
- Figure 24. Intermediate stage PL in which F-actin is mainly oriented parallel to leading edge.



lamelloplasm. Axial bundles of F-actin did not always extend from the leading edge of PL's, appearing to originate in the lamellar cortex (Fig. 27). Unipolar PL's with less definite leading edges often had F-actin bundles which crossed at acute angles, originating in filopodia along a broad arc of the leading edge (Fig. 28). PL's which were distinctly bipolar had broad, definite bands of F-actin extending from one pole to the other (Fig. 29). PL's of indistinct or multiple polarity often had F-actin bundles which crossed at several different angles and in various orientations (Fig. 30). F-actin bundles in adjacent areas of touching or overlapping cells often were aligned in the same direction (Figs. 31, 32).

PL's which were fully spread, non-polarized had a variety of different F-actin configurations (Figs. 33, 34, and 35). Large F-actin bundles were occasionally not prominent, but the fine cytoplasmic network of F-actin was invariably present.

Cytoskeleton of PL's From Treated Insects

Anti-tubulin staining

The MT cytoskeleton of PL's was not significantly different in larvae infected with axenic nematodes at 1, 2, and 3 hrs PI, or in PL's of larvae injected with serum 2, 3, and 4hrs PInj. However, by 4hrs PI with nematodes, alterations in the pattern of anti-tubulin

Figures 25-28. Fluorescence micrographs showing F-actin distribution in intermediate (Fig. 25) and unipolarized (Figs. 26-28) spreading stage PL's.

Figure 25. Intermediate spreading stage PL (arrow) with oblique bundles of F-actin. x1,170.

Figure 26. Unipolarized PL (arrow) with longitudinally-oriented F-actin bundles. Also visible are cytoplasmic, filopodial, and subplasmalemmal F-actin bundles. x1,100.

Figure 27. Unipolarized PL (arrow). Note subplasmalemmal F-actin at leading edge. x1,100.

Figure 28. Unipolarized PL (arrow) with less definite leading edge. x1,170.

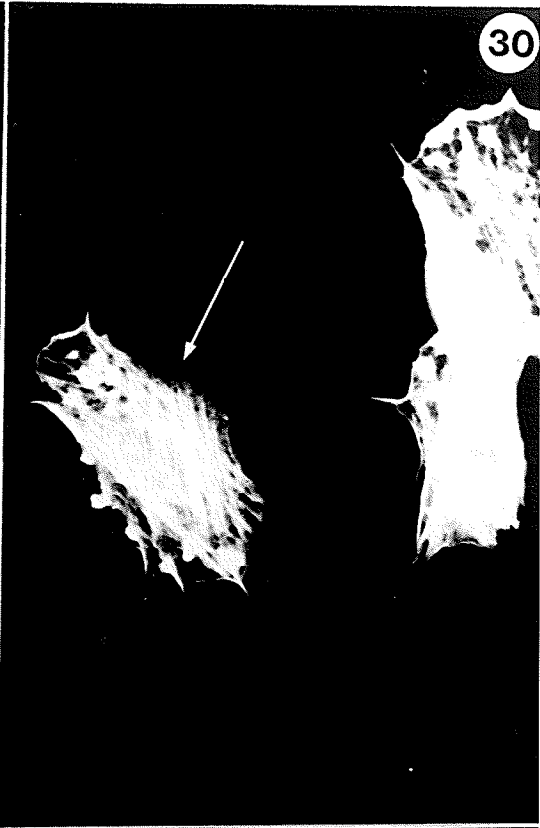


Figures 29-32. Fluorescence micrographs showing F-actin distribution in PL's.

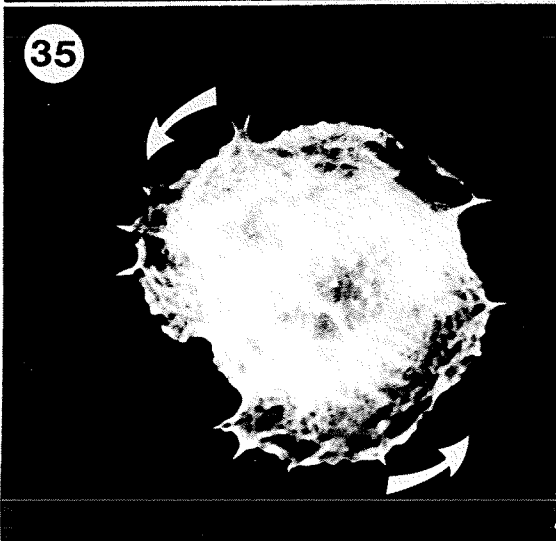
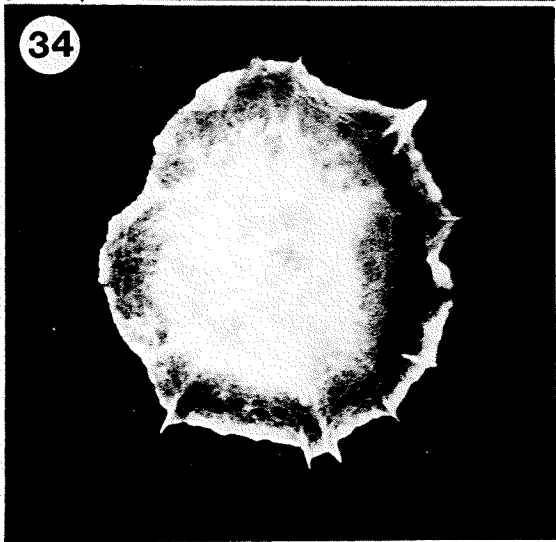
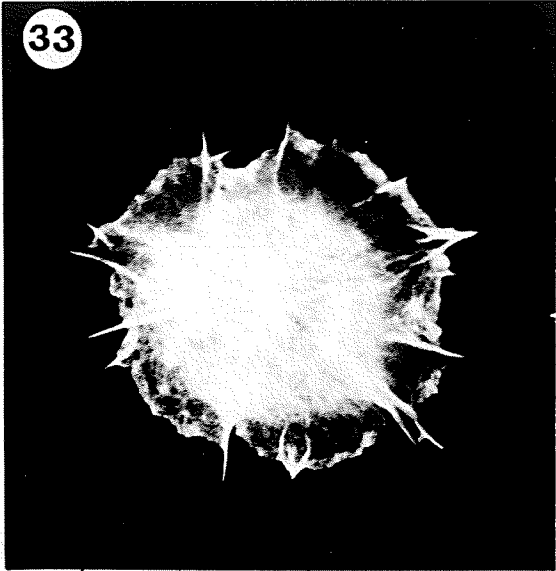
Figure 29. Bipolar PL. Note F-actin bundles extending between poles. x1,100.

Figure 30. F-actin distribution in multipolar PL's. x1,100.

Figures 31-32. Overlapping PL's. Arrows indicate F-actin bundles in adjacent cells aligned in same direction. x1,170.



Figures 33-35. Fluorescence micrographs showing F-actin distribution in fully spread, non-polarized PL's. Note variation in filopodial F-actin bundles. PL in Fig. 35 is undergoing torsion (direction indicated by arrows). x1,220.



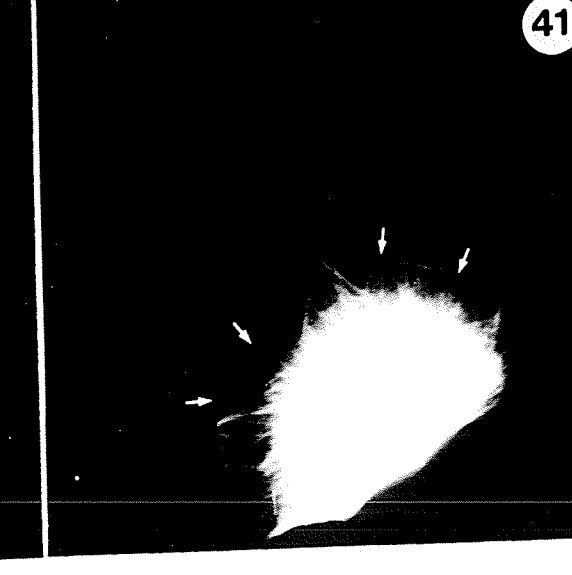
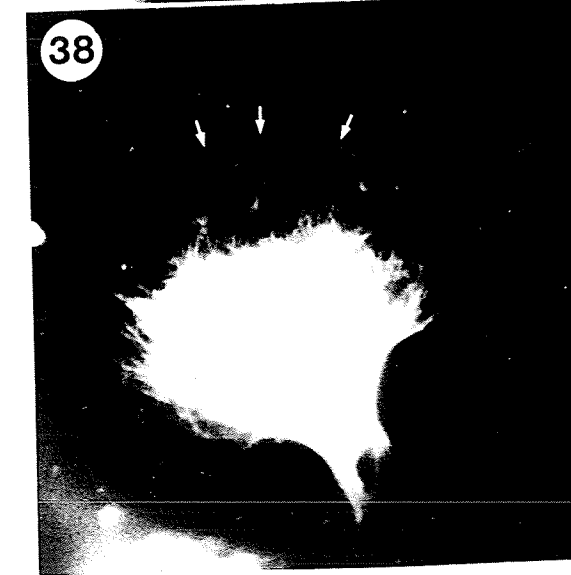
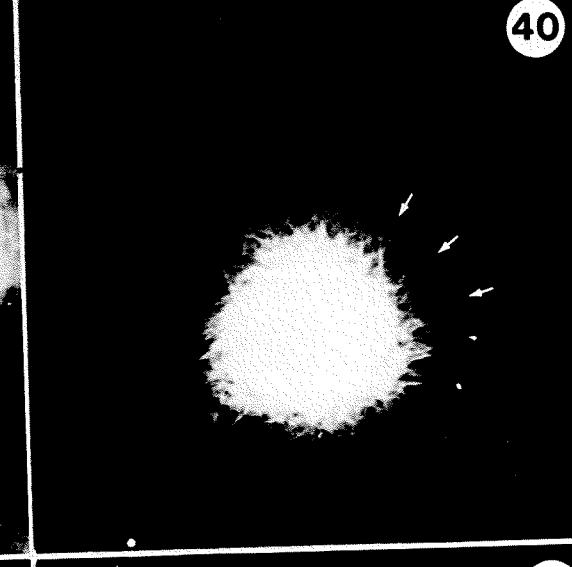
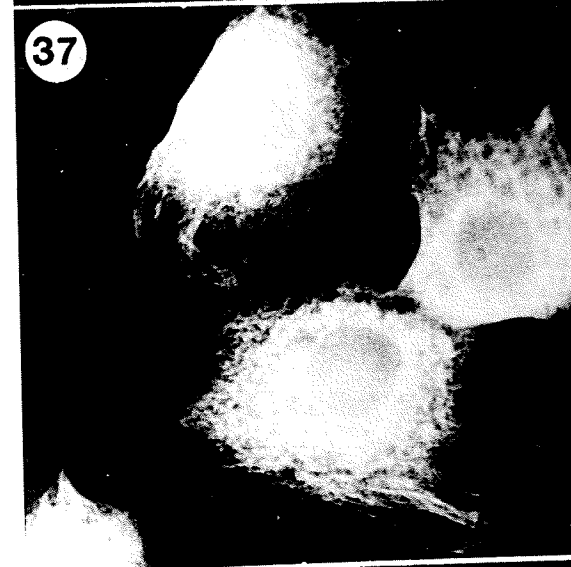
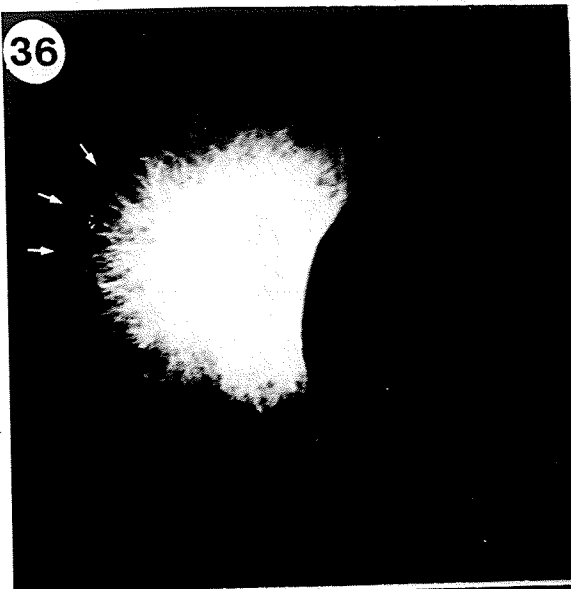
immunofluorescence was evident in some PL's. Many PL's at intermediate stages of spreading showed few MT bundles (Figs. 36, 37). The perinuclear region of such cells had an intensely fluorescent band of MT's, and the area of cytoplasm immediately adjacent had a high density of short MT's; however, only a few MT's extended to the cell cortex. This was also evident in PL's after undergoing polarized spreading (Fig. 38).

As well, to a lesser extent, PL's from larvae 1hr PI with axenically-derived serum showed similar disruptions in MT distribution (Figs. 39, 40). Occasionally, PL's from control larvae showed similar perturbations in MT distribution (Fig. 41), but these occurred at a far lower relative frequency than in treated larvae.

F-actin distribution

Hemocytes from larvae 4hrs PI with nematodes were examined to determine if there were differences in F-actin distribution. Changes in the F-actin pattern were more striking than those in the MT pattern. High proportions of PL's from nematode-injected animals exhibited F-actin staining patterns markedly different from controls in the intermediate, polarized, and non-polarized spreading stages. Intermediate spreading stage PL's usually had less intense staining around the nucleus, and few, if any, major filamentous bundles (Fig. 42). F-actin bundles originating in filopodia tended to terminate in

Figures 36-41. Fluorescence micrographs showing MT distribution in PL's from infected insects. Arrows indicate cell periphery. Note that MT bundles are short and in most instances do not extend to the edge of the cell. x1,170.



the cortical lamelloplasm, and the subplasmalemmal F-actin network was less prominent (Fig. 42).

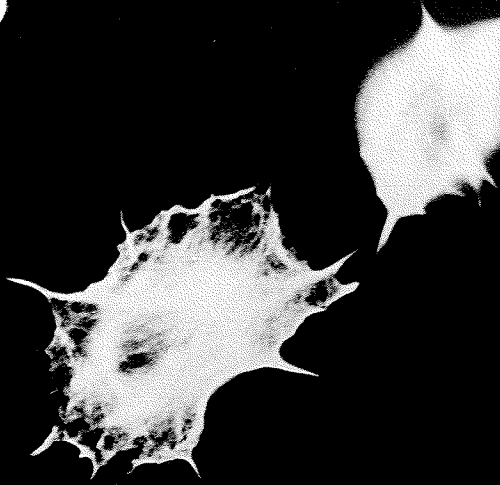
PL's undergoing polarized spreading also showed disruptions in F-actin distribution. In most cells at this stage, major F-actin bundles were far less obvious than in normal hemocytes, and few actin filaments originating in filopodia extended past the cortical region (Fig. 43). Perinuclear F-actin was less intensely stained, as was the fine cytoplasmic network of F-actin. In both of the preceding stages, there were fewer fluorescent granules in the cytoplasm. Subplasmalemmal F-actin bundles were also not as obvious as in control cells. Finally, non-polarized, spread cells from infected animals also showed marked differences in F-actin staining patterns. Fluorescence in the nuclear region was less intense, and there were fewer major bundles traversing these cells (Fig. 44); there were also fewer filopodial F-actin bundles which extended into the lamellopodium (Fig. 45).

DISCUSSION

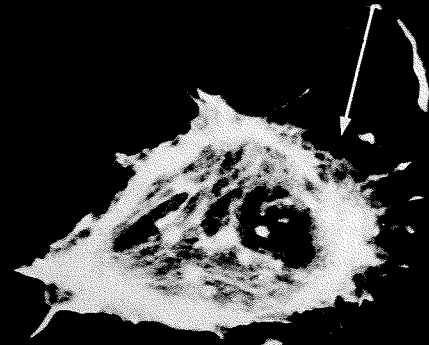
Data showed that a well-developed cytoskeleton, containing both MT's and F-actin, is present in G. mellonella PL's. The organization of the cytoskeleton correlated with cell shape. Based on previous time-lapse observations of PL movement, the shape can be reorganized relatively quickly.

Figures 42-45. Fluorescence micrographs showing F-actin distribution in PL's from infected insects. Note lack of large F-actin bundles, absence of fine F-actin (arrows in Figs. 33 and 34) and relatively sparse subplasmalemmal F-actin. Arrow in Fig. 45 indicates sparse F-actin in center of a non-polarized PL. Fig. 42 x1,200. Figs. 43 and 44 x1,050. Fig. 45 x1,180.

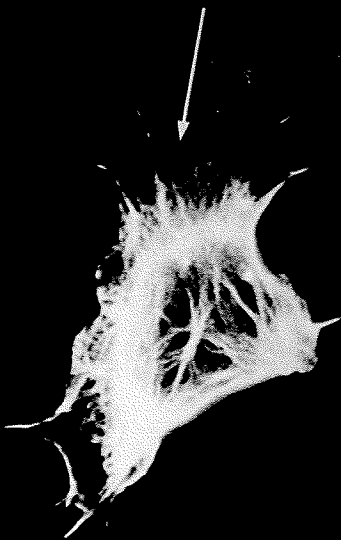
42



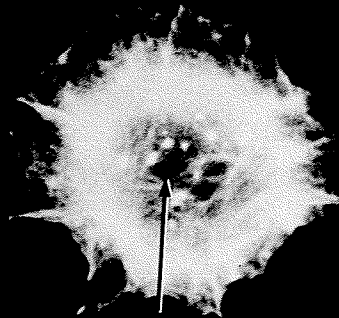
43



44



45



Microtubule Cytoskeleton

Normal distribution

The overall distribution and orientation of MT's in G. mellonella PL's are similar to that of mammalian fibroblasts in culture (Small et al., 1985; Dustin, 1984; Weber et al., 1978). The MT pattern at early PL settling/spreading stages also correlate to that of mouse 3T3 cells (Osborne and Weber, 1976). In both cell types, lamellar extension occurred first, followed by the incursion of fine bundles of MT's. These facts are consistent with the observation that MT's are probably not necessary for flattening and early lamellar extension, since MT inhibitors do not uncouple these processes (Vasiliev, 1982).

The MT distribution in later stages of cell spreading closely corresponded to PL shape. Vertebrate fibroblasts with relatively simple MT organization usually have one MT organizing center (MTOC) in the cytocenter; since MT's in PL's appeared to originate in the perinuclear region, it is likely that one or more MTOC's exist in this region. Olmstead et al. (1984) speculated that MT's originate at other, less defined MTOC's rather than in the perinuclear region. Further study on the origin of MT's in PL's could provide insight on how changes in the MT framework are established or controlled.

Curving of MT's in lamellae of later spreading stage PL's was

probably due to MT-MT and MT-MF interaction. Schliwa and Van Blerkom (1981) found that, when MT's are allowed to assemble in vitro, they do so in straight tubes. Also, when actin filaments are removed or disrupted, the porportion of straight MT segments increase. Varying degrees of curving are therefore dependant on interaction between cytoskeletal elements.

MT's in other cultured cells end peripherally in one of three places: at the termination of stress fibres; at the base of the leading edge; or within the leading edge of cells (Dustin, 1984). MT's usually terminated in or close to the leading edge of insect PL's, and thus were probably involved in stable contact formation and ruffling, as also reported by Small et al., (1985) in vertebrate cells.

Distribution of MT's in cells from experimental groups

Alterations in MT distribution in PL's from treated larvae suggest that, directly or indirectly, nematodes may inhibit MT growth or assembly. The fact that there were no apparent changes in MT patterns in PL's 2, 3, and 4hrs PI_{inj} with serum indicates that, if the effect of nematode infections on MT's is the result of factors excreted by nematodes, these excretions must be continually produced. The absence of notable differences in MT patterns in PL's from larvae 1, 2, and 3hrs PI also suggest that such nematode excretions gradually accumulate in the hemolymph.

There is a strong functional correlation suggested by disruptions in MT pattern and nematode-induced inhibition of PL locomotion (see Chapter 3). Ratcliffe and Rowley (1979) suggested the use of MT inhibitors to examine cell locomotion during parasitic encapsulation in insects. Previous experiments with vertebrate fibroblasts have already shown the importance of MT's in the maintenance of cell shape and in cell locomotion (Small et al., 1985; Brinkley et al., 1981). Despite the fact that MT alterations were not visible until 4hrs PI, it is likely that nematode secretions could have a local effect on PL's near to or in contact with them. This could potentially inhibit adherence and spreading of PL's on the nematode cuticle.

F-Actin Cytoskeleton

Normal distribution

The diverse pattern of F-actin distribution in PL's conforms to the range of patterns described in other cell types (Pollard, 1981). Briefly, four F-actin staining patterns were observed in PL's: (1) F-actin bundles in filopodia; (2) submembranous actin filaments between filopodia and along the cell periphery; (3) fine, diffuse cytoplasmic F-actin; and (4) large stress fibre bundles. Each of these forms of F-actin have been previously reported in a variety of cultured cell types (Pollard, 1981; Stossel, 1984; Small, 1981).

PL's at early spreading stages usually had filopodial F-actin, submembranous actin bundles at the anterior-most cell periphery, and the diffuse cytoplasmic F-actin. Most cells beyond early spreading stages also had well-developed stress fibres. In cells presumably migrating at the time of fixation, stress fibres were arranged parallel to the direction of movement. Although stress fibres can contract under different experimental conditions (Isenberg et al., 1976), there are conflicting reports in the literature as to their role in force generation during locomotion. Vasiliev (1982), Abercrombie (1980), and Pollack et al. (1975) attribute cell locomotion to tension exerted by stress fibres on focal contacts in the leading edge of the cell. In contradiction to this, Pollard et al. (1982) and Couchman and Rees (1979) have described motile tissue culture cells which lack focal contacts and stress fibres, and show that less motile cells have better defined stress fibres. This may, in fact, indicate two different modes of locomotion in fibroblastic cells, the latter being dependant on close contact formation (Rees et al., 1982), in which movement may be generated by the activity of the fine cytoplasmic F-actin network (Geiger, 1983). Most PL's which were presumably locomoting had both the fine cytoplasmic network of F-actin and stress fibres. On the basis of my own video time-lapse observations of migrating PL's, it is likely that even if stress fibres are not involved in generating force for forward movement, they probably have some role in the rapid posterior retraction phase of unipolarized cell locomotion.

Wang (1984) used a highly sensitive, image intensified video microscopy system coupled with time-lapse photography to study actin distribution in living fibroblasts. He showed that stress fibres in rapidly advancing cells are continually assembled, disassembled, and reorganized; fibres misaligned in advancing cells are often realigned in the direction of movement. This is consistent with the presence of large stress fibres in many presumably motile PL's, and would explain the misalignment of some stress fibres in intermediate spreading stage PL's.

The observed alignment of F-actin in touching or overlapping PL's may be explained by the observations of Heaysman and Pegrum (1973). These authors showed that, in collisions between leading-lamellae, electron-dense areas appear under the plasmalemma in the contact area and lead to the association of microfilaments lying parallel to the axis of collision. Further ultrastructural research on the cytoskeleton of PL's would clarify these membrane cytoskeletal associations in the contact area, both between cells and between cells and the substrate.

Finally, the fluorescent granular structures found in almost all normal PL's are similar to the F-actin aggregates found in transformed cells (Carley et al., 1981). These authors found F-actin aggregates, labelled by nitrobenzoxadiazole-phalloidin, near the ventral surface of cells transformed by RNA or DNA tumor viruses, chemical mutagens, or spontaneously transformed cells. The reasons

for the ubiquitous presence of these aggregates in PL's is unknown. They could either be the result of procedures used to culture PL's (ie. PTU exposure), a chronic viral infection, or they could simply be part of the normal PL cytoskeletal morphology. The latter is strongly suspected, mainly due to the relative lack of such aggregates in the PL's of nematode-infected animals.

Distribution of F-actin in cells from infected larvae

As in alterations observed in the MT cytoskeleton, nematode parasites induced definite changes in the F-actin cytoskeleton. Stress fibres, fine cytoplasmic F-actin, and submembranous F-actin bundles were less prominent in PL's from nematode-infected animals, and this strongly implies an effect on cell locomotion.

The overall modifications of PL cytoskeleton caused by nematodes correlates very well with the cell motility data. Axenic nematodes induced obvious changes in cell locomotion (Chapter 3). Since the MT and MF cytoskeletons are implicated in cell motility in a variety of cell types, including G. mellonella PL's, it is highly significant that there are, in fact, changes in the cytoskeleton. This provides experimental evidence that nematodes, by as yet unknown factors, modify the cell behaviour -- cytoarchitectural association. This may be a critical component of the host-parasite relationship, whereby the nematode is able to evade the cellular immune response of the host.

GENERAL SUMMARY

The results presented demonstrate that the entomophagous nematode S. feltiae induces a variety of alterations in Galleria sp. hemocytes, and these reflect an impairment of the cellular immune response. Striking differences occurred in the in vitro locomotion of PL's, and these correlated well with alterations in the microtubule-microfilament cytoskeleton. This clearly demonstrates that the nematode can disrupt processes involved in cellular encapsulation. Inhibition of phagocytosis and alterations in the surface membrane of GR's, while only speculatively linked to the encapsulation response, imply that S. feltiae may also influence immune recognition.

The actual mechanism by which these changes were brought about are as yet unknown. Factors either excreted by the nematodes or induced as a result of them may simply have been toxic to hemocytes and/or may have inhibited metabolism. This may explain the lower rates of locomotion and changes in cytoskeleton, as cell movement and assembly of microtubules and microfilaments require metabolic energy (Vasiliev, 1982; Dustin, 1984; Alberts et al., 1983). Furthermore, inhibitors of glycolysis and oxidative phosphorylation prevent capsule maturation (Ratner and Vinson, 1983).

However, other, more specific mechanisms cannot be ruled out. Since S. feltiae secrete very specific inhibitors of immune proteins (Gotz et al., 1981), and considering that nematode parasites have had

millions of years to evolve specialized mechanisms to cope with host immunological responses (Anderson, 1982), it is likely that S. feltiae may secrete other factors which specifically target insect hemocytes.

Future work on this system should include attempts to isolate factor(s) involved in eliciting the observed alterations in insect hemocytes. This would not only provide more information on the biology of S. feltiae, but also has implications in biological control and hopefully, will add to our understanding of basic cellular processes.

REFERENCES

- Abercrombie, M. 1970. Contact inhibition in tissue culture.
In vitro 6: 128-142.
- Abercrombie, M. 1980. The crawling movement of metazoan cells.
Proc. R. Soc. Lond. B 207: 129-147.
- Alberts, B., D. Bray, J. Lewis, M. Raff, K. Roberts, J.D. Watson.
1983. Molecular Biology of the Cell. Garland Publishing,
Inc., New York. pgs. 1146.
- Amirante, G.A. and F.G. Mazzalai. 1978. Synthesis and localization
of hemoagglutinins in hemocytes of the cockroach Leucophaea
maderae L. Dev. Comp. Immunol. 2: 735-740.
- Anderson, R.C. 1984. The origins of zooparasitic nematodes. Can. J.
Zool. 62: 317-328.
- Anderson, R.S. 1976. Expression of receptors by insect macrophages.
In Phylogeny of Thymus and Bone Marrow-Bursa Cells.
R.K. Wright and E.L. Cooper (Eds.). Elsevier/North-Holland,
Amsterdam. pgs. 27-34.

- Armstrong, P.B. 1977. Interaction of motile blood cells of the horseshoe crab, Limulus. Studies on contact paralysis of pseudopodial activity and cellular overlapping. Exp. Cell Res. 107: 127-138.
- Arnold, J.W. 1959. Observations on amoeboid motion of living haemocytes in the wing veins of Blaberus giganteus (L) (Orthoptera:Blattidae) Can. J. Zool. 37: 371-375.
- Baerwald, R.J. and G.M. Boush. 1970. Time-lapse photographic studies of cockroach hemocyte migrations in vitro. Exptl. Cell Res. 63: 208-213.
- Beck, S.D. 1960. Growth and development of the greater wax moth, Galleria mellonella (L.) (Lepidoptera:Galleriidae). Wis. Acad. Sci. Arts Lett. 49: 137-148.
- Beeman, S.C., M.E. Wilson, L.A. Bulla, Jr., and R.A. Consigli. 1983. Structural characterization of the hemocytes of Plodia interpunctella. J. Morphol. 175: 1-16.

- Boemare, N., C. Laumond, and J. Luciana. 1982. Pathologic Animale. -
Mise en evidence d'une toxicogenese provoquee par le Nematode
axenique entomophage Neoplectana carpocapsae Weiser chez
l'insecte axenique Galleria mellonella L. C.R. Acad. Sc.
paris.t.295 (III) 543-546.
- Boman, H.G., I. Nilsson-Faye, and T. Rasmuson. 1974. Why is insect
immunity interesting? In Lipmann Symposium: Energy, Bio-
synthesis and Regulation. D. Richter (Ed.). Walter de Gruyter
Verlag, New York. pgs. 103-121.
- Bourguignon, Y.W. and G.J. Bourguignon. 1984. Capping and the
cytoskeleton. Int. Rev. Cytol. 87: 195-224.
- Brahni, Z. and E.L. Cooper. 1974. Characteristics of the agglutinin
in the scorpion, Androctonus australis. In Contemporary
Topics in Immunobiology (Vol. 4), Invertebrate Immunology.
E.L. Cooper (Ed.). Plenum Press, New York. pgs. 261-70.
- Brennan, B.B. and T.C. Cheng. 1975. Resistance of Moniliformis
dubious to the defense reactions of the American cockroach,
Periplaneta americana. J. Invertebr. Pathol. 26: 65-73.

- Brewer, F.D. and S.B. Vinson. 1971. Chemicals affecting the encapsulation of foreign materials in an insect. *J. Invertebr. Pathol.* 18: 287-289.
- Brinkley, B.R., S.M. Cox, D.A. Pepper, L. Wible, S.L. Brenner, and R.L. Pardue. 1981. Tubulin assembly sites and the organization of cytoplasmic microtubules in cultured mammalian cells. *J. Cell Biol.* 90: 554-562.
- Burnett, F.M. 1968. Evolution of the immune process in vertebrates. *Nature.* 218: 426-430.
- Carley, L.S., L.S. Barak, and W.W. Webb. 1981. F-actin aggregates in transformed cells. *J. Cell Biol.* 90: 797-802.
- Cawthorn, R.J. and R.C. Anderson. 1977. Cellular reactions of field crickets (*Acheta pennsylvanicus* Burmeister) and German cockroaches (*Blatella germanica* to *Physaloptera maxillaris* Molin (Nematoda:Physalopteroidea) *Can. J. Zool.* 55: 368-375.
- Chain, B.M. and R.S. Anderson. 1981. Rapid plasmatocyte depletion in an insect following experimental infection. *Am. Zool.* 21: 981-987.

- Chain, B.M. and R.S. Anderson. 1983. Inflammation in insects: the release of a plasmatocyte depletion factor following interaction between bacteria and haemocytes. *J. Insect Physiol.* 29: 1-4.
- Cheng, T.C. 1983. The role of lysosomes in molluscan inflammation. *Amer. Zool.* 23: 129-144.
- Cheung, P.Y.K., E.A. Grula, and R.L. Burton. 1978. Hemolymph responses in Heliothis zea to inoculation with Bacillus thuringiensis or Micrococcus lysodeikticus. *J. Invertebr. Pathol.* 31: 148-156.
- Condon, W.J., and R. Gordon. 1977. Some effects of mermithid parasitism of the larval blackflies Prosimulium mixtum fuscum and Simulium venustum. *J. Invertebr. Pathol.* 29: 56-62.
- Couchman, J.R. and D.A. Rees. 1979. Actomyosin organisation for adhesion, spreading, growth and movement in chick fibroblasts. *Cell Biol. Int. Rep.* 3: 431-439.
- Davies, D.H. and T.M. Preston. 1985. The behaviour of insect plasmatocytes in vitro: Changes in morphology during settling, spreading, and locomotion. *J. Exptl. Zool.* 236: 71-82.

- De Brabander, M., J. De Mey, R. Van de Veire, F. Aerts, and G. Geuens. 1977. Microtubules in mammalian cell shape and surface modulation: an alternative hypothesis. *Cell Biol. Int. Rep.* 1: 453-461.
- De Groot, C. and J. Wormmeester. 1981. Capping of surface immunoglobulin on rabbit and mouse lymphocytes. I. Kinetics. *Eur. J. Cell Biol.* 24: 9-15.
- Dustin, P. 1984. *Microtubules*. Springer-Verlag, New York. pgs. 482.
- Edds, K.T. 1977. Dynamic aspects of filopodial formation by reorganization of microfilaments. *J. Cell Biol.* 73: 479-491.
- Evans, J.J.T. 1968. Natural substrates of the phenoloxidase in the pupal blood of the Chinese oak silkworm Antheraea pernyi. *J. Insect Physiol.* 13: 1699-1711.
- Evans, P.M. and B.M. Jones. 1974. Studies on cellular adhesion aggregation. *Exptl. Cell Res.* 88: 56-62.

- Foley, D.A. and T.C. Cheng. 1972. Interaction of molluscs and foreign substances: the morphology and behaviour of hemolymph cells of the American oyster, Crassostrea virginica, in vitro. J. Invertebr. Pathol. 19: 383-394.
- Gaugler, R. and G.M. Boush. 1979. Effects of ultraviolet radiation and sunlight on the entomogenous nematode, Neoaplectana carpocapsae. J. Invertebr. Pathol. 32: 291-296.
- Geiger, B. 1983. Membrane-cytoskeleton interaction. Biochimica et Biophysica Acta. 737: 305-341.
- Godman, G., B. Woda, and R. Kolberg. 1980. Redistribution of contractile and cytoskeletal components induced by cytochalasin. I. In Hmf cells, a nontransformed fibroblastoid line. Eur. J. Cell Biol. 22: 733-744.
- Goldman, R.D. and D.M. Knipe. 1973. Functions of cytoplasmic fibres in non-muscle cell motility. Cold Spring Harbor Symp. Quant. Biol. 37: 523-534.
- Gotz, P., A. Boman, and H.G. Boman. 1981. Interactions between insect immunity and an insect-pathogenic nematode with symbiotic bacteria. Proc. R. Soc. Lond. B 212: 333-350.

- Gotz, P. and H.G. Boman. 1985. Insect immunity. In Comprehensive Insect Physiology, Biochemistry and Pharmacology. Vol. 3 C.A. Kerkut and L.J. Gilbert (Eds.). Pergamon Press, Oxford. pgs. 453-485.
- Gupta, A.P. 1979. Hemocyte types: their structures, synonymies, interrelationships, and taxonomic significance. In Insect Hemocytes. A.P. Gupta (Ed.). Cambridge University Press, New York. pgs. 85-128.
- Heaysman, J.E.M. and S.M. Pegrum. 1973. Early contact between fibroblasts. *Exptl. Cell Res.* 78: 71-78.
- Huebner, E. and E. Anderson. 1972. A cytological study of the ovary of Rhodnius prolixus I. The ontogeny of the follicular epithelium. *J. Morph.* 136: 459-494.
- Hughes, R.C. 1976. Membrane Glycoproteins. Butterworths Publishers, Inc., Boston. pgs. 205.
- Inoue, S. 1986. Video Microscopy. Plenum Press, New York. pgs. 584.

Isenberg, G., P.C. Rathke, N. Hulsmann, W.W. Franke, and K.E.

Wohlfarth-Bottermann. 1976. Cytoplasmic actomyosin fibrils in tissue culture cells. Direct proof of contractility by visualization of ATP-induced contraction in fibrils isolated by laser microbeam dissection. *Cell Tiss. Res.* 166: 427-444.

Kabat, E.A. 1976. *Structural Concepts in Immunology and Immunology*. Second ed. Holt, Rinehart and Winston, New York. pgs. 547.

Kawanishi, C.Y., C.M. Splittstoesser, and H. Tashiro. 1978.

Infection of the European chafer, Amphimallon majalis, by Bacillus pepsillae. II. Ultrastructure. *J. Invertebr. Pathol.* 31: 91-102.

Kitano, H. 1969. Experimental studies on the parasitism of Apanteles glomeratus L. with special reference to its encapsulation-inhibiting capacity. *Bull. Tokyo Gekugei Univ.* 21: 95-136.

Lackie, A.M. 1980. Invertebrate immunity. *Parasitol.* 80: 393-412.

Lackie, A.M. 1981a. Immune recognition in insects. *Devel. Comp. Immunol.* 5: 191-204.

- Lackie, A.M. 1981b. Humoral mechanisms in the immune response of insects to larvae of Hymenolepis diminuta (Cestoda). *Parasite Immunol.* 3: 201-208.
- Lackie, A.M. 1986. The role of substratum surface-charge in adhesion and encapsulation by locust hemocytes in vivo. *J. Invertebr. Pathol.* 47: 377-386.
- Lackie, A.M. and J.M. Lackie. 1979. Evasion of the insect immune response by Moniliforms dubius (Acanthocephala): further observations on the origin of the envelope. *Parasitol.* 79: 297-311.
- Lawrence, P.O. 1986. Host-parasite hormonal interactions: an overview. *J. Insect Physiol.* 32: 295-298.
- Leonard, C., K. Soderhall, and N.A. Ratcliffe. 1985. Studies on prophenoloxidase and protease activity of Blaberus cranifer haemocytes. *Insect Biochem.* 15: 803-810.
- Lowry, O.H., N.J. Rosebrough, A.L. Farr, and R.J. Randall. 1951. Protein measurement with the Folin phenol reagent. *J. Biol. Chem.* 193: 265-275.

- Lynn, D.C. and S.B. Vinson. 1977. Effects of temperature, host age, and hormones upon the encapsulation of Cardiochiles nigriceps eggs by Heliothis spp. J. Invertebr. Pathol. 29: 50-5.
- Lysenko, O. and J. Weiser. 1974. Bacteria associated with the nematode Neoaplectana carpocapsae and the pathogenicity of this complex for Galleria mellonella larvae. J. Invertebr. Pathol. 24: 332-336.
- Nappi, A.J. 1975. Parasite encapsulation in insects. In Invertebrate Immunity. K. Maramorosch and R.E. Shope (Eds.). Academic Press, New York. pp. 293-326.
- Nappi, A.J. and M. Silvers. 1984. Cell surface changes associated with cellular immune reactions in Drosophila. Science. 225: 1166-1168.
- Nappi, A.J. and J.G. Stoffolano, Jr. 1972. Distribution of haemocytes in larvae of Musca domesticus and Musca autumnalis and possible chemotaxis during parasitization. J. Invertebr. Pathol. 18: 169-79.
- Neuwirth, M. 1973. The structure of the hemocytes of Galleria mellonella (Lepidoptera). J. Morphol. 139: 105-124.

- Nicolson, G.L. 1974. The interactions of lectins with animal cell surfaces. *Int. Rev. Cytol.* 39: 89-190.
- Olmsted, J.B., J.V. Cox, C.F. Asnes, L.M. Parysek, and H.D. Lyon. 1984. Cellular regulation of microtubule organization. *J. Cell Biol.* 99: 285-325.
- Osborn, M. and K. Weber. 1976. Tubulin-specific antibody and the expression of microtubules in 3T3 cells after attachment to a substratum. *Exptl. Cell Res.* 103: 331-340.
- Osborn, M. and K. Weber. 1982. Immunofluorescence and immunocytochemical procedures with affinity purified antibodies: tubulin-containing structures. In *Methods in Cell Biology*, Vol. 24. Academic Press. pgs. 97-132.
- Parish, C.R. 1977. Simple model for self- non-self discrimination in invertebrates. *Nature (Lond.)* 267: 711-33.
- Partridge, T. and P.S. Davies. 1974. Limpet haemocytes II. The role of spikes in locomotion and spreading. *J. Cell Sci.* 14: 319-330.

- Poinar, G.O. 1974. Insect immunity to parasitic nematodes. In Contemporary Topics in Immunology, Vol. 4, Invertebrate Immunology. E.L. Cooper (Ed.). Plenum Press, New York. pgs. 167-78.
- Poinar, G.O. 1979. Nematodes for Biological Control of Insects. CRC Press, Boca Raton, Florida. pgs. 198.
- Poinar, G.O. and P.T. Himsworth. 1967. Neoaplectana parasitism of Galleria mellonella L. J. Invertebr. Pathol. 9: 241-246.
- Poinar, G.O., R. Leutenegger, and P. Gotz. 1968. Ultrastructure of a melanotic capsule in Diabrotica (Coleoptera) in response to a parasitic nematode (Mermithidae). J. Ultrastruct. Res. 25: 293-306.
- Pollack, R., M. Osborn, and K. Weber. 1975. Patterns of organization of actin and myosin in normal and transformed cultured cells. Proc. Natl. Acad. Sci. USA. 72: 994-998.
- Pollard, T.D. 1981. Cytoplasmic contractile proteins. J. Cell Biol. 91: 156s-165s.
- Pollard, T.D., S.C. Selden, and P. Maupin. 1984. Interaction of actin filaments with microtubules. J. Cell Biol. 99: 33s-37s.

Ratcliffe, N.A. and S.J. Gagen. 1976. Cellular defense reactions of insect hemocytes in vivo: An ultrastructural analysis of module formation in Galleria mellonella and Pieris brassicae larvae. J. Invertebr. Pathol. 28: 373-82.

Ratcliffe, N.A. and S.J. Gagen. 1977. Studies on the in vivo cellular reactions of insects: An ultrastructural analysis of nodule formation in Galleria mellonella. Tissue Cell. 9: 73-85.

Ratcliffe, N.A. and A.F. Rowley. 1979. Role of hemocytes in defense against biological agents. In Insect Hemocytes. A.P. Gupta (Ed.). Cambridge University Press, New York. pgs. 331-414.

Ratcliffe, N.A., A.F. Rowley, S.W. Fitzgerald, and C.P. Rhodes. 1985. Invertebrate immunity: basic concepts and recent advances. Int. Rev. Cytol. 97: 183-347.

Ratner, S. and S.B. Vinson. 1983a. Phagocytosis and encapsulation: cellular immune responses in Arthropoda. Amer. Zool. 23: 185-194.

Ratner, S. and S.B. Vinson. 1983b. Encapsulation reactions in vitro by haemocytes of Heliothis virescens. J. Insect Physiol. 29: 855-863.

- Rees, D.A., J.R. Couchman, C.G. Smith, A. Woods, and G. Wilson. 1982. Cell-substratum interactions in the adhesion and locomotion of fibroblasts. Proc. R. Soc. Lond. B 299: 169-176.
- Renwrautz, L.R. and T.C. Cheng. 1977. Identification of agglutinin receptors on hemocytes of Helix pomatia. J. Invertebr. Pathol. 29: 88-96.
- Reynolds, E.S. 1963. The use of lead citrate at high pH as an electron-opaque stain in electron microscopy. J. Cell Biol. 17: 208-212.
- Rizki, M.T.M. 1962. Experimental analysis of hemocyte morphology in insects. Amer. Zool. 2: 247-56.
- Salt, G. 1963. The defence reactions of insects to metazoan parasites. Parasitol. 53: 527-642.
- Salt, G. 1968. The resistance of insect parasitoids to the defence reactions of their hosts. Biol. Rev. (Cambridge) 43: 200-32.
- Salt G. 1970. The Cellular Defence Reactions of Insects. Cambridge University Press, Cambridge. pgs. 118.

- Schliwa, M. and J. van Blerkom. 1981. Structural interaction of cytoskeletal components. *J. Cell Biol.* 90: 222-235.
- Scott, M.T. 1971. Recognition of foreignness in invertebrates. II. In vitro studies of cockroach phagocytic haemocytes. *Immunol.* 21: 817-828.
- Scott, M.T. 1972. Partial characterization of the hemagglutinating activity in hemolymph of the American cockroach (Periplaneta americana). *J. Invertebr. Pathol.* 19: 66-71.
- Silverstein, S.C., R.M. Steinman, and Z.A. Cohen. 1977. Endocytosis. *Annu. Rev. Biochem.* 46: 669-772.
- Seryczynska, H., M. Kamionek, and H. Sandner. 1974. Defensive reactions of caterpillars of Galleria mellonella L. in relation to bacteria Achromobacter nematophilus. Poinar et Thomas (Eubacteriales:Achromobacteriaceae) and bacteria-free nematodes Neoaplectana carpocapsae Weiser (Nematoda:Steinernematidae). *Bull Acad. Polon. Sci., Ser. Sci. Biol.* 20: 193-196.
- Small, J.V. 1981. Organization of actin in the leading edge of cultured cells: influence of osmium tetroxide and dehydration on the ultrastructure of actin meshworks. *J. Cell Biol.* 91: 695-705.

Small, J.V., G. Rinnerthaler, Z. Afnur, and B. Geiger. 1985. Cytoskeletal changes associated with fibroblast locomotion: involvement of ruffling and microtubules in the establishment of new substrate contacts at the leading edge. In Proc. 1st Int. Congr. Contractile Proteins. Sansari (Ed.). Temple Univ. pgs.

Stossel, T.P. 1984. Contribution of actin to the structure of the cytoplasmic matrix. *J. Cell Biol.* 99: 15S-21S.

Sundqvist, K.G. and A. Ehrnst. 1976. Cytoskeletal control of surface membrane mobility. *Nature* 264: 226-231.

Sykes, J.A. and E.B. Moore. 1959. A new chamber for tissue culture. *Proc. Soc. Exp. Biol. and Med.* 100: 121-127.

van der Knaap, W.P.W., T. Sminia, R. Schutte, and L.H. Boerrigter-Barendsen. 1983. Cytophilic receptors for foreignness and some factors which influence phagocytosis by invertebrate leucocytes: in vitro phagocytosis by amoebocytes of the snail Lymnaea stagnalis. *Immunol.* 48: 377-384.

Vasiliev, J.M. 1982. Spreading and locomotion of tissue cells: factors controlling the distribution of pseudopodia. *Proc. R. Soc. Lond. B* 299: 145-327.

- Vey, A. and C. Vago. 1971. Reaction anticryptogamique de type granulome chez les insectes. Ann. Inst. Pasteur (Paris) 121: 527-532.
- Vinson, S.B. 1974. The role of foreign surface and female parasitoid secretions on the immune response of an insect. Parasitol. 68: 27-33.
- Vinson, S.B. 1977. Microplitis croceipes: Inhibitions of the Heliothis zea defense reactions to Cardiochiles nigriceps. Exptl. Parasitol. 41: 112-17.
- Vinson, S.B. and J.R. Scott. 1974. Parasitoid egg shell changes in a suitable and unsuitable host. J. Ultrastruct. Res. 47: 1-15.
- Wang, Y.L. 1984. Reorganization of actin filament bundles in living fibroblasts. J. Cell Biol. 99: 1478-1485.
- Weber, K., P.C. Rathke, and M. Osborn. 1978. Cytoplasmic micro-tubular images in glutaraldehyde-fixed tissue culture cells by electron microscopy and by immunofluorescence microscopy. Proc. Natl. Acad. Sci. U.S.A. 75: 1820-1824.

Welch, H.E. and J.F. Bronskill. 1962. Parasitism of mosquito larvae by the nematode DD136 (Nematoda:Neoaplectanidae). *Can J. Zool.* 40: 1276-1285.

Wigglesworth, V.B. 1979. Hemocytes and growth in insects. In *Insect Hemocytes*. A.P. Gupta (Ed.). Cambridge University Press, New York. pgs. 303-318.

Witkowski, J.A. and W.D. Brighton. 1972. Influence of serum on attachment of tissue cells to glass surfaces. *Exptl. Cell Res.* 70: 41-48.

Yeaton, R.W. 1981. Invertebrate lectins: I. Occurrence. *Dev. Comp. Immunol.* 5: 391-402.

Yoshino, T.P. 1981. Concanavalin A-induced receptor redistribution on Biomphalaria glabrata hemocytes: characterization of capping and patching responses. *J. Invert. Pathol.* 38: 102-112.

Yoshino, T.P., L.R. Renwranz, and T.C. Cheng. 1979. Binding and redistribution of surface membrane receptors for concanavalin A on oyster hemocytes. *J. Exp. Zool.* 207: 439-450.

Zar, J.H. 1974. *Biostatistical analysis*. Prentice-Hall, Inc. Englewood Cliffs, N.J.